ASN NEURO REVIEW ARTICLE

ASN NEURO 4(5):art:e00093.doi:10.1042/AN20120021

Fueling and imaging brain activation

Gerald A Dienel[1]
Department of Neurology, University of Arkansas for Medical Sciences, Little Rock, AR 72205, U.S.A.

Cite this article as: Dienel GA (2012) Fueling and imaging brain activation. ASN NEURO 4(5):art:e00093.doi:10.1042/AN20120021

ABSTRACT

Metabolic signals are used for imaging and spectroscopic studies of brain function and disease and to elucidate the cellular basis of neuroenergetics. The major fuel for activated neurons and the models for neuron–astrocyte interactions have been controversial because discordant results are obtained in different experimental systems, some of which do not correspond to adult brain. In rats, the infrastructure to support the high energetic demands of adult brain is acquired during postnatal development and matures after weaning. The brain's capacity to supply and metabolize glucose and oxygen exceeds demand over a wide range of rates, and the hyperaemic response to functional activation is rapid. Oxidative metabolism provides most ATP, but glycolysis is frequently preferentially up-regulated during activation. Underestimation of glucose utilization rates with labelled glucose arises from increased lactate production, lactate diffusion via transporters and astrocytic gap junctions, and lactate release to blood and perivascular drainage. Increased pentose shunt pathway flux also causes label loss from C1 of glucose. Glucose analogues are used to assay cellular activities, but interpretation of results is uncertain due to insufficient characterization of transport and phosphorylation kinetics. Brain activation in subjects with low blood-lactate levels causes a brain-to-blood lactate gradient, with rapid lactate release. In contrast, lactate flooding of brain during physical activity or infusion provides an opportunistic, supplemental fuel. Available evidence indicates that lactate shuttling coupled to its local oxidation during activation is a small fraction of glucose oxidation. Developmental, experimental, and physiological context is critical for interpretation of metabolic studies in terms of theoretical models.

Key words: astrocyte, gap junction, glucose, lactate, metabolism, neuron.

INTRODUCTION

During the past five decades, enormous progress has been made towards understanding the local energy demands of living brain and the relationships between brain function and fluxes in metabolic pathways that satisfy developmental, energetic, neuroprotective, and biosynthetic requirements of working brain cells. The knowledge base enables use of haemodynamic and metabolic signals in brain imaging and spectroscopic studies as functional surrogates. These signals register the location, direction and magnitude of local changes in brain function under various conditions, including rest, activation, pharmacological intervention and diseases. Major advances in the understanding of brain metabolism and blood flow are driven by evolution of methodology, ranging from micro-analytical and biochemical assays, molecular biological studies, quantitative autoradiography, PET (positron emission tomography), MRS (magnetic resonance spectroscopy), fMRI (functional magnetic resonance imaging) and fluorescence microscopy. Development of new reporter molecules facilitated a shift from global to local methods and to cellular assays of metabolic capacity and rates. The goal of understanding cellular and subcellular contributions to energetics of brain function and disease and the brain images based on these signals is a long-standing, formidable problem requiring complementary combinations of quantitative *in vivo* approaches to address technically difficult issues.

Functional metabolic activity and brain activation

In this review, the concept of *functional metabolic activity* is broadly used to describe metabolic processes associated with brain functions, and includes all processes that enable a cell to stay alive and carry out its roles in tissue. Functional metabolic activities include so-called 'housekeeping'

[1] email gadienel@uams.edu

Abbreviations: 2-NBDG, 2-[*N*-(7-nitrobenz-2-oxa-1,3-diazol-4-yl)amino]-2-deoxyglucose; 6-NBDG, 2-[*N*-(7-nitrobenz-2-oxa-1,3-diazol-4-yl)amino]-6-deoxyglucose; a–v, arteriovenous; BOLD, blood oxygen-level dependent; CBF, cerebral blood flow; 4-CIN, α-cyano-4-hydroxycinnamate; CMR, cerebral metabolic rate; DG, 2-deoxy-D-glucose; FDG, 2-fluoro-2-deoxy-D-glucose; fMRI, functional magnetic resonance imaging; GABA, γ-aminobutyric acid; Glc-6-P, glucose 6-phosphate; GLUT, glucose transporter; LDH, lactate dehydrogenase; MAS, malate–aspartate shuttle; MCT, monocarboxylic acid transporter; MRS, magnetic resonance spectroscopy; PDH, pyruvate dehydrogenase; PET, positron emission tomography; TCA, tricarboxylic acid.

processes (e.g., macromolecule turnover and axonal transport), biosynthesis of many types of neurotransmitters, signalling within and among cells and maintenance and restoration of membrane potentials. The calculated energetic costs associated with ion fluxes greatly exceed those of other processes (Attwell and Laughlin, 2001; Howarth et al., 2010). *Brain activation* refers to stimulation of brain cells by a specific paradigm in which signalling activities, ion fluxes and demand for ATP rise over and above that of the basal or 'resting' state of the specific experimental condition and protocol. The *resting state* is an energy-consuming state that involves active information processing via many modalities and pathways, and its level can vary markedly with experimental condition, for example, in comatose, anaesthetized and conscious subjects. Detailed knowledge of the biochemical, cellular, and network basis for the metabolic signals used to generate brain images and calculate rates of metabolic pathways is essential to properly interpret their relationships to normal brain activity and disease processes. Glucose is the major, obligatory fuel for normal adult brain, but the pathways, processes and cell types that consume the additional glucose required during activation compared with baseline and the fates of products of glucose metabolism in working brain are not adequately understood.

The literature relevant to brain energy metabolism and imaging is enormous. It spans many decades of work in complex, interrelated fields that use different technologies and different experimental systems ranging from purified cell types in tissue culture to human brain. Since most reviews of this work focus on specific aspects of neuroenergetics and selectively address topics of interest, it is difficult for investigators, especially those who do not work in the field, to develop a broad overview. The goal of this review is to provide a comprehensive perspective of brain activation. Major topics can be read and studied in increments and more details of these and related subjects can be found in cited reviews and references and in a recent volume on brain energetics (Gibson and Dienel, 2007) that contains excellent reviews of many aspects of brain energy metabolism and function. Unfortunately, length constraints prevent citation of many interesting and important studies in the present work.

To provide a common framework for a discussion of 'fuelling brain activation', the brain's infrastructure is described first, and includes major glucose metabolism pathways, types of assays commonly used to measure metabolic rate in brain *in vivo*, metabolic capacity and glucose supply–demand relationships. Then results of *in vivo* studies of brain activation are presented, with emphasis on findings in normal, conscious adult animals and humans. Important issues related to energetics of activation include the disproportionate rise in non-oxidative metabolism, incomplete trapping of metabolites of labelled glucose and the controversial role of lactate.

BRAIN METABOLIC ACTIVITY: PATHWAYS AND ASSAY PROCEDURES

Overview of major pathways of glucose utilization

Glucose metabolism fulfils important functions in adult brain related to neuroenergetics, neurotransmission, energy storage, biosynthesis and oxidative defence (Figure 1A). The major energy-producing pathways are glycolysis (glucose to pyruvate) and oxidative metabolism (pyruvate to CO_2) via the TCA (tricarboxylic acid) cycle and the electron transport chain. Neuromodulators and neurotransmitters must be produced endogenously from substrates derived via these two pathways because passage of neuroactive compounds from blood to brain across the blood–brain barrier is highly restricted. Without the blood–brain barrier, dietary consumption of neuroactive compounds such as MSG (monosodium glutamate) would disrupt the integrity of brain signalling activities. Biosynthesis of amino acids, monosaccharides and complex carbohydrates is essential for neurotransmission and macromolecular turnover, and requires the use of glucose as the carbon source. Some biosynthetic reactions and defence against oxidative stress depend on NADPH production via the pentose-phosphate shunt pathway. Since NADH generated by glycolysis cannot traverse the mitochondrial membrane, shuttling of reducing equivalents from the cytoplasm into mitochondria is necessary for pyruvate formation and maximal ATP yield from glucose (Figure 1A). Regeneration of NAD^+ also occurs in cytoplasm via LDH (lactate dehydrogenase), which converts pyruvate into lactate. However, this lactate must then be released from the cell for glycolytic rate to be sustained, because lactate accumulation will reverse the direction of the equilibrative LDH reaction due to mass action. Lactate release eliminates pyruvate as an oxidative fuel for the cell in which it is produced. When labelled glucose is used to evaluate the rate of glucose utilization [CMR_{glc} (cerebral metabolic rate) for glucose] lactate efflux causes loss of a highly labelled metabolite of glucose and underestimation of CMR_{glc}. Glucose has many essential functions fulfilled by glycolytic and pentose shunt pathways that cannot be satisfied by oxidizable substrates, for example, ketone bodies and lactate (Figure 1).

Glucose phosphorylation: The gateway step for glucose metabolism

The steady-state brain-to-plasma ratio for glucose is 0.2–0.3 in animals and humans (Dienel et al., 1991; Gruetter et al., 1998). In normal rat brain, glucose levels are in the range of 2–3 μmol/g, and brain glucose content exceeds 1 mmol/l as long as arterial plasma glucose level is above 5 mmol/l. The first irreversible step of glucose metabolism is catalysed by hexokinase (Figure 1A), which has a K_m for glucose of

A. Multi-functional roles of glucose metabolism

Energetics, neurotransmission, redox, biosynthesis

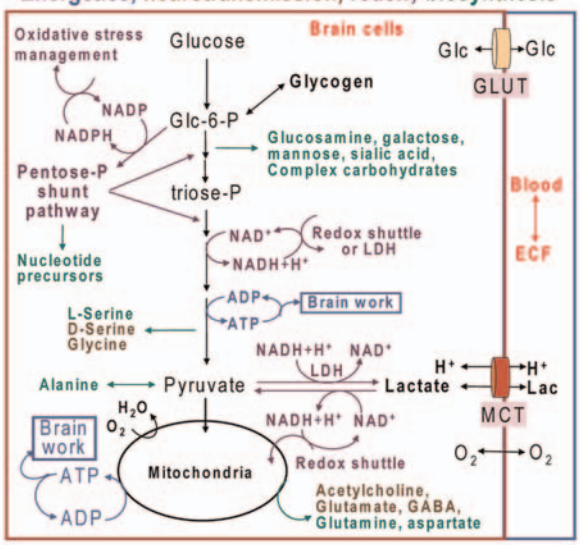

B. Measures of metabolic activity

a. Metabolic rate assays

Global: CMR = (A-V)CBF

Hexokinase reaction (CMR_{glc})

DG → DG-6-P, FDG→FDG-6-P

2-NBDG→2-NBDG-6-P

Glycolysis pathway

Glc consumption, Lac production

Glc→H_2O

Pentose phosphate shunt pathway

Release of labeled CO_2 from C1-labeled Glc

Oxidative pathways (V_{TCA}, CMR_{O2})

Glc, Lac, Pyr, Acetate → TCA cycle

O_2→H_2O

b. Pathway relationships

$OGI = CMR_{O2}/CMR_{glc}$ (maximum = 6.0)

$OCI = CMR_{O2}/CMR_{total\ carbohydrate}$

c. Metabolite concentration change

Δ[Metabolite] = Δ(input to pool) – Δ(output from pool)

C. Signals are generated from metabolic tracers in different pathways according to functional activity

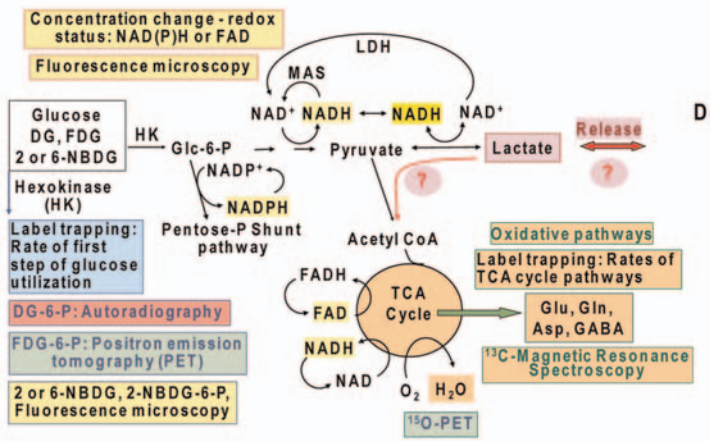

D. Relative transport and phosphorylation rates

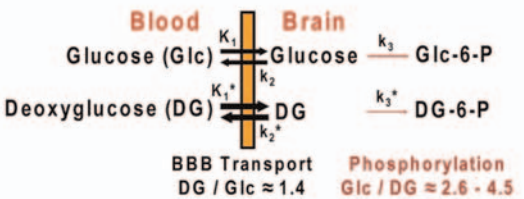

- Routine DG method: Lumped constant = 0.48
  2 Glc taken up and phosphorylated for each DG
- Glc supply capacity > demand:
  $T_{max}/CMR_{glc} \approx 2\text{-}3$

E. Glucose level vs. Methylglucose distribution ratio

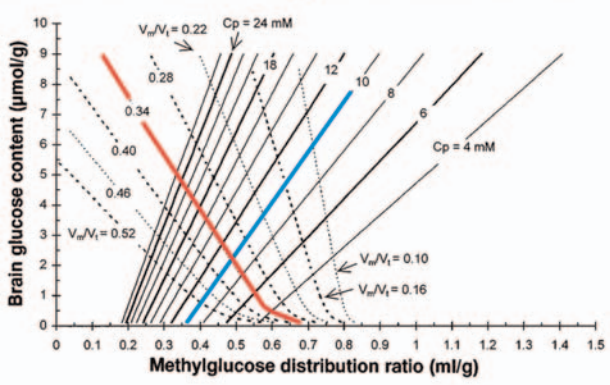

F. Malate-aspartate shuttle (MAS) and label trapping

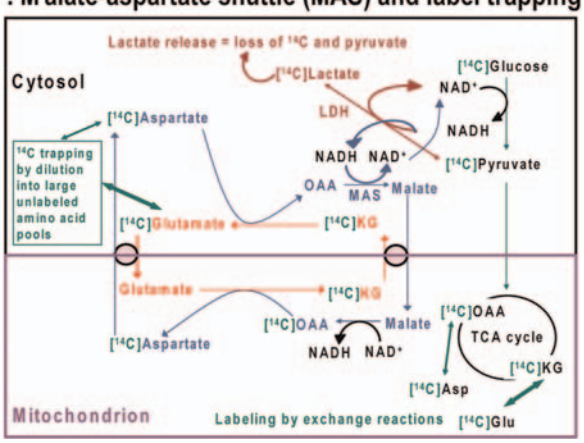

Figure 1 **Major pathways for glucose metabolism and methods to assay pathway rates**

(**A**) Colour coding identifies different aspects of the glycolytic, pentose-phosphate shunt pathway, oxidative pathway, biosynthetic routes associated with synthesis of various compounds including acetylcholine and amino acid neurotransmitters, and redox shuttling. Note that oxidizable alternative substrates (e.g., lactate, acetate, amino acids or ketone bodies) cannot satisfy many important upstream functions fulfilled by glucose metabolism. Reproduced with permission from: Dienel GA (2011) Brain lactate metabolism: the discoveries and the controversies. J Cereb Blood Flow Metab, doi:10.1038/jcbfm.2011.175. (**B**) Different aspects and pathways of glucose metabolism can be measured by local and global methods using glucose analogues or glucose labelled in specific carbon atoms. Oxidative pathways are assessed with many labelled precursors and by direct assay of oxygen consumption. Overall pathway relationships are assessed by comparison of oxygen and glucose or total carbohydrate utilization. Note that metabolite concentration changes reflect the difference between input and output, not flux through the pool. (**C**) Brain imaging and spectroscopic studies depend on signals derived from metabolic activity to calculate pathway rates and redox changes. Glucose analogues (DG, FDG and 2-NBDG) have limited metabolism, are trapped as the hexose 6-phosphate, and are used to assay the hexokinase step and calculate total glucose utilization rate. Incorporation of label from glucose into TCA cycle-derived amino acids enables calculation of oxidative rates and glutamate–glutamine cycling. Respiration is assayed by PET or MRS by assaying incorporation of labelled oxygen into water. Fluorescence of endogenous redox compounds (NADH, NADPH and FAD) are used to localize and quantify redox changes under different conditions. Lactate can be released to maintain redox balance or serve as an supplementary fuel when present in high concentrations. Reprinted from Basic Neurochemistry 8th Ed, Mary C. McKenna, Gerald A. Dienel, Ursula Sonnewald, Helle S. Waagepetersen, Arne Schousboe, Chapter 11 - Energy Metabolism of the Brain, 200–231, Copyright (2012), with permission from Elsevier. (**D**) Use of glucose analogues to measure glucose utilization rate requires knowledge of relative rates of transport and phosphorylation of the analogue and of glucose at various glucose concentrations. DG is transported into brain faster than glucose, whereas glucose is phosphorylated by hexokinase faster than DG and the capacity for glucose transport into brain exceeds the demand for glucose. The thickness of the arrows for transport and phosphorylation are scaled to represent relative values for the rate constants for uptake into brain from arterial plasma (K_1, K_1*, where the asterisk denotes the glucose analogue, that is, tracer [^{14}C]DG), efflux from brain to blood (k_2 and k_2*), and phosphorylation by hexokinase (k_3 and k_3*). The DG/Glc transport coefficient (K_1*/K_1) determined in rat brain ranges from approximately 1.3 to 1.5 (Cunningham and Cremer, 1981; Pardridge et al., 1982; Crane et al., 1983; Fuglsang et al., 1986; Hargreaves et al., 1986; Holden et al., 1991). The DG/Glc phosphorylation coefficient (k_3*/k_3) determined in rat brain ranges from approximately 0.22 to 0.38 (Sols and Crane, 1954; Cunningham and Cremer, 1981; Pardridge et al., 1982; Crane et al., 1983; Kapoor et al., 1989; Holden et al., 1991). The ratio of maximal transport (T_{max}) to maximal phosphorylation rate (V_{max}) for glucose is estimated to be approximately 3:1(Buschiazzo et al., 1970; Holden et al., 1991), and the ratio of T_{max} to CMR_{glc} is estimated to be in the range of approximately 1.5–2.5 (or higher) in rat and human brain (Cremer et al., 1981; Pardridge et al., 1982; Hargreaves et al., 1986; Cremer et al., 1988; Gruetter et al., 1998; Choi et al., 2001; de Graaf et al., 2001; Shestov et al., 2011), whether using the standard or reversible Michaelis–Menten kinetic model (Cunningham et al., 1986). The lumped constant of the [^{14}C]DG method takes these kinetic differences into account, with the net result that about two glucose molecules are phosphorylated for each DG phosphorylated (Sokoloff et al., 1977). This means that, with no correction for product loss, accumulation of metabolites of glucose should exceed DG-6-P accumulation by approximately 2-fold due to greater phosphorylation coefficient. Note that these relationships are not established for neurons, astrocytes, or oligodendrocytes or for 2-NBDG and 6-NBDG, the fluorescent glucose analogues, so differences among cell types cannot be interpreted (**E**) Contour map showing the steady-state brain-to-plasma distribution ratio of the non-metabolizable analogue 3-*O*-methylglucose and brain glucose concentration. When metabolic rate is constant and plasma glucose level held at different but fixed levels, the relationship between glucose level and methylglucose distribution ratio is illustrated by the dotted lines. The red line represents the normal resting rat brain for which V_{max}/T_{max} (ratio of maximal phosphorylation to maximal transport capacities) is 0.34. As plasma glucose concentration (Cp) is reduced, brain glucose level falls and the methylglucose distribution ratio rises, particularly at the lowest brain glucose levels. The continuous lines illustrate the relationships for varying demand at fixed plasma glucose level. When plasma glucose is fixed, for example, at 10 mmol/l (blue line) and metabolism is increased (i.e. V_{max}/T_{max} rises), brain glucose level and methylglucose distribution ratio both decrease (the blue line falls below the red line). In contrast, when metabolic rate is reduced (e.g., by anaesthesia), brain glucose level and methylglucose distribution ratio rise (blue line). Reproduced with permission from: Dienel GA, Cruz NF, Adachi K, Sokoloff L, Holden JE (1997), Determination of local brain glucose level with [^{14}C]methylglucose: effects of glucose supply and demand, Am J Physiol., 273(5 Pt 1):E839–49. The lumped constant for DG is relatively stable during normoglycaemia and hypoglycaemia, but rises when brain glucose level falls (Dienel et al., 1991; Holden et al., 1991); methylglucose distribution ratio can be used to determine brain glucose level and the appropriate value for the lumped constant (Dienel et al., 1997). Thus, supply and demand govern the relationship between glucose and non-metabolizable and metabolizable glucose analogues. Measured and theoretical values are in good agreement for deoxyglucose and methylglucose. Similar relationships are anticipated for the relationships between intracellular and extracellular glucose levels and metabolic demand. These relationships must also be established for the non-metabolizable fluorescent tracer 6-NBDG. The 'lumped constant' must be determined for 2-NBDG. (**F**) Pyruvate production and flux through the glycolytic pathway requires regeneration of NAD^+ from NADH by means of the MAS. This pathway also shuttles TCA cycle intermediates and amino acids across the mitochondrial membrane, and is essential for trafficking of labelled intermediates from mitochondria to the larger unlabelled cytoplasmic amino acid pools. Lactate production removes pyruvate as an oxidative substrate for that cell and reduces label mixing by replacing the MAS to regenerate NAD^+. Lactate oxidation requires the MAS activity (see **A**). Reprinted from Neurochem Int. 45(2-3), Dienel GA, Cruz NF, Nutrition during brain activation: does cell-to-cell lactate shuttling contribute significantly to sweet and sour food for thought? 321–513, Copyright (2004), with permission from Elsevier.

~0.05 mmol/l (Grossbard and Schimke, 1966; Bachelard, 1967; Wilson, 2003). Thus, when the intracellular glucose level exceeds 0.5 mmol/l, hexokinase is >90% saturated. When intracellular glucose level falls below this level, hexokinase becomes unsaturated and its rate falls progressively with decreasing glucose level. On the other hand, increasing the steady-state plasma and brain glucose levels from the normoglycaemic to hyperglycaemic range does not change local rates of glucose utilization in rat brain (Orzi et al., 1988; Schuier et al., 1990) or in isolated synaptosomes (Bradford et al., 1978). CMR_{glc} is governed by energy demand and by feedback and allosteric control mechanisms, *not* fuel supply, except when it becomes limiting during hypoglycaemia.

The glycolytic and oxidative pathways are tightly regulated at many enzymatic steps, including hexokinase, phosphofructokinase, pyruvate kinase and pyruvate, isocitrate and α-ketoglutarate dehydrogenases. Lowry (1975) emphasized the necessity for control mechanisms, using the following example: if the glycolytic enzymes could operate without constraint, metabolism of an unlimited glucose supply would

cause all available ATP into be converted into triose phosphate plus ADP and lactate, with the final result of no ATP and no P_i (inorganic phosphate) that is, complete energy failure and inability to phosphorylate glucose (Lowry, 1975). Metabolic regulation of pathway fluxes and tight linkage of glucose utilization to energy demand is essential. ADP controls respiration and becomes available as co-substrate for energy-producing phosphorylation reactions after its generation by ATP hydrolysis during brain work.

Branch point reactions

Glc-6-P (glucose 6-phosphate) has different fates (Figure 1A). Glc-6-P can be converted into fructose 6-phosphate and continue down the glycolytic pathway to pyruvate. This pathway also provides precursors for synthesis of other carbohydrates (e.g., mannose, galactose and glucosamine), amino acids (e.g., serine, glycine and alanine), pyruvate for oxidative metabolism, and lactate to regenerate NAD^+ when glycolytic rate exceeds oxidative rate or under hypoxic conditions. Glc-6-P can enter the pentose-phosphate shunt pathway to generate NADPH, which is necessary for the reactions involving glutathione for protection against oxidative stress (Dringen et al., 2007). Astrocytes synthesize glycogen from Glc-6-P to generate an energy store that is used during activation. Regulation of phosphofructokinase by many metabolites is the major rate-controlling step of glycolysis, and shifts in the levels of regulatory compounds can serve to coordinate the rates of different pathways (Lowry and Passonneau, 1966). Pyruvate is also a branch-point metabolite that can be converted into alanine, lactate, oxaloacetate or acetyl-CoA.

Most energy is derived from oxidative reactions

Oxygen diffuses from blood into brain cells and is consumed in the electron transport chain via cytochrome oxidase to generate water and CO_2. Brain is a highly oxidative organ, and oxidative metabolism of pyruvate provides most of the ATP in brain due to its high yield of ATP (~32 ATP/glucose, which is less than the theoretical maximum due to proton leakage across the mitochondrial membrane) compared with that from glycolysis (net of 2 ATP) and glycogenolysis (3 ATP per preformed glucose unit because ATP is not needed to generate Glc-6-P). Maximal ATP yield from glucose or glycogen and production of pyruvate for oxidation in the TCA cycle requires that reducing equivalents from NADH produced by the glycolytic pathway be transferred into the mitochondria via a redox shuttle system (Figure 1A). In normal resting brain, the ratio of the CMR_{O2} to that for glucose that is, CMR_{O2}/CMR_{glc} or the OGI (oxygen-glucose index; Figure 1B), is somewhat less than the theoretical maximum of 6.0 (i.e. $1\ glucose + 6O_2 \rightarrow 6CO_2 + 6H_2O$), probably due to biosynthesis and release of small amounts of lactate and other compounds from brain to blood.

Aerobic glycolysis

The notion of *aerobic* glycolysis arose from observations that lactate is formed in the presence of adequate levels and delivery of oxygen to brain, in contrast with hypoxia (reduced oxygen levels) and anoxia (no oxygen; *anaerobic* glycolysis) in which lactate formation rises markedly due to insufficient levels of oxygen to support oxidative metabolism. Aerobic glycolysis is evident in resting brain, which releases small amounts of lactate. In human brain local rates of glucose utilization exceed oxygen consumption to differing extents (Vaishnavi et al., 2010). During brain activation the CMR_{O2}/CMR_{glc} ratio usually falls (see below), indicating that non-oxidative metabolism of glucose increases disproportionately more than oxygen consumption. The rise in CMR_{O2} is generally modest compared with increases in blood flow and CMR_{glc}. Prevalence of aerobic glycolysis during brain activation is a perplexing phenomenon, because the brain's capacity to increase CMR_{O2} is high. For example, CMR_{O2} increases by almost 3-fold at seizure onset, but does not match the 4-fold rise in CMR_{glc}, and the CMR_{O2}/CMR_{glc} ratio falls (Table 1). The oxygen/glucose metabolic ratio increases after 1 h of continuous seizures when both rates exceed twice normal and can be maintained at this level for at least 2 h (Table 1). Why this excess respiratory capacity is not used during normal functional activation remains to be established.

Increased non-oxidative metabolism of glucose during brain activation may arise from preferential use of glycolysis-derived ATP to fuel ATPases involved in ion pumping, which would be associated with increased lactate production. However, other biosynthetic reactions may also contribute to disproportionate increases in glucose utilization. Increased pentose shunt pathway flux causes oxidative decarboxylation of glucose without oxygen consumption; the equivalent of one glucose molecule lost as CO_2 for every six that enter the pathway. The magnitude of the *mismatch* in the rise in CMR_{O2} and CMR_{glc} represents the maximal amount of lactate produced that is *not oxidized* in the region of interest and, therefore *not used as fuel* by activated cells. During brain activation, lactate can be released from brain to blood in greater quantities than at rest. In contrast, during exhaustive exercise when blood lactate levels rise markedly (increasing from ~0.5–1 to 15–20 mmol/l), lactate diffuses down its concentration gradient into the brain and is metabolized there as a supplementary fuel (Quistorff et al., 2008). A striking and unexplained observation is that CMR_{O2}/CMR_{glc} and the OCI (oxygen-carbohydrate index or $CMR_{O2}/CMR_{glc+0.5lac}$; Figure 1B) fall markedly even as lactate is taken up and oxidized in greater amounts during and after exhaustive exercise.

Metabolic signals are used to localize and quantify functional activity

Many analytical approaches employing labelled and unlabelled substrates are commonly used to measure rates of specific metabolic steps or pathway fluxes at global and local levels in brain *in vivo*, in brain slices, and in cultured cells (Figure 1B). In fact, signals generated from specific metabolic

Table 1 High capacity for up-regulation of CMR_{glc} and CMR_{O2} in adult rodent brain

Condition	Rate ($\mu mol \cdot g^{-1} \cdot min^{-1}$) CMR_{glc}	CMR_{O2}	Ratio CMR_{O2}/CMR_{glc}	Reference
Control (rat) – global assays	0.77	4.4	5.7	(Borgstrom et al., 1976)
Bicuculline-induced seizures				
Onset: first 1–2 min*†	3.17	12.2	3.8	
After 60 min of seizures	1.99	10.3	5.2	
Bicuculline-induced seizures*				(Meldrum and Nilsson, 1976)
For 1, 5, 10, 20, 60, or 120 min		~9 to 13		(Siesjo, 1978)
Control (rat)‡		4.60		(Blennow et al., 1979)
Homocysteine-induced seizures†		7.23		
Control (mouse) – forebrain	0.76			(Lowry et al., 1964)
Decapitation ischaemia†§	6.5			
Conscious rat‡		1.34		(Buchweitz-Milton and Weiss, 1990)
+Salbutamol (β-adrenoceptor agonist)‡		3.30		

* Rats were paralysed and mechanically ventilated while maintained on 70% N_2O/30%O_2 and seizures were induced by intravenous injection of bicuculline. Nitrous oxide does not affect CMR_{O2} (Carlsson et al., 1976). The rise in CMR_{glc} is within the range estimated in other studies by the increase in tissue lactate concentration (see references cited by Borgstrom et al., 1976). Notably, the 2–3-fold increase in CMR_{O2} was sustained for as long of 2 h of continuous seizures and was accompanied by increased rates of blood flow to brain that peaked at approximately 4–9-fold above control during the first minute and remained elevated by 3–4-fold at intervals up to 2 h.

† The authors state that the increase in brain lactate concentration during the initial 1–2 min approximately equals the decrease in levels of glucose plus glycogen. Note that lactate is retained in brain for a brief interval in the seizing brain of the intact animal, although some can be released to blood because living brain is an 'open system'. In contrast, the decapitated head is a 'closed system' with no influx or efflux.

‡ Units of reported values (ml of O_2/100 g per min) were converted into $\mu mol \cdot g^{-1} \cdot min^{-1}$ by dividing by 2.24.

§ Adult mice were decapitated into liquid nitrogen and rates calculated from changes in metabolite levels.

reactions and pathways are the basis for detection and quantification of changes in local functional activity because energy demand increases the flux of glucose into and through these pathways (Figure 1C). Metabolic assays can be designed to measure the overall, initial, intermediate or terminal steps of glucose metabolism (Figures 1B and 1C).

Metabolite concentration is the net result of its rates of formation and removal (Figure 1B), and, without additional information, it is not appropriate to interpret changes in concentration in terms of pathway flux. Comparison of percentage changes in metabolite concentrations can be problematic because equivalent percentage changes can correspond to large differences in concentration. For example, in carefully handled rats (to minimize sensory stimulation) the brain lactate level is approximately 0.5–1 μmol/g, whereas glucose is 2–3 μmol/g. Influx of glucose from blood occurs at the same rate as glucose utilization, whereas influx of lactate from blood is much lower. Fluxes through these pools are not equivalent, and percentage changes in metabolite levels only reveal an input–output mismatch. A 20% decrease in levels of extracellular lactate and glucose after an activating stimulus might be regarded as equivalent, but lactate level is much lower, so more glucose would have been consumed [see Tables 7 and 8 and related text in Dienel (2011)].

The rate of the first irreversible step of glycolysis, the hexokinase reaction, is assayed by means of intracellular trapping of phosphorylated products of radiolabelled or fluorescent glucose analogues (Figure 1C). Alternatively, glucose that has specific carbon atoms labelled with radioactive (^{11}C, ^{14}C, ^{3}H) or stable (^{13}C) isotopes is used to evaluate pathway rates and oxidative metabolism by means of label release in by-products (lactate, CO_2 or H_2O) or trapping of label in the large unlabelled amino acid pools derived from the TCA cycle (Figure 1C). Conversion of ^{15}O or ^{17}O-labelled oxygen into labelled water is used to calculate rates of oxidative metabolism by PET or MRS respectively. Fluorescence microscopy is used to localize and measure changes in the concentrations of endogenous compounds that participate in redox reactions and levels of various voltage- and pH-sensitive dyes in different cellular compartments. NAD(P)H and FAD fluorescence is used to evaluate the rate and magnitude of *relative concentration change* ($\Delta F/F$) (Figure 1C), but $\Delta F/F$ must be interpreted with caution because the levels of NADH or FAD are very low under resting conditions and fractional changes in concentration during activation are small (<5–10%). The relationships between pathway fluxes and incremental changes in metabolite or cofactor levels are not generally known, and they need to be established for conditions of interest. For example, it may not be appropriate to interpret a rise in lactate or NADH level as increased glycolysis. Lactate is probably in equilibrium with pyruvate, and its level would increase with a higher steady-state level of pyruvate. Increased mitochondrial NADH could arise from Ca^{2+}-mediated stimulation of mitochondrial dehydrogenases, causing NADH to be generated faster than it is oxidized in the electron transport chain.

To summarize, metabolic assays have established the major and supplementary fuels for living brain and regional heterogeneity of metabolic capacity and activity. *In vivo* assays at the cellular and subcellular level are restricted by temporal-spatial and technical limitations of current methods. Incomplete understanding of cellular neuroenergetics underlies controversies related to the contributions of specific pathways in different cell types during activating conditions, particularly with respect to lactate generation, oxidation and release.

Assay of the hexokinase reaction: deoxyglucose

Sols and Crane (1954) recognized that DG (2-deoxy-D-glucose) isolates the hexokinase reaction because the lack of the

2-hydroxy group prevents conversion of DG-6-P into fructose 6-phosphate and further metabolism via the glycolytic pathway. Two decades later, Sokoloff et al. (1977) developed the use of [^{14}C]DG and [^{18}F]FDG (2-fluoro-2-deoxy-D-glucose) (Reivich et al., 1979) for *in vivo* assays of local CMR_{glc} simultaneously in all regions of brain in living subjects. In brief, the quantitative method requires determination of time course of the specific activity of the tracer in arterial plasma (i.e. the ratio of the labelled compound to glucose at each timed interval) and the amount of total ^{14}C or ^{18}F in brain regions of interest at the end of the experimental interval. Rate constants for DG and glucose influx, efflux and phosphorylation determined in a separate group of subjects are used to estimate (i) time-activity integral (i.e. integrated specific activity or area under the curve) of the labelled precursor in brain from that measured in plasma and (ii) amount of unmetabolized precursor remaining in brain at the end of the experimental period; the level of unmetabolized DG is only approximately 5–10% of the total ^{14}C in brain at 45 min, but is a higher fraction of the total at early times after pulse labelling (Sokoloff et al., 1977). Uncertainties in the true values of rate constants have a negligible effect in routine 30–45 min assays, but they do have a large influence on estimates of precursor level in shorter assays with labelled DG and glucose (Adachi et al., 1995) and on the tissue integrated specific activity (see Figure 10 in Sokoloff, 1986). For this reason, the results of 5–10 min *in vivo* autoradiographic assays with either tracer may not be as accurate as desired (Brondsted and Gjedde, 1988; Lear and Ackermann, 1988; Adachi et al., 1995), but levels of labelled precursor and products can be directly measured in tissue extracts to avoid errors in their estimates. Also, the plasma time-activity integral can be used to calculate the minimal metabolic rate (at short experimental times the plasma integral exceeds that in brain due to restricted tracer entry into brain across the blood–brain barrier; Sokoloff et al., 1977). The 'lumped constant' of the DG method is the correction factor that accounts for differences in rates of transport and phosphorylation of glucose and DG; it converts the rate of DG phosphorylation into glucose phosphorylation. DG is transported ~1.4 times faster than glucose, whereas glucose is phosphorylated ~2.6–4.5-fold faster than DG (Figure 1D). The measured value of the lumped constant is 0.48, which indicates that about two glucose molecules are phosphorylated for each DG-6-P formed in tissue. CMR_{glc} is calculated by dividing the quantity of DG-6-P formed during the experimental interval by the product of the lumped constant and integrated specific activity in brain (Sokoloff et al., 1977). At steady state, the rate of each reaction in a multi-step pathway is the same as the pathway flux, so the *rate of the hexokinase step represents total glucose utilization*. However, hexokinase assays do not provide information about downstream metabolism of Glc-6-P. The principles of the DG method are discussed in more detail below because the use of fluorescent glucose analogues to assay rates of glucose transport or phosphorylation at a cellular level requires the same detailed studies that were used to establish and validate the DG method in brain.

Product stability

Glucose-6-phosphatase activity is detectable in extracts of brain tissue and brain cells, but this activity has negligible effects on DG-6-P accumulation (Nelson et al., 1986; Dienel et al., 1988; Gotoh et al., 2000). Some DG-6-P is converted into other compounds (e.g., DG-1-P, DG-1,6-P_2, 6-phosphodeoxygluconate; Dienel and Cruz, 1993; Dienel et al., 1993) and incorporated into glycogen (Nelson et al., 1984), but all of these labelled compounds would be retained in cells where formed. With long experimental times (>60 min), there is slow loss of label from brain that is commonly ascribed to phosphatase activity. However, this loss could arise from entry of the acid-labile DG-1-P (Dienel et al., 1990) or its metabolites (e.g., glycosidic derivatives at C1, such as UDP-DG, DG-glycogen, DG-glycolipid or DG-glycoprotein) into acidic compartments (e.g., lysosomes), thereby generating DG that can diffuse from brain and give the appearance of phosphatase activity. DG-6-P is sufficiently stable to allow a 30–45 min experimental period, thereby minimizing the amount of unmetabolized DG in tissue at the end of the assay interval, as well as effects of uncertainties in true values of the rate constants.

Lumped constant stability

The lumped constant has two components, lambda and phosphorylation coefficient. The factor lambda is the ratio of the distribution space for DG to that for glucose at steady state (i.e. $[K^*_1/(k^*_2+k^*_3)]/[K_1/(k_2+k_3)]$), where K_1, k_2 and k_3 are the rate constants for influx efflux, and phosphorylation respectively and the asterisks denote DG (see Figure 1D). The phosphorylation coefficient is the ratio of the rate of phosphorylation of DG to that of glucose (Figure 1D) by Type I hexokinase, the predominant brain isoform (Grossbard and Schimke, 1966; Wilson, 2003). Lambda is the component of the lumped constant that is sensitive to glucose concentration due to the greater relative phosphorylation by hexokinase compared with carrier-mediated transport for glucose than for DG (Figure 1D). Lambda (and the lumped constant) is relatively stable within the normo- and hyper-glycaemic range, but it increases progressively as brain tissue glucose level falls below ~1 μmol/g due to reduced competition of DG with glucose for phosphorylation (Orzi et al., 1988; Schuier et al., 1990; Dienel et al., 1991; Holden et al., 1991). This rise must be taken into account when calculating rates of glucose utilization from DG phosphorylation during hypoglycaemia. Also, if the hexokinase isoform changes, the phosphorylation coefficient must be adjusted, for example, for brain cells with glucokinase (Roncero et al., 2000) and tumours with different hexokinase isoforms (Kapoor et al., 1989). Values for the lumped constant are relatively stable under normal physiological conditions and under anaesthesia, but can differ under pathophysiological states and with species (Sokoloff, 1986).

Use of methylglucose to determine glucose level and local lumped constant

The steady-state brain/plasma distribution ratio for the non-metabolizable analogue 3-*O*-methylglucose can be used to determine local brain glucose concentration, from which the value of the lumped constant can be determined (Dienel et al., 1991, 1997; Holden et al., 1991). The contour map in Figure 1(E) illustrates the complex interrelationships between the methylglucose distribution ratio and brain glucose concentration as glucose supply and demand is varied. For example, when the plasma glucose level of conscious, resting rats is clamped at different concentrations, the distribution ratio for methylglucose rises as brain glucose levels falls, as illustrated by the red line in Figure 1(E) that corresponds to the normal metabolism/transport ratio, $V_m/V_t=0.34$. When CMR_{glc} is either increased (raise V_m/V_t) or decreased (reduce V_m/V_t), changes in steady-state plasma glucose concentration produce different glucose–methylglucose relationships (dotted lines above and below the red line, Figure 1E). For example, pentobarbital anaesthesia reduces $CMR_{glc,}$ and the glucose–methylglucose relationship falls along the dotted contour line $V_m/V_t=0.22$ (Dienel et al., 1997). A different set of relationships is obtained when plasma glucose level is kept constant and glucose utilization rate is varied (continuous lines, Figure 1E). For example, when plasma glucose is 10 mmol/l (blue line, Figure 1E), increasing metabolic rate causes both the brain glucose level and methylglucose distribution ratio to fall, whereas reducing CMR_{glc} increases glucose level and methylglucose distribution ratio. A different contour line is obtained for each plasma glucose concentration as demand is varied (continuous lines to the left and right of the blue line, Figure 1E). The complex relationships between glucose and a non-metabolizable analogue that competes with glucose for influx and efflux are well-described by Michaelis–Menten kinetics.

Cellular basis of glucose utilization using glucose analogues: DG, 2-NBDG {2-[*N*-(7-nitrobenz-2-oxa-1,3-diazol-4-yl)amino]-2-deoxyglucose} and 6-NBDG {2-[*N*-(7-nitrobenz-2-oxa-1,3-diazol-4-yl)amino]-6-deoxyglucose}

Deoxyglucose

The cellular and subcellular contributions to neuroenergetics have been of long-standing interest since the inception of the DG method. For example, an early study by Sharp (1976) used [^{3}H]DG and frozen emulsion-based autoradiography to demonstrate that grain counts in neuronal perikarya were similar to those in neurophil in four brain structures in resting rats and that grain densities increased to a similar extent in perikarya and neuropil during swimming. High-resolution studies using [^{3}H]DG revealed grain accumulation over single cell bodies, some of which contained tyrosine hydroxylase (Hokfelt et al., 1983, 1984; Duncan et al., 1987). Quantitative *in vivo* cellular assays with [^{3}H- or ^{14}C]DG are not yet possible due to high loss of DG-6-P caused by membrane damage during immunoassays to identify cell types. The study with the least loss of DG-6-P (~50%) during tissue processing reported similar amounts of [^{14}C]DG-6-P in neuronal and astrocytic soma during *resting* conditions (Nehlig et al., 2004). This is a major advance, but interpretation of cellular metabolic activities is limited by label quantification only in cell bodies that may have much lower CMR_{glc} than their synapse-associated processes, particularly during brain activation. Also, incorporation of DG into glycogen, glycoprotein and glycolipid would result in labelled metabolites that are resistant to washout during fixation and processing to identify cell types. Low-level but preferential labelling of glycogen in astrocytes (Nelson et al., 1984) or other compounds in neurons could bias interpretation of the cellular basis of metabolic activity when there is high washout.

Application of DG methodology to estimate glucose utilization rates at the cellular level requires knowledge of lumped constant for each cell type to convert cellular DG-6-P concentration (sometimes represented by grain counts) into equivalent units of glucose phosphorylation. Transport differences between neurons, astrocytes, oligodendrocytes and microglia may influence the value of the factor lambda, whereas the phosphorylation coefficient would be the same for the cells containing type I hexokinase. The relationship between transport and metabolism in each cell type is a key factor. The rate of change of intracellular concentration of glucose or a glucose analogue can be expressed as $dCe/dt=K_1Cp-k_2Ce-k_3Ce$, where Cp and Ce represent extracellular and intracellular hexose concentrations respectively analogous to plasma and overall brain tissue levels and the rate constants illustrated in Figure 1(D). At steady state, the rate of change is zero and $K_1Cp=Ce(k_2+k_3)$ and the intracellular/extracellular distribution ratio, $Ce/Cp=K_1/(k_2+k_3)$. The factor lambda for a given cell type is the ratio of the distribution space for DG to that for glucose, and the glucose dependence of this factor would arise from relative transport-phosphorylation rate constants in each cell type, as discussed above. The rate constants can be influenced by the GLUT (glucose transporter) isoform, number, and catalytic activity and the amount of hexokinase; these values could be expected to vary with developmental stage and tissue culture condition. Cell-type differences in hexose transport can be anticipated because catalytic turnover rate per molecule of transporter (k_{cat}) for the neuronal GLUT3 for glucose is about six times higher than the astrocytic GLUT1 (Simpson et al., 2007). As with the intact brain, relationships between the factor lambda and extracellular glucose concentration need to be established for each cell type. To the author's knowledge, values for the lumped constant for brain cell types have not been published.

2-NBDG and 6-NBDG

Two fluorescent glucose analogues have been used for real-time assays of transport (6-NBDG) or phosphorylation (2-NBDG) in individual cells *in vitro* and *in vivo*. 2-NBDG is used to assay the hexokinase reaction, whereas 6-NBDG cannot be

phosphorylated, and it is used to assay transport. Little is known about 2-NBDG-6-P stability and the intracellular distribution, diffusion, or binding of 2-NBDG, 2-NBDG-6-P, or 6-NBDG to intracellular structures or compartments in brain cells. The larger, more-hydrophobic fluorescent moiety of NBDG may alter its distribution compared with glucose or DG. For example, 6-NBDG binds to haemoglobin and accumulates in erythrocytes but not erythrocyte ghosts, suggesting that protein binding can influence intracellular accumulation (Speizer et al., 1985). In *Escherichia coli* 2-NBDG is phosphorylated, but is subsequently converted into an unidentified non-fluorescent compound (Yoshioka et al., 1996). Notably, 6-NBDG transport by GLUT1 at 24°C is 2000–3000-fold slower than glucose and 3-O-methylglucose transport at 4°C (see discussion in Cloherty et al., 1995; Mangia et al., 2009a). The brain/plasma or intracellular-to-extracellular distribution ratio for 6-NBDG will depend on glucose supply and demand, but a different contour map compared with that for methylglucose (Figure 1E) is anticipated.

Intracellular levels of 6-NBDG or 2-NBDG-6-P in neurons and astrocytes cannot be compared and interpreted in terms of cellular glucose transport or utilization without detailed knowledge of their relationships to glucose supply and demand, as determined for DG and methylglucose. Intracellular levels of 6-NBDG report glucose concentration at steady state, not glucose phosphorylation rate, as incorrectly interpreted by Pellerin and Magistretti (2011) when discussing the data of Chuquet et al. (2010). Chuquet et al. (2010) reported a greater rise in 6-NBDG level in astrocytes compared with neurons during whisker stimulation of urethane-anaesthetized rats, and concluded that glucose is primarily taken up into astrocytes, reflecting increased metabolic activity in the astrocytic network. An alternative explanation for this finding is *reduced* utilization of glucose in astrocytes, causing intracellular glucose level to rise along with the 6-NBDG intracellular-to-extracellular ratio, as observed for methylglucose (blue line, Figure 1E). Reduced astrocytic glucose utilization could arise from glycogenolysis, increased level of Glc-6-P, and greater inhibition of hexokinase, as predicted by metabolic modelling (DiNuzzo et al., 2010b). To sum up, interpretation of data obtained with DG, 2-NBDG and 6-NBDG in terms of glucose transport, concentration or utilization at the cellular level requires detailed knowledge of and consideration of supply-demand relationships as functions of glucose level in each cell type. Different relationships are anticipated for assays in cultured cells compared with adult brain *in vivo* due to maturational changes in transporters and enzymes. Comparisons of results obtained in immature cells or tissue need to be validated as equivalent to findings in the same cell types in adult tissue.

Assay of specific pathways and cell–cell interactions with labelled glucose

Variously-labelled [^{14}C]glucose has been used for some 50 years to evaluate glucose metabolism *in vivo* and *in vitro*, and ^{13}C-labelled glucose has been extremely useful for selective *in vivo* and *in vitro* assays of specific pathways (Figure 1). Differential labelling by C1- and C6-labelled glucose is used to quantify the pentose shunt pathway because C1 is decarboxylated. C2-labelled glucose is used to assay pyruvate carboxylase, and C3- or C4-labelled glucose is used to measure the PDH (pyruvate dehydrogenase) reaction that releases these carbon atoms as CO_2. Retention of label derived from C6 of glucose is highest compared with other labelling positions because decarboxylation of C6 requires three turns of the TCA cycle; label from all positions, including C6, is, however, lost when lactate is released. *In vivo* ^{13}C-MRS assays of incorporation of ^{13}C from [1-, 2-, or 6-^{13}C]glucose or from [^{13}C]acetate into glutamate and glutamine in conjunction with metabolic modelling are used to calculate rates of pyruvate carboxylation, glucose oxidation, glutamate/glutamine cycling and GABA (γ-aminobutyric acid) turnover (Figure 1C; see for example, Henry et al., 2006; Rothman et al., 2011). ^{13}C-labelled glucose has the advantage that the fates of individual carbon atoms can be tracked *in vivo*. Emphasis has been placed on the oxidative pathways from which label is incorporated into TCA cycle-derived amino acids and trapped by dilution in large unlabelled amino acid pools. A lumped constant correction factor is not required because the unlabelled and ^{13}C- or ^{14}C-labelled precursors have the same kinetics. Labelled glucose does, however, have the disadvantage that many of its metabolites are diffusible (e.g., lactate, amino acids and CO_2) and label can be quickly lost from activated tissue in substantial quantities, causing reduced trapping of labelled metabolites and underestimation of metabolic activation. Limitations of MRS studies include use of anaesthesia to immobilize experimental animals, low sensitivity to detect compounds present in small amounts and *no information about the upstream fate of glucose* is gained from assays of oxidative pathways. Parallel assays of total CMR_{glc} with deoxyglucose and of the oxidative pathways with labelled glucose are essential for a more complete understanding of metabolic activity during brain activation (Figure 1C).

MAS (malate-aspartate shuttle)

The MAS is the major redox shuttle in brain for regeneration of cytoplasmic NAD^+ (McKenna et al., 2006; Pardo et al., 2006). This shuttle also has a key role in metabolic assays with labelled glucose and lactate because it transfers label from mitochondria to cytosol, where it is diluted in the larger unlabelled amino acid pools (Figure 1F). Exit of labelled α-ketoglutarate and oxaloacetate from the TCA cycle, their transamination to glutamate and aspartate and participation of these compounds in the MAS provide a mechanism for label 'trapping'. Reduced trafficking of compounds between mitochondria and cytosol via the MAS [e.g., when glycolytic flux exceeds MAS or oxidation rates, during hypoxia, or during mitochondrial calcium overload (see below)] stimulate lactate production and reduce pyruvate availability as an

oxidative fuel. This causes less retention of glucose-derived label, due, in part, to (i) release of labelled lactate to blood and (ii) longer retention of labelled metabolites in the mitochondria, which may enhance the loss of label as $^{14}CO_2$ due to increased cycling of compounds within the TCA cycle and greater exposure to decarboxylation reactions (Figures 1A–1F). Utilization of lactate as an oxidative fuel also requires stoichiometric MAS activity to oxidize the NADH produced in cytoplasm by LDH (Figure 1A).

Inhibition of the MAS during neuronal activation by calcium influx into mitochondria has been proposed as a mechanism for increased neuronal lactate production during brain stimulation (Contreras and Satrustegui, 2009) and for the inability of neurons to metabolize extracellular lactate in place of glucose to satisfy the ATP demands associated with neuronal depolarization (Bak et al., 2009, 2012). Small Ca^{2+} signals transmitted to neuronal mitochondria stimulate MAS shuttle activity (Pardo et al., 2006), whereas Ca^{2+} entry through the Ca^{2+} uniporter activates the mitochondrial pyruvate, isocitrate and α-ketoglutarate dehydrogenases and inhibits the shuttle. The MAS and TCA cycle share α-ketoglutarate as a common substrate, and retention of α-ketoglutarate within the TCA cycle reduces its efflux via the oxoglutarate carrier, thereby impairing MAS activity; efflux of Ca^{2+} from the mitochondria restores shuttle activity (Contreras and Satrustegui, 2009). The point at which *in vivo* MAS activity is reduced by Ca^{2+} remains to be established, but these findings provide a mechanistic explanation for the notion that (i) neuronal lactate oxidation may be optimal under resting and less-active conditions and (ii) neurons may generate and release lactate during stronger activation if MAS flux is lower than glycolytic rate (Bak et al., 2012). Reduced MAS activity due to inhibitor treatment impairs glucose oxidation in cultured neurons and astrocytes (Fitzpatrick et al., 1988), brain slices (Fitzpatrick et al., 1983) and synaptosomes (Kauppinen et al., 1987; Cheeseman and Clark, 1988) and lactate oxidation in synaptosomes (McKenna et al., 1993). These findings support modelling studies that predict greater glucose utilization by neurons compared with astrocytes, and shuttling of lactate from neurons (Simpson et al., 2007; Mangia et al., 2009a; DiNuzzo et al., 2010a, 2010b; Mangia et al., 2011).

Summary

DG and FDG are extremely useful for quantitative assays of the hexokinase reaction in living brain. The influence of rate constants on calculated CMR_{glc} is low with the routine 30–45 min DG method. The value of the lumped constant, the factor that converts DG phosphorylation into glucose phosphorylation, is relatively stable when glucose levels are within or above the normoglycaemic range, but appropriate corrections must be made when assays are carried out under hypoglycaemic or other abnormal conditions. Cellular assays with DG, 2-NBDG or 6-NBDG require detailed knowledge of glucose supply and demand relationships before these analogues can be used to determine and compare glucose levels and utilization rates in astrocytes and neurons. ^{13}C-MRS assays of substrate metabolism in conjunction with metabolic modelling have the unique advantage that incorporation of individual carbon atoms of various substrates into metabolites of interest can be evaluated in living brain. Detailed understanding of brain activation requires parallel assays of all substrates consumed by brain, fluxes in glycolytic, pentose shunt and oxidative pathways and quantification of products released from brain.

METABOLIC INFRASTRUCTURE OF BRAIN: CAPACITY EXCEEDS DEMAND

Development of adult capabilities for metabolism, transport and fuel use

Many model systems are used to study brain function and cell–cell interactions, and it is essential to take into account the transport and metabolic characteristics of the model compared with normal adult brain. Brain cells have very low levels of enzymes and transporters prior to birth, and large (>5-fold) developmental changes occur in rats during the 30-day postnatal interval for glycolytic (Figure 2A) and mitochondrial (Figure 2B) enzymes, as well as for glucose and MCTs (monocarboxylic acid transporters) (Figure 2C). Myelination in rat brain also peaks at about age 21 days. Suckling rats use lactate and ketone bodies along with glucose as a significant fuel (Figure 2D), and after weaning (age ~20 days) there are substantial increases and decreases in activities or amounts of cellular components. Mitochondrial capacity for β-hydroxybutyrate oxidation is highest at 20–22 days, and falls thereafter (Figure 2E-a) along with β-hydroxybutyrate dehydrogenase activity and endothelial MCT levels (Cremer, 1982; Nehlig and Pereira de Vasconcelos, 1993; Vannucci and Simpson, 2003). At 20 days of age, PDH activity is about half that of the adult (Figure 2B), and during the next 10 days, the capacity for pyruvate oxidation rises ~60% (Figure 2E–b). Figure 2 emphasizes large differences for glycolytic, oxidative and transport *capacities* in pre-natal brain cells, early postnatal, weanling and adult tissue, and does not take into account the effects of concomitant development of the neurotransmitter systems that govern cellular activities and neuroenergetics.

Enzymatic capacities greatly exceed glucose utilization rate *in vivo*

The maximal velocity of an enzyme (V_{max}) is proportional to protein amount when assayed under optimal conditions. In normal adult brain, activities of different metabolic enzymes vary enormously, and most greatly exceed the fluxes through

A. Development of glycolytic enzymes

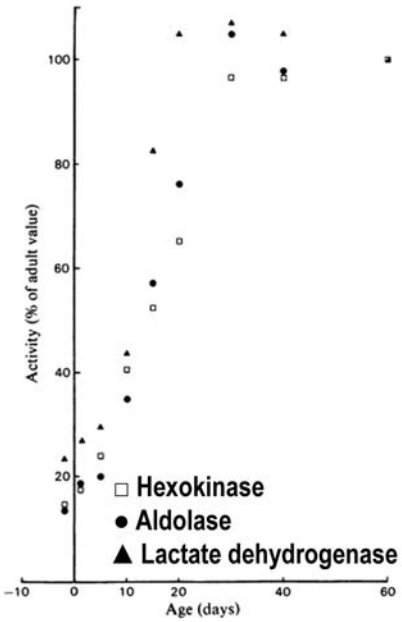

B. Development of mitochondrial enzymes

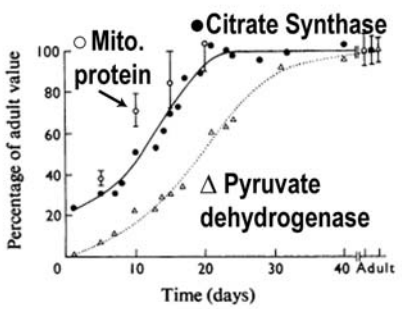

C. Regional glucose (GLUT) and monocarboxylic acid (MCT) transporter developmental patterns

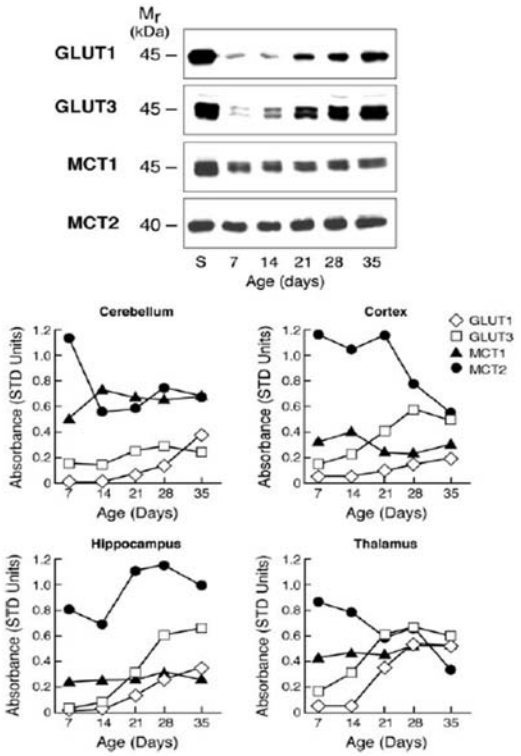

D. Developmental changes in fuel utilization

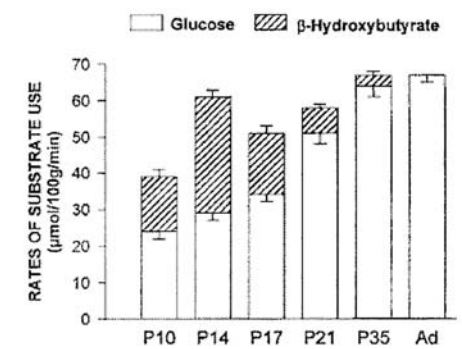

E. Developmental changes in fuel oxidation

a. β-Hydroxybutyrate + malate

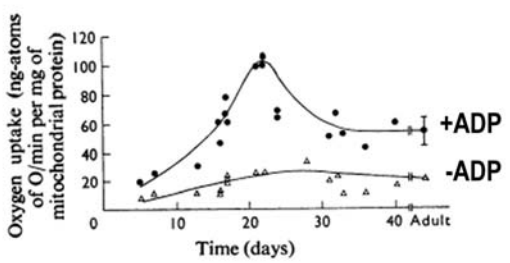

b. Pyruvate + malate

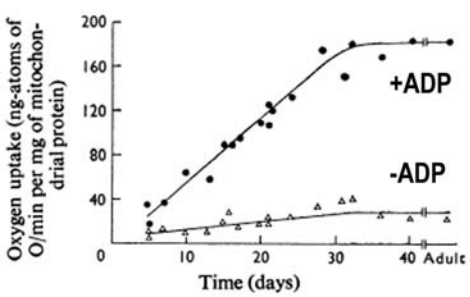

Figure 2 **Postnatal development of enzymatic and transporter capacities and fuel utilization in rat brain**

Brain maturation involves an enormous increase in metabolic capacity along with selective changes in specific enzymes, transporters and fuel utilization during postnatal development that vary temporally with brain region and mammalian species (Baquer et al., 1975; Cremer et al., 1975; Cremer, 1982; Nehlig et al., 1988; Clark et al., 1993; Nehlig and Pereira de Vasconcelos, 1993). Representative patterns in different pathways are illustrated. (**A**) Comparative development of three glycolytic enzymes in rat cerebral cortex, expressed as a percentage of respective values in the 50-day-old adult. Glycolytic capacity increases approximately 5-fold from birth to adult, with large changes after 20 days (approximate age of weaning). Leong SF, Clark JB. (1984), Regional enzyme development in rat brain. Enzymes of energy metabolism, Biochem J;218(1):139–45 copyright the Biochemical Society. (**B**) TCA cycle enzymes show different developmental patterns, with the postnatal rise in PDH lagging that of citrate synthase and mitochondrial protein. Note that PDH activity is a negligible percent of adult value at birth, and by day 20 it is only 60% of the adult value. Land JM, Booth RF, Berger R, Clark JB (1977), Development of mitochondrial energy metabolism in rat brain., Biochem J 164:339–348 copyright the Biochemical Society. (**C**) Nutrient transporters in the vascular-free membranes of different brain regions have different developmental profiles. Western blots are shown for hippocampus (top) and patterns in four brain regions are shown graphically (bottom). The patterns for the glucose transporter in astrocytes (GLUT1) and neurons (GLUT3) rise in parallel, with larger increments for GLUT3. The MCTs in astrocytes (MCT1) and neurons (MCT2) also show distinct regional patterns, particularly the decrease in MCT2 level in cerebral cortex after the age of 21 days. Figure previously published in Am J Physiol Endocrinol Metab, Vannucci and Simpson, 285, 2003, and pp. 339–348 ©The American Physiological Society (APS). (**D**) Ketone bodies, for example, β-hydroxybutyrate, are a significant brain fuel during the postnatal (P) suckling period, and they continue to be used along with glucose until the age of 35 days in the rat, after which glucose is the major fuel. Glucose and total fuel utilization rise during postnatal development, but the proportions vary with age. After weaning the MCT at the blood–brain barrier is reduced markedly, diminishing ketone body and lactate transport capacity by approximately 10-fold in adult (Ad) compared with immature rats (Cremer et al., 1979). This figure was published in: Nehlig A. Cerebral energy metabolism, glucose transport and blood flow: changes with maturation and adaptation to hypoglycaemia. Diabetes Metab. 1997;23(1):18-29. Copyright© 1997 Elsevier Masson SAS. All rights reserved. (**E**) (a) Maximal respiration rate with β-hydroxybutyrate as fuel is attained at approximately 20 days and requires the presence of ADP as co-substrate for ATP synthesis. Note that ketone body utilization falls (see **D**) before attaining maximal capacity, which is lower in adult rat brain. (b) Pyruvate-supported respiration progressively rises with age, paralleling the rise in PDH activity (see **B**). At 20 days the rate is approximately 70% that of the adult value. Land JM, Booth RF, Berger R, Clark JB (1977), Development of mitochondrial energy metabolism in rat brain., Biochem J 164:339–348 copyright the Biochemical Society.

their respective pathways (McIlwain and Bachelard, 1985). Enzyme amount or maximal activity determines capacity but does not reflect actual *in vivo* flux. For example, glycolytic flux is $<5\%$ of V_{max} of hexokinase assayed *in vitro*, due, in part, to feedback inhibition of hexokinase by Glc-6-P (Lowry and Passonneau, 1964; Bachelard, 1967; McIlwain and Bachelard, 1969). Thus, brain has the capacity to increase the flow of glucose through the hexokinase step by ~20-fold, well above the 4–8.5-fold increases in CMR_{glc} observed during an energy crisis caused by seizures or ischaemia (Table 1). Relative hexokinase activity (that was normalized by the original authors to that of fumarase, a TCA cycle enzyme) is similar in whole brain, astrocytes, neurons and synaptosomes isolated from adult brain, whereas it is much lower in oligodendroglia (Figure 3A). Maximal activities of hexokinase, phosphofructokinase and cytochrome oxidase all tend to be higher in structures with higher CMR_{glc}, but the correlations between CMR_{glc} and enzyme amount are poor (Figure 3B). Brain has a very high oxidative capacity, and 2.5–3-fold increases in CMR_{O2} can be sustained for as long as 2 h during seizures (Table 1). A large excess respiratory capacity has also been documented in studies of glucose-supported oxygen consumption in synaptosomes isolated from adult rodents (Choi et al., 2009, 2011; Nicholls, 2009), and many laboratories have demonstrated up-regulation of glycolytic and oxidative fluxes in cultured neurons and by as much as 5–10-fold in synaptosomes (reviewed in Dienel, 2011). Pathway fluxes can be regulated by feedback inhibition, allosteric interactions and post-translational modification of enzymes. Neurons are capable of increasing glucose utilization, contrary to claims made by others (Herrero-Mendez et al., 2009; Jolivet et al., 2010; Pellerin and Magistretti, 2011).

Up- or down-regulation of enzyme or transporter levels that sometimes accompany altered physiological states in normal brain may tend to maintain excess capacity relative to actual flux. In fact, bioengineering studies have shown that glycolytic flux does not change when rate-limiting enzymes are up-regulated manyfold (Schaaff et al., 1989; Urbano et al., 2000), indicating that metabolic flux regulation prevails over enzyme protein amount. Also, changes in mRNA and protein levels need not be predictive of functional flux changes (e.g., Koehler-Stec et al., 2000; Nehlig et al., 2006). Due to excess capacity, adaptive changes in enzyme or transporter amount may not even be required to maintain the elevated fluxes in the altered states of normal brain when up-regulated. However, there may be exceptions to the notion of excess capacity, particularly during abnormal or pathophysiological conditions may damage enzymes and alter relationships between enzyme amount, enzyme activity, and reaction rates.

Comparison of (i) uneven distribution of selected glycolytic and oxidative enzymes with the corresponding rates of glucose utilization in laminated regions of hippocampus, olfactory bulb and olfactory cortex (Borowsky and Collins, 1989) and (ii) consideration of results of other studies of local metabolic activities led Collins (1997) to coin the term 'red brain–white brain'. He concluded the following: "Studies of the metabolic architecture of brain have revealed parallels with the organization of metabolism in 'red and white' muscle. First, the oxidative and glycolytic enzyme profile of a particular brain area is heavily influenced by the type of synaptic input. Secondly, oxidative enzymes are highest in areas that are tonically stimulated by ongoing physiological activity. Thirdly, brief phasic activity stimulates glycolytic metabolism more than oxidative metabolism. Fourthly, the relative balance of oxidative and glycolytic enzymes in any one area is a reflection of the history of the use of that area. Functional zones are continuously remodelling their metabolic architecture in

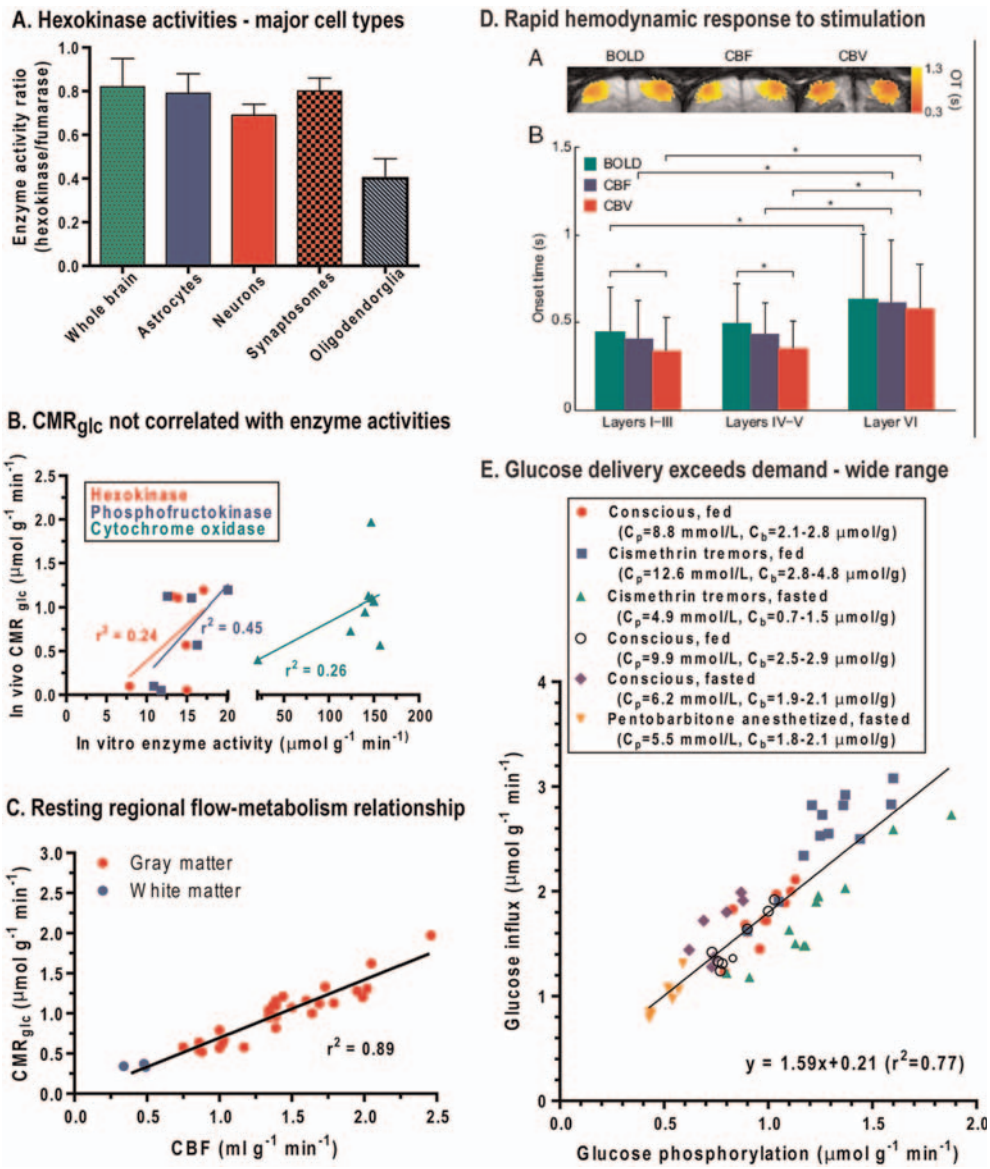

Figure 3 **Enzyme activities, glucose utilization rate and fuel supply–demand relationships in adult rat brain**
(**A**) Hexokinase activities relative to those of fumarase in whole rat brain homogenate and in isolated synaptosomes and major cell types. Data from Snyder and Wilson (1983). (**B**) Local glucose utilization rates (CMR_{glc}) tend to be higher in brain structures with higher enzyme amounts (i.e. maximal *in vitro* activity assayed under optimal conditions), but the correlations are poor. CMR_{glc} values are from Sokoloff et al. (1977), hexokinase and phosphofructokinase activities from Leong et al. (1981) and cytochrome oxidase activities from Hevner et al. (1995). Each point represents a different brain structure. (**C**) Local rates of glucose utilization are linearly related to local rates of CBF in conscious resting rat brain. Each point represents a different brain structure. Plotted from data of Sokoloff et al. (1977) and Sakurada et al. (1978) and reproduced from This figure was published in: From Molecules to Networks. An Introduction to Cellular and Molecular Neuroscience, 2 Edition, Byrne JH, Roberts JL (eds), Dienel GA, Energy Metabolism in the Brain, pp 49-110, Copyright Elsevier (2009). (**D**) Mean OT (onset time) for the BOLD, CBF and CBV (cerebral blood volume) changes in layers of cerebral cortex after bilateral electrical stimulus to both forelimbs of α-chloralose-anaesthetized rats. OTs varied but were very fast, between 340 and 610 ms. Re-printed with permission from: Hirano Y, Stefanovic B, Silva AC, (2011), Spatiotemporal evolution of the functional magnetic resonance imaging response to ultrashort stimuli, J Neurosci, 31:1440-1447. (**E**) Unidirectional glucose influx and glucose phosphorylation were assayed simultaneously in different regions of rat brain of conscious or anaesthetized, fed or fasted rats with or without cismethrin-induced tremors (plotted from data of Cremer et al., 1983; Hargreaves et al., 1986). Glucose delivery was approximately 160% that of CMR_{glc} over a wide range of arterial plasma (C_p) and brain (C_b) glucose concentrations and CMR_{glc}.

response to changing needs." Evaluation of local and cellular oxidative and non-oxidative capacities and rates needs to take into account the characteristics of afferent and efferent pathways of interest, previous and current activity, functions of stations of various pathways and relationships to blood flow (Gjedde and Marrett, 2001; Gjedde et al., 2002).

Blood flow–fuel delivery–metabolism relationships *in vivo*: glucose supply exceeds demand

Flow–metabolism

Adult brain depends on continuous delivery of glucose and oxygen by the blood, and inadequate blood levels of either substrate or interruption of blood flow leads to impaired brain function. Local rates of blood flow [CBF (cerebral blood flow)] and CMR_{glc} are highly correlated in resting animals over a 5-fold range, with lowest flow and metabolic rates in white matter and heterogeneously higher rates in grey matter structures (Figure 3C). Regional GLUT1 levels and capillary density are highly correlated with CMR_{glc} (Zeller et al., 1997), and GLUT1 and MCT1 levels are also highly correlated (Maurer et al., 2004). Based on methylglucose distribution, glucose levels are relatively uniform throughout the brain despite the heterogeneous metabolic rate (Sokoloff et al., 1977), and similar conclusions were drawn from MRS studies of brain glucose level (Pfeuffer et al., 2000). The capacity for fuel delivery (i.e. capillary density, blood flow rate, transporter levels) is closely related to metabolic rate at a local level.

Oxygen delivery

One of the hallmarks of brain activation is a rapid increase in the rate of blood flow to activated structures (Attwell et al., 2010; Paulson et al., 2010). BOLD (blood oxygen-level dependent)-fMRI signal increases are registered within seconds after stimulus onset, with a somewhat longer time-to-peak intervals, depending on the stimulus paradigm and microanatomy (e.g. layers of cerebral cortex) of the structures of interest (Shen et al., 2008; Hirano et al., 2011). Haemodynamic responses to stimulation (increased BOLD signal, CBF and cerebral blood volume) can, however, be very fast, and have been registered within 350–500 ms after stimulus onset (Figure 3D; see also Table 1 and related text in Masamoto and Kanno, 2012). The capacity for increased CBF under extreme conditions is extraordinary, for example, CBF rises 9-fold within the first minute after seizure onset (Meldrum and Nilsson, 1976). The prevalence of large, rapid BOLD effects indicates that, after a brief lag, oxygen delivery exceeds oxygen consumption by activated brain and provides a large gradient for oxygen diffusion to cells furthest from capillaries (Buxton, 2010; Hyder et al., 2010; Vazquez et al., 2010; Devor et al., 2011). Oxygen delivery to human and animal brain exceeds CMR_{O2} by a factor of 2–3 (Uludag et al., 2004; Buxton, 2010; Hyder et al., 2010), but there is some evidence that oxidative metabolism may respond to stimulation faster than haemodynamic components (Vazquez et al., 2010). The small, transient increases in brain lactate level evoked by visual stimulation concomitant with increases in total creatine and BOLD signals (Mangia et al., 2007b) probably arise from function-induced changes in relative fluxes of the glycolytic and oxidative pathway, rather than from oxygen insufficiency. Modelling of flow and metabolism generated the hypothesis that the large increase in blood oxygen availability is necessary to maintain tissue oxygen levels, particularly at sites most distant from capillaries (Buxton, 2010).

Glucose delivery

Many studies in brain of experimental animals and humans have shown that glucose delivery exceeds glucose utilization rate by 1.5-fold over a wide range of glucose concentrations and metabolic rates in anaesthetized or conscious subjects. For example, data compiled from studies by Cremer et al. (1983) (Figure 3E) show that glucose influx into rat brain exceeds CMR_{glc} and is directly proportional to CMR_{glc} over a 3–4-fold range. These rats had mean plasma glucose levels ranging from 4.9 to 12.6 mmol/l and brain glucose levels of 0.7–4.8 μmol/g. Even during abrupt, 4–5-fold increases in glycolysis during seizures, glucose delivery nearly matches the higher demand (Duffy et al., 1975; Howse and Duffy, 1975). Surplus glucose delivery compared with demand has also been demonstrated in studies that combined ^{14}C- or ^{13}C-metabolic assays with mathematical modelling (Holden et al., 1991; Gruetter et al., 1998; de Graaf et al., 2001; Duarte et al., 2009; Shestov et al., 2011). To sum up, oxygen and glucose transport capacities of grey and white matter are sufficiently high to sustain large increases in CMR_{O2} and CMR_{glc} in normoxic subjects with plasma glucose level above the mildly hypoglycaemic level. There may, however, be a short lag, on the order of seconds, before reactive hyperaemia and fuel delivery to activated cells rises to its maximal extent.

'Buffering' by endogenous fuel

Oxygen and glucose in the blood in brain and in brain tissue can serve as transient buffers when there is an abrupt supply–demand mismatch at stimulus onset. The extraction fraction (E) that is, the arterial (A) minus venous (V) concentration of a substance divided by its arterial concentration, $E = 100^*[A-V]/A$, is approximately 50% for oxygen and approximately 12% for glucose in rat brain, for example, (Madsen et al., 1998, 1999). The solubility of oxygen in water is very low and there is no reservoir in brain, so oxygen extraction would have to rise to provide more oxygen to tissue until delivery increases. In contrast, total glucose concentration in rat brain (intracellular plus extracellular) is ~20% of that in arterial plasma and generally within the range of 2–3 μmol/g. This amount is sufficient to accommodate more than a 100% increase in CMR_{glc} for at least a minute, as shown in the hypothetical example in Table 2. Increasing CMR_{glc} from 1 to 2 $\mu mol \cdot g^{-1} \cdot min^{-1}$ would consume 1 μmol/g of glucose in 30 s. Half of the glucose would come from blood at the normal resting delivery rate, with the remainder from the glucose contained in brain. Doubling CMR_{glc} would reduce tissue glucose level by

Table 2 Glucose buffering capacity and ATP yields from up-regulation of glycolysis and oxidation

Physiological state*	CMR_{glc}* ($\mu mol \cdot g^{-1} \cdot min^{-1}$)	Glucose consumed† in 30 s ($\mu mol \cdot g^{-1}$)	CMR_{O2}* ($\mu mol \cdot g^{-1} \cdot min^{-1}$)	ATP yield* ($\mu mol \cdot g^{-1} \cdot min^{-1}$)	
				Glycolysis	Oxidation
Rest	1	0.5	6	2	192
Activation: 5%	1.05	0.525	6.3	2.1	201.6‡
10%	1.1	0.55	6.6	2.2	211.2
30%	1.3	0.65	7.8	2.6	249.6
50%	1.5	0.75	9	3	288
100%	2	1†	12	4‡	384

* The resting rate of glucose utilization rate (CMR_{glc}) of 1 $\mu mol \cdot g^{-1} \cdot min^{-1}$ approximates the mean value for the entire rat cerebral cortex. For the purpose of illustration, this resting rate is associated with a ratio of oxygen/glucose consumption (CMR_{O2}/CMR_{glc}) set equal to 6, the maximal theoretical molar ratio (1 glucose+$6O_2 \rightarrow 6CO_2+6H_2O$). ATP yields were calculated for rest and different hypothetical levels of metabolic activation using 2ATP per glucose for the glycolytic pathway and 32 ATP per glucose for the oxidative pathway.
† Normal rat brain glucose concentration is approximately 20–25% of that in arterial plasma, and is generally within the range of 2–3 $\mu mol/g$ in non-fasted adult animals (Dienel et al., 1991; Holden et al., 1991). At steady state during rest, net glucose delivery matches glucose utilization rate and at rest would be equal to 1 $\mu mol \cdot g^{-1} \cdot min^{-1}$. Note that even if glucose delivery does not rise to match increased demand for glucose during activation to evoke a 100% increase in CMR_{glc} there is enough unmetabolized glucose in brain tissue to support this high metabolic rate for 1 min and still maintain the brain glucose level above 1 $\mu mol/g$ and saturate hexokinase (K_m~0.05 mmol/l; Grossbard and Schimke, 1966). Thus, if brain glucose level is 2 $\mu mol/g$ and 1 $\mu mol/g$ is delivered in 1 min, consumption of 2 $\mu mol/g$ in 1 min due to a 100% increase in CMR_{glc} would still leave 1 $\mu mol/g$ unmetabolized glucose in brain.
‡ Note that the net ATP yield from a 5% increase in CMR_{O2} (201.6–192=9.6) is 4.8 times greater than from a 100% rise in glycolysis (4−2=2) in astrocytes and in neurons, and this oxygen-glucose metabolic mismatch would be associated with an overall fall in the CMR_{O2}/CMR_{glc} ratio from 6 to 3.15 (i.e., 6.3 divided by 2).

0.5 µmol or 25% if the resting value were 2 µmol/g. Thus, hexokinase will remain saturated (1 mmol/l glucose is 20 times the K_m for glucose, ~ 0.05 mmol/l) and can operate at V_{max} when disinhibited by downstream consumption of Glc-6-P. These conclusions are consistent with experimental evidence obtained during extreme situations, for example, electroconvulsive or chemically induced seizures that evoke large hyperaemic responses, increased utilization of blood glucose, and consumption of some endogenous glucose and glycogen (King et al., 1967a; King et al., 1967b; Howse et al., 1974; Duffy et al., 1975; Miller et al., 1982). Compensatory responses to huge, abrupt increases in energy demand can maintain adequate brain glucose and ATP levels for intervals ranging from 10 to 30 s to more than several minutes.

It is widely recognized by researchers in the metabolism field that the preponderance of ATP generated from glucose metabolism comes from oxidative pathways due to the 16–18-fold higher ATP yield compared with glycolysis (e.g., Hyder et al., 1997; Mangia et al., 2007b; Lin et al., 2010a, 2010b). This fact is illustrated by hypothetical data in Table 2. A modest 5% rise in CMR_{O2} in a neuron or astrocyte during a 50% fall in the CMR_{O2}/CMR_{glc} ratio produces 4.8 times more ATP than a 100% increase in glycolysis (Table 2). These data suggest that the rise in non-oxidative metabolism during brain activation may be related to specific pathways that utilize glucose (e.g., pentose-phosphate shunt to generate NADPH) or preferential use of glycolytically generated ATP for specific purposes, as opposed to overall energetics (also see Shulman et al., 2009). This argument applies to the complex, interactive activities of all brain cells in tissue and is consistent with excess glucose supply compared with demand under normal resting and activating conditions. However, the energetics of subcellular microdomains in neurons and astrocytes may differ from the tissue average, as suggested by increased glycogen turnover during activation. Cellular and subcellular compartmentation of metabolism is an active research topic, but until methods with high spatial and temporal resolution are established for use in intact adult tissue, it is difficult to ascribe the pathway of origin of ATP and its use for specific functions.

Glycogen – a dynamic fuel consumed during brain activation and abnormal conditions

Swanson et al. (1992) discovered that whisker stimulation increased local glycogen degradation in the whisker barrel field of sensory cortex. This seminal study stimulated the conceptual shift of the functional role of glycogen in brain from an emergency energy store to a participant in brain energetics during activation (recently reviewed by Hertz et al., 2007; Schousboe et al., 2007; Hertz and Gibbs, 2009; DiNuzzo et al., 2011; Obel et al., 2012). The predominance of glycogen in astrocytes supports the notion that these cells require glucose buffering to carry out their normal activities during activation. Resting glycogen utilization in forebrain of normal conscious rodents is very low, <0.01 $\mu mol \cdot g^{-1} \cdot min^{-1}$ (Table 3A), compared with rates of utilization of blood-borne glucose that range from ~0.5 to 1.7 $\mu mol \cdot g^{-1} \cdot min^{-1}$ in grey matter (Table 3B). Glycogen turnover in human brain is also quite low, even when assayed during modest hypoglycaemia or in diabetic patients with hypoglycaemic unawareness (Table 3A). Very few studies have directly measured glycogen turnover during sensory stimulation of conscious subjects. The available data indicate that, when the animals are very carefully handled prior to the experimental assay, their brain glycogen levels are high, in the range of 5–12 µmol/g (Table 3A). When more glycogen is available, it may be consumed in substantial quantities during sensory stimulation compared with when its pre-stimulus levels are much lower. The astrocytic functions supported by utilization of glycogen *in vivo* remain to be established, but metabolic modelling by DiNuzzo et al. (2010b) supports their hypothesis that an important role for glycogen during brain activation is to fuel astrocytes while maintaining Glc-6-P levels high enough to inhibit hexokinase, thereby reducing astrocytic consumption of glucose in interstitial fluid and

Table 3 **Glycogen and glucose utilization during normal and pathophysiological conditions**

Mean glycogen utilization rates were either reported by the cited studies, calculated from net glycogen consumed during a specified time interval, or determined by MRS during and after labelling of brain glycogen with [1-^{13}C]glucose. Glycogenolysis rates can be compared with mean local rates of glucose utilization in the same or related structures in a representative [^{14}C]deoxyglucose study in normal resting rats. Comparisons are also made during ischaemia, when rates were calculated from changes in levels of energy metabolites.

Substrate and brain structure	Rate ($\mu mol \cdot g^{-1} \cdot min^{-1}$)	Reference(s)
A. Glycogen utilization rate or label clearance rate		
Rest, conscious mouse forebrain. Total glycogen	0.010*	(Watanabe and Passonneau, 1973)
Limit dextrin (inner core)	0.004	
Rest, α-chloralose-anaesthetized rats, cerebral cortex/dorsal caudate labelled during hyperglycaemia	0.008†	(Choi et al., 1999)
Rest, conscious euglycaemic human occipital cortex of normal subjects or Type 1 diabetics with hypoglycaemic unawareness	0.003–0.005‡	(Oz et al., 2007, 2009, 2012)
Sensory stimulation (5 min), conscious rat cerebral cortex	0.58§	(Cruz and Dienel, 2002)
Sensory stimulation (5 min)+15 min recovery	0.20§	
Sensory stimulation (10 min) cerebral cortex	0.055§	(Dienel et al., 2007a)
Hypoglycaemia, conscious rat forebrain during lethargy	0.04–0.07‖	(Ghajar et al., 1982)
Hypoglycaemia, conscious rat parietal cortex+hippocampus	0.03¶	(Suh et al., 2007)
Hypoglycaemia, conscious rat, three brain regions	0.01–0.02§	(Herzog et al., 2008)
Hypoglycaemia, glycogen degradation rate after insulin infusion into α-chloralose-anaesthetized rats	0.038**	(Choi et al., 2003)
Hypoglycaemia, human occipital cortex		(Oz et al., 2009)
Insulin-induced hypoglycaemia, ^{13}C-washout rate	0.002††	
Euglycaemia, ^{13}C-washout rate	0.0005	
Euglycaemia turnover rate (synthesis=degradation)	0.003	
Seizures, bicuculline for 20 min, range for three rat brain regions	0.11–0.16§	(Folbergrova et al., 1981)
Anoxia, mouse cerebral cortex, range for two assays in controls between 15 and 90 s after onset of anoxia	0.8–1.4§	(Gross and Ferrendelli, 1980)
Ischaemia, initial flux after decapitation, unanaesthetized adult mouse forebrain	2.2 (peak rate=3)	(Lowry et al., 1964)
Ischaemia, 20 s interval between decapitation and freezing mouse brain, range for four brain regions	0.2–2.6§	(Gatfield et al., 1966)
Ischaemia, 2 min before freezing sciatic nerve from anaesthetized rabbit	0.17§	(Stewart et al., 1965)
Aglycaemia, maximally stimulated rat or mouse optic nerve during ~30 min aglycaemic perfusion *in vitro*	0.02–0.03‡‡	(Wender et al., 2000; Brown et al., 2003)
Aglycaemia, astrocyte culture, initial 10 min interval	0.36§	(Dringen et al., 1993)
Aglycaemia+10 mmol/l azide, initial 10 min interval	0.50§	
B. Glucose utilization rate		
Resting rat brain tissue		
Visual pathway		
Optic nerve	0.13§§	Estimated rate
Optic chiasm	0.16	(Grunwald et al., 1988)
Superior colliculus	0.69	
Lateral geniculate	0.76	
Visual cortex	0.93	
Auditory pathway		
Cochlear nucleus	1.01	
Superior olivary nucleus	1.40	
Lateral lemniscus	0.94	
Inferior colliculus	1.69	
Medial geniculate	1.08	
Auditory cortex	1.36	
Other regions of cerebral cortex		
Sensorimotor cortex	0.96	
Parietal cortex	0.87	
Frontal cortex	0.92	
Piriform cortex	1.09	
Entorhinal cortex	0.49	
Cingulate cortex	0.99	
White matter		
Corpus callosum	0.25	
Genu of corpus callosum	0.20	
Internal capsule	0.22	
Cerebellar white matter	0.25	
Ischaemia		
Decapitation ischaemia, 20 s interval before freezing mouse brain, range for four brain regions	1.15–3.18§	(Gatfield et al., 1966)
Ischaemia, 2 min before freezing sciatic nerve from anaesthetized rabbit	0.32§	(Stewart et al., 1965)

* Rates determined by tracer [^{14}C]glucose labelling, label clearance assays and metabolic modelling.
† Glycogen turnover rate (i.e., synthesis rate=degradation rate when pool size constant) estimated during 4 h labelling with [1-^{13}C]glucose to produce a constant plasma glucose level of 15 mmol/l and during label clearance for at least 3 h after cessation of label infusion. Net synthesis of glycogen during the hyperglycaemic infusion was anticipated by the authors, and the rate was probably overestimated.
‡ Glycogen turnover rate calculated from rates of label incorporation and loss during and after programmed infusion of [1-^{13}C]glucose in normal subjects with blood glucose level clamped at ~6 mmol/l. Label washout rate after an 11 h [1-^{13}]glucose infusion was ~0.0005 $\mu mol \cdot g^{-1} \cdot min^{-1}$.
§ Glycogen or glucose utilization rates were calculated as net amount of glycogen (expressed in glucose units) or glucose consumed divided by the duration of the experimental interval. To compare results from different studies, values or rates reported in units 'per mg protein' were converted into wet weight, assuming 100 mg protein/g wet weight.
‖ Range corresponds to the fall in glycogen level (1.47 μmol/g) from control to lethargy divided by either 20 or 35 min that corresponds to the beginning and end of the lethargy interval respectively (see Figure 1 and Table 3 in Ghajar et al., 1982).
¶ Rate was calculated from glycogen consumed (i.e., the net increase in glycogen caused by inhibition of glycogen phosphorylase with CP-316,819 compared with saline-treated controls, ~3 μmol/g) divided by the net increase in duration of neuronal activity prior to onset of isoelectric electroencephalogram during hypoglycaemia compared with hypoglycaemic saline-controls (~90 min) (see Figure 3 and text, p. 48 in Suh et al., 2007). Glucose depletion relieves inhibition of phosphorylase by CP-316,819, and the additional glycogen can be consumed as needed.
** Glycogen was first labelled by infusion of [1-^{13}C]glucose for 4 h to clamp brain glucose at approximately 3 μmol/g. Glycogen degradation rate was calculated from label washout during a ~2 h interval of insulin-induced hypoglycaemia that reduced brain glucose to approximately 0.1 μmol/g.
†† Label washout rate assayed during 2.5 h interval of euglycaemia (blood glucose, ~5.2 mmol/l) or hypoglycaemia (blood glucose, ~3.6 mmol/l) following an 11 h prelabelling period of infusion of [1-^{13}C]glucose when both groups of subjects were euglycaemic (7.2 mmol/l). Turnover rate was calculated for euglycaemic control subjects.
‡‡ Isolated mouse or rat optic nerves were first incubated with cerebrospinal fluid (aCSF) containing 10 mmol/l glucose for 1h, then perfused with artificial aCSF containing zero glucose while maximal compound action potentials (CAPs) were evoked every 30 s by electrical stimulation. Glycogen levels prior to stimulus onset were ~5–10 pmol/μg optic nerve protein; assuming 100 mg protein/g optic nerve, initial glycogen levels were ~0.5–1 μmol/g. Estimated glycogenolysis rates were calculated from net glycogen consumed during the interval between stimulus onset and CAP failure from data in Figure 3(B) and related text of Wender et al. (2000) and in Figure 2(D) of Brown et al. (2003).
§§ Glucose utilization rate in optic nerve was not measured by Grünwald et al. (1988). Estimated rate was calculated from the relative rate of glucose utilization in optic nerve versus optic chiasm in urethane-anaesthetized monkeys as follows. Optic nerve/optic chiasm ≈0.82, estimated from Figure 4 of Sperber and Bill (1985) times the measured rate for optic chiasm (0.16, from Grünwald et al., 1988): $0.82 \times 0.16 = 0.13$.

increasing availability of tissue glucose and blood-borne glucose for activated neurons.

Recent studies of memory and learning have opened a new, fascinating chapter regarding the functional roles of astrocytic glycogen. For example, 1-day-old chicks quickly learn to associate bead colour with an aversive taste, and detailed analysis of the time courses for blockade and rescue of learning and memory consolidation by various compounds led to the conclusion that glycogenolysis provides precursors for astrocytic synthesis of glutamate, not to provide energy for neurons (Gibbs et al., 2008; Hertz and Gibbs, 2009). However, mechanisms for the roles of glycogen and glutamate remain to be established in this paradigm. Suzuki et al. (2011) identified up-regulation of phospho-CREB (cAMP-response-element-binding protein), Arc, and phospho-cofilin as molecular events that occur during long-term memory consolidation of avoidance learning by adult rats and linked these changes to glycogenolysis and lactate transport. Suzuki et al. (2011) bring readers' attention to astrocyte-neuron lactate shuttling in their introduction by stating that "...lactate transport between astrocytes and neurons has been shown from glutamate-stimulated glycolysis (Pellerin and Magistretti, 1994; Magistretti et al., 1999)...". This statement is not true. In fact, these two reports only show lactate efflux to culture media and formalize a hypothetical shuttle model respectively. These studies provide no evidence for astrocyte-to-neuron lactate shuttling, which has been a very controversial topic due to lack of direct evidence for substantial cell-to-cell transport (Dienel, 2011). Intriguing aspects of the Suzuki study are the temporal effects of lactate loading with respect to glycogenolysis and roles of different MCTs in memory. For example, it is not clear why lactate given 15 min before a training event prevents the memory-blocking effects of MCT antisense oligonucleotides injected one h before the training. When assayed 13 h after MCT1, 2 or 4 antisense injection the total MCT isoform levels (i.e. plasma membrane transporters plus intracellular stores) were reduced by ~30–50%. The time courses of declines are not known, but if linear, the rates of decrease would be ~2–4%/h and the decrement in total MCT level for a given isoform at 1 h after training would be only 4–8%. Lactate injections (100 nmol) into hippocampus prevented the memory decrements associated with antisense treatment against MCT1 or 4, but not MCT2. Depending on the distribution of the injected lactate into the volume of the hippocampus, the resultant concentration is estimated to be within the range of 1–5 μmol/g, and higher in the vicinity of the injection site. Assuming a rate of lactate efflux to blood of 15–22% of CMR_{glc} when brain lactate content is elevated (Hawkins et al., 1973; Cruz et al., 1999) and hippocampal CMR_{glc} of 0.8 $\mu mol \cdot g^{-1} \cdot min^{-1}$ (Sokoloff et al., 1977), the time for efflux of all injected lactate to blood could range from ~10 to 30 min, assuming no metabolism, which would increase its clearance rate. Thus, the injected lactate has a very limited duration to influence memory, and its effective span would end at least 30–45 min before total MCT isoform level is anticipated to fall by <10%. This apparent discordance suggests that other factors may be more important for memory formation than astrocyte-neuron lactate transport. Conceivably, large changes in the NADH/NAD^+ ratio (redox state) caused by lactate influx from extracellular fluid into neurons and astrocytes and redox-induced changes in astrocytic Ca^{2+} signalling may evoke longer lasting effect on actions of transcription factors (Garriga-Canut et al., 2006; Requardt et al., 2012; Wilhelm and Hirrlinger, 2012) and initiate memory-sparing events that are detectable at later times. The Suzuki study did not directly demonstrate cell-to-cell lactate shuttling, nor rule out the use of glycogen by astrocytes as a key element in memory consolidation, but it characterizes an interesting experimental paradigm to further evaluate temporal roles of glycogen and lactate. Newman et al. (2011) also linked glycogen-derived lactate to memory processing in a recent study that extends their previous findings that glucose potently enhances memory processes in humans and rats. In this study, they reported mirror-image percentage changes in extracellular glucose (decrease) and lactate (increase) during behavioural testing and associated the changes with

energetics of cognitive testing. However, the absolute values of extracellular metabolite levels were not reported, and percentage changes in concentration are difficult to interpret because fluxes through the extracellular glucose and lactate pools are likely to be very different, as discussed above. Performance in a short-term spatial working memory task was enhanced by lactate injection, and impaired in a dose-dependent manner by inhibitors of glycogenolysis or lactate transport. Memory impairment due to inhibition of glycogen breakdown could be rescued by high doses of lactate or glucose, but effects of 4-CIN (α-cyano-4-hydroxycinnamate) on lactate transport were not reversed by glucose or lactate. To try to exclude effects of inhibition of mitochondrial pyruvate transport by 4-CIN, the authors showed that *in vitro* assays of succinate dehydrogenase activity were not altered. However, this is not a sufficient test to exclude competitive inhibition by 4-CIN of oxidation glucose-derived pyruvate *in vivo*.

Abnormal conditions that reduce glucose or oxygen supply or increase metabolic demand also enhance utilization of glycogen reserves. During modest hypoglycaemia, supply of glucose from blood cannot fully satisfy the brain's continuous demand for fuel, and glycogenolysis is stimulated by 2–7-fold in rodents to supplement glucose delivery from blood to brain (Table 3A). During severe pathophysiological conditions (seizures, anoxia, ischaemia), glycogenolysis abruptly rises 10–100-fold, with highest rates during ischaemia that reach 2–3 $\mu mol \cdot g^{-1} \cdot min^{-1}$ (Table 3A). These accelerated rates of glycogen degradation exceed normal rates of glucose utilization, but they are only approximately 1/3 of the corresponding rate of consumption of endogenous glucose in ischaemic brain after decapitation (Tables 1, 3A and 3B). Aglycaemia caused by removal of glucose from cultured astrocytes causes glycogen depletion at rates within the range of that observed in the intact brain (Table 3A). White matter typically has much lower rates of glucose utilization compared with grey matter structures (Table 3B), and estimated rates of glycogenolysis in the ischaemic sciatic nerve and in the optic nerve given intense electrical stimulation in the absence of glucose are only a minor fraction of those in grey matter (Table 3A). Preservation of maximally evoked compound action potentials by glycogen is ascribed to lactate shuttling from astrocytes to axons (Brown and Ransom, 2007), although the cell(s) that actually oxidize the lactate remain to be identified. These findings are of interest because they reveal the very small quantitative contribution of glycogenolysis (0.02–0.03 $\mu mol \cdot g^{-1} \cdot min^{-1}$, Table 3A) that is sufficient to maintain intensively activated action potentials. The estimated rate of glycogenolysis is only ~10–20% of CMR_{glc} in resting white matter and a few per cent of that in many grey matter structures (Tables 3A and 3B). Thus, the energy demands of maximally stimulated compound action potentials in optic nerve and the 'protective contributions' of the associated lactate shuttling are quite low. Most of the glucose consumed by optic nerve in conscious, resting rats supports other energy-consuming processes, consistent with the white matter energy budget of Harris and Attwell (2012).

To sum up, glycogen is a significant supplementary fuel during brain activation under normal and abnormal conditions, and its utilization is also associated with memory and learning. During extreme conditions, glycogen utilization can preserve neuronal function, even though its rate is much lower than that of glucose contained in tissue or of glucose delivered by blood to grey or white matter.

CMR_{glc} during rest and activation in conscious and anaesthetized subjects

Functional activation of CMR_{glc} in conscious subjects

The close relationship between cellular signalling and neuroenergetics enables the use of metabolic signals to evaluate the location and magnitude of functional activities during brain activation and diseases (Figure 1). Many laboratories have used energetic signals to study brain function, and Table 4 provides some representative examples of global and local studies. The whole brain weighted-average metabolic rate determined with the [^{14}C]DG method is in good agreement with values determined with global assays that calculate metabolic rate according to the Fick principle, CMR=CBF(A-V). Local and global assays of whole-brain glucose utilization with different methods give equivalent results, but global assays cannot detect large changes in small structures.

Generalized somatosensory stimulation due to gentle brushing of the whiskers, paws, head and back of previously sequestered, conscious rats evoked a 44% increase in global CMR_{glc}, from 0.75 to 1.08 $\mu mol \cdot g^{-1} \cdot min^{-1}$ (Table 4). However, local increases in CMR_{glc} in the parietal and whisker barrel field of somatosensory cortex were much larger, rising from ~1 $\mu mol \cdot g^{-1} \cdot min^{-1}$ at rest to 1.4–2 $\mu mol \cdot g^{-1} \cdot min^{-1}$ during stimulation, depending on the cortical region and layer (Dienel et al., 2007a). Stimulation of the visual system by increasing light intensity or the frequency of on-off pattern flashes evoked graded increases in CMR_{glc} up to 70–115% of the resting value in the dorsal superior colliculus (Table 4). Acoustic stimulation raises CMR_{glc} in different brain regions in the auditory pathway by 55–80% (Table 4). Both self-rewarding and 'investigator-imposed' electrical stimulation evoke large increases in CMR_{glc} in many regions (Table 4). To summarize, different stimulus paradigms increase CMR_{glc} in specific pathways of conscious rats by as much as 100%, with rates rising above the respective resting values by 0.3–1 $\mu mol \cdot g^{-1} \cdot min^{-1}$.

Blunted CMR_{glc} responses to activation in anaesthetized rats

Anaesthesia is used to immobilize experimental animals during electrophysiological, MRS and PET studies in which movement would compromise the experiment. Suppression of CMR_{glc} by anaesthesia (Table 4) is consistent with

Table 4 Glucose utilization in rat brain: effects of functional activation of various pathways in conscious and anaesthetized rats

Experimental paradigm/structure	Conscious rats			Anaesthetized rats			Reference
	CMR_{glc} ($\mu mol \cdot g^{-1} \cdot min^{-1}$)		Net change	CMR_{glc} ($\mu mol \cdot g^{-1} \cdot min^{-1}$)		Net change	
	Unstimulated	Stimulated	$\mu mol \cdot g^{-1} \cdot min^{-1}$ (% difference)	Unstimulated	Stimulated	$\mu mol \cdot g^{-1} \cdot min^{-1}$ (% difference)	
Range for normal resting or anaesthetized visual, auditory, parietal, and sensory-motor cortex ([^{14}C]DG method)	1.07–1.57			0.64–0.81 (thiopental)		−0.43 (−40%) to −0.76 (−48%)	(Sokoloff et al., 1977)
Cerebellar cortex	0.57			0.44		−0.13 (−23%)	
Whole brain, weighted average ([^{14}C]DG)	0.68			–			
Whole brain, Kety–Schmidt method	0.66			0.33 (pentobarbital)		−0.33 (−50%)	(Linde et al., 1999)
	0.75	1.08	0.33 (44%)*				(Madsen et al., 1999)
	Concious rats						
Visual stimulation of stratum griseum superficiale of the superior colliculus							
Dark	0.7						(Miyaoka et al., 1979)
Light intensity (lux): 0.3		1.0	0.3 (43%)				
1.4		1.25	0.55 (79%)				
7		1.5	0.8 (114%)				
On-off pattern (Hz): 0	0.85						(Collins et al., 1987)
4		0.98	0.13 (15%)				
8		1.13	0.28 (33%)				
16		1.34	0.49 (58%)				
33		1.45	0.6 (71%)				
Mean net change (mean %)			**0.45 (59%)**				
Broadband click acoustic stimulation	Sham	Stimulated					(Cruz et al., 2005)
Superior olive	0.56	0.87	0.31 (55%)*				
Lateral lemniscus	0.51	0.92	0.41 (80%)*				
Inferior colliculus	0.75	1.20	0.45 (60%)*				
Mean net change (mean %)			**0.39 (65%)**				
	Unstimulated		Stimulated		Net change		
Self-rewarding electrical stimulation	Ipsi	Contra	Ipsi	Contra	Ipsi versus Contra		(Esposito et al., 1984)***
Ventral tegmental area	0.56	0.58	0.93	1.95	1.02 (110%)*		
Substantia nigra pars compacta	0.61	0.63	0.97	1.21	0.24 (25%)*		
Medial forebrain bundle	0.59	0.58	0.72	1.18	0.46 (64%)*		
Horizontal limb diagonal band of Broca	0.69	0.71	0.88	1.19	0.31 (35%)*		
Mean net change (mean %)					**0.51 (59%)**		
Electrical stimulation of dorsal raphe nucleus (serotonergic system)	Unstimulated		Stimulated		Net change		(Cudennec et al., 1988)†
Red nucleus, parvocellular	0.87		1.40		0.53 (61%)*		
Red nucleus, magnocellular	0.81		1.29		0.48 (59%)*		
Substantia nigra pars compacta	0.84		1.40		0.56 (67%)*		
Substantia nigra pars reticulata	0.60		0.89		0.29 (48%)*		
Zona incerta	0.99		1.51		0.52 (53%)*		
Habenular nucleus, lateral	1.50		1.64		0.14 (9%)		
Habenular nucleus, medial	0.86		0.91		0.05 (6%)		
Dorsal tegmental nucleus	1.24		1.72		0.48 (39%)*		
Median raphe nucleus	1.12		1.56		0.44 (39%)*		

Table 4 **Continued.**

Pontine reticular nucleus	0.68	1.15	0.47 (69%)*
Frontoparietal somatosensory	1.42	2.11	0.69 (49%)*
Frontal sensorimotor	1.39	1.88	0.49 (35%)*
Mean net change (mean %)			**0.43 (45%)**

	Conscious rats			0.5% Halothane anaesthesia			
Ipsilateral effects of electrical stimulation of substantia nigra	Sham	Stimulated	Net change	Sham	Stimulated	Net change	(Savaki et al., 1983)‡
Substantia nigra pars compacta	0.55	0.73	0.18 (33%)*	0.75	0.88	0.13 (17%)	
Substantia nigra pars reticulatea	0.43	1.40	0.97 (226%)*	0.55	1.10	0.55 (100%)*	
Ventral tegmental area	0.45	0.59	0.14 (31%)*	0.53	0.52	−0.01 (−2%)	
Posterior striatum, ventro-medial	0.89	1.17	0.28 (31%)*	0.89	0.99	0.10 (11%)	
Subthhalamic nucleus	0.71	0.99	0.28 (39%)*	0.80	0.92	0.12 (15%)*	
Globus pallidus	0.43	0.70	0.27 (63%)*	0.45	0.62	0.17 (38%)*	
Interpeduncular nucleus	0.84	1.06	0.22 (26%)*	1.06	0.91	−0.15 (−14%)*	
Habenula, medial	0.68	0.86	0.18 (26%)*	0.71	0.70	−0.01 (−1%)	
Mean net change (mean %)			**0.32 (59%)**			**0.11 (21%)**	

	Conscious rats			Chloral hydrate anaesthesia			
Apomorphine (dopamine agonist)	Saline	Drug	Net change	Saline	Drug	Net change	(Grome and McCulloch, 1983) §
Cerebellar cortex	0.44	0.83	0.39 (89%)*	0.31	0.32	0.01 (3%)	
Cerebellar nuclei	0.81	0.95	0.14 (17%)*	0.56	0.60	0.04 (7%)	
Substantia nigra pars compacta	0.66	0.80	0.14 (21%)*	0.49	0.36	−0.13 (−27%)*	
Substantia nigra pars reticulatea	0.52	0.94	0.42 (81%)*	0.35	0.40	0.05 (14%)	
Red nucleus	0.68	0.89	0.21 (31%)*	0.39	0.41	0.02 (5%)	
Subthalamic nucleus	0.71	1.26	0.55 (77%)*	0.45	0.51	0.06 (13%)	
Habenular nucleus, medial	0.70	0.69	−0.01 (−1%)	0.54	0.59	0.05 (9%)	
Habenular nucleus, lateral	1.00	0.80	−0.20 (−20%)*	0.47	0.55	0.08 (17%)	
Globus pallidus	0.48	0.67	0.19 (40%)*	0.32	0.39	0.07 (22%)*	
Sensory-motor cortex, layer IV	0.90	1.48	0.58 (64%)*	0.51	0.55	0.04 (8%)	
Sensory-motor cortex, layer VI	0.65	1.20	0.55 (85%)*	0.44	0.45	0.01 (2%)	
Anterior cingulate cortex	0.94	0.80	−0.14 (−15%)*	0.64	0.60	-0.04 (−6%)	
Mean net change (mean %)			**0.24 (39%)**			**0.02 (6%)**	

	Conscious rats			α-Chloralose anaesthesia			
Whisker stimulation	Unstimulated	Stimulated	Net change	Unstimulated	Stimulated	Net change	(Nakao et al., 2001)‖
Spinal trigeminal nucleus	0.61	1.44	0.83 (131%)*	0.44	1.11	0.67 (158%)*	

Table 4 **Continued.**

	Conscious rats			α-Chloralose anaesthesia			
Principal sensory trigeminal nucleus	0.58	1.13	0.55 (92%)*	0.47	1.0	0.53 (112%)*	
Ventral posteromedial thalamic nucleus	1.00	1.75	0.75 (75%)*	0.49	0.68	0.19 (39%)*	
Somatosensory cortex, barrel field	0.94	1.48	0.54 (54%)*	0.39	0.50	0.11 (28%)*	
Mean net change (mean %)			**0.67 (88%)**			**0.38 (84%)**	
Electrical stimulation of forepaw							
Primary somatosensory cortex				0.254	0.394	0.14 (55%)*	(Ueki et al., 1988)¶
				0.521	0.731	0.21 (40%)*	(Ueki et al., 1992)**
				0.25 (oxidative)	0.74 (oxidative)	0.49 (196%)*	(Hyder et al., 1996)††
				0.25 (oxidative)	1.05 (oxidative)	0.8 (320%)*	(Hyder et al., 1997)‡‡
				0.25 (oxidative)	0.37 (oxidative)	0.12 (48%)*	(Yang and Shen, 2006)§§
Mean net change (mean %)						**0.47 (189%)**	
Electrical stimulation of dorsal raphe nucleus							(Bonvento et al., 1991) ‖‖
Red nucleus				0.42	0.54	0.12 (29%)*	
Substantia nigra				0.37	0.43	0.06 (16%)*	
Zona incerta				0.42	0.52	0.10 (24%)*	
Habenular nucleus				0.56	0.71	0.15 (27%)*	
Dorsal tegmental nucleus				0.52	0.79	0.27 (52%)*	
Median raphe nucleus				0.53	0.61	0.08 (15%)*	
Pontine reticular nucleus				0.37	0.45	0.08 (22%)*	
Mean net change (mean %)						**0.12 (26%)**	
Electrical stimulation of climbing fibres of cerebellar Purkinje cells							(Caesar et al., 2008)¶¶
Cerebellar cortex				0.200	0.248	0.048 (24%)*	

* Statistically significantly different from respective control value (see original reports for actual P values). % Difference = 100*(experimental-control)/control. Specific responses to each condition vary according to the stimulus paradigm, pathway, and neurotransmitter systems activated. Comparisons between conscious and anaesthetized animals should be made structure by structure. However, different studies did not measure the same structures, and for comparison of overall differences due to activation or anaesthesia, the arithmetic mean net (incremental) changes due to activation and the mean percent changes were calculated for all structures in each experimental group.

*** Rats self-stimulated at 200–250 μA delivered at 100 Hz in 400 ms trains at a rate of 60–80 responses/min for 55 min. Ipsi, hemisphere ipsilateral to stimulus electrode; Contra, contralateral hemisphere.

† Stimulus intensity 200 μA, frequency 10 Hz, pulse duration 2 ms pulse; 45 min stimulation.

‡ Train of 30 pulses, pulse duration 0.5 ms, intensity 100 μA; train duration 100 ms, repeated every 4s for 17 min.

§ Chloral hydrate dose: 100 mg/kg, intravenous followed by 3 mg/kg per min infusion.

‖ Rats were given unilateral vibrissal stimulation while conscious or ventilated (30%O_2/70%N_2) and anaesthetized (acute intravenous injection of α-chloralose (50 mg/kg), followed by continuous intravenous infusion of 40 mg/kg per h). Rates of glucose utilization (i.e., total CMR_{glc} assayed as flux through the hexokinase step) determined with the [^{14}C]deoxyglucose (DG) method approximately 3 h after termination of halothane in the unanaesthetized group and approximately 45 min after changing from halothane to α-chloralose in the anaesthetized group. Approximate mean values for CMR_{glc} were estimated from Figure 1 of Nakao et al. (2001) and used to calculate the net increase in rate due to whisker stimulation. The actual percent differences between stimulated and unstimulated sides were stated by the authors, and small errors in interpolating values from their Figure will cause apparent discrepancies in percentage differences. The rate of oxygen consumption (CMR_{O2}) was not measured in the Nakao study. It is not known whether CMR_{O2}/CMR_{glc} falls during whisker stimulation. Assuming maximal oxidation of glucose during the resting state, i.e., $CMR_{O2}/CMR_{glc}=6$, then maximal CMR_{O2} in the spinal trigeminal nucleus, sensory trigeminal nucleus, ventral posterior medial thalamic nucleus, and barrel cortex respectively is 3.7, 3.5, 6 and 5.6 $\mu mol \cdot g^{-1} \cdot min^{-1}$ in conscious rats and 2.6, 2.8, 2.9, and 2.3 $\mu mol \cdot g^{-1} \cdot min^{-1}$, in anaesthetized rats.

¶ Ueki et al. (1988) used the routine [^{14}C]DG method to determine total CMR_{glc} in ventilated, α-chloralose-anaesthetized rats (80 mg/kg infused intravenous) in the non-activated primary somatosensory cortex and homologous contralateral cortex activated by unilateral electrical stimulation of one forepaw (5 V square-wave pulse 0.3 ms at 3 Hz).

** Ueki et al. (1992) compared effects of α-chloralose (80 mg/kg, intravenous; ventilation with 30%O_2/70%N_2) with halothane (inhalation: 0.5% in 70% N_2O/30% O_2), pentobarbital (40 mg/kg, intravenous; ventilation with 30%O_2/70%N_2), and nitrous oxide (inhalation: 70% N_2O/30% O_2) on CMR_{glc} during unilateral electrical stimulation of one forepaw (5 V square-wave pulse 0.3 ms at 3 Hz). *Total* CMR_{glc} increased only in the chloralose-anaesthetized rats.

†† Data are from Table 1 of Hyder et al. (1996); values are calculated with dilution assumed from pyruvate/lactate exchange. Rates of incorporation of ^{13}C from [1-^{13}C]glucose into glutamate C4 were assayed by MRS in α-chloralose-anaesthetized rats (20 mg/kg per 30 min, intraperitoneal; ventilated with 70% N_2O/30%O_2) during unilateral electrical stimulation of the forepaw (5 V square-wave pulse 0.3 ms at 3 Hz) according to the procedure of Ueki et al. (1988). Glucose oxidation (TCA cycle, V_{TCA}) rates were calculated by metabolic modelling, and the tabulated oxidative CMR_{glc} was calculated as half of the TCA cycle rate (due to formation of two pyruvate/glucose) and represents only glucose oxidized, not total glucose utilization. Assuming $CMR_{O2}/CMR_{glc}=6$,

unconsciousness, reduced brain function, and lower ATP demand. By depressing the metabolic baseline, anaesthesia can reveal abnormal CMR_{glc} that might otherwise be masked by the higher activity in the conscious state (Frey and Agranoff, 1983). Global assays in resting, awake and pentobarbital (40 mg/kg)-anaesthetized rats show that the CMR_{O2}/CMR_{glc} ratios are similar, ~5.8, despite the 40% decrease in metabolism under pentobarbital (Linde et al., 1999). However, the CMR_{O2}/CMR_{glc} fell to 4.9 in resting halothane-anaesthetized rats (1% in 70% N_2O/30% O_2) due to increases in CBF and CMR_{glc} with no change in CMR_{O2}; lactate efflux to blood rose 3-fold, from 2 to 6% of the glucose entering brain (Linde et al., 1999). Metabolic responses to electrical stimulation of the forepaw are detected under α-chloralose (80 mg/kg) but not under pentobarbital (40 mg/kg), halothane (0.5%) and nitrous oxide (70% in 30% O_2) anaesthesia (Ueki et al., 1992). α-Chloralose has, therefore been commonly used for functional studies.

When responses to activation of different pathways and neurotransmitter systems in conscious and anaesthetized rats were assessed in parallel in the same study (Table 4), the major findings were that anaesthesia generally depressed CMR_{glc} and diminished both the absolute incremental change and the percentage change of CMR_{glc} responses to activation compared with conscious subjects. CMR_{glc} in anaesthetized-stimulated rats did, however, sometimes exceed the conscious resting rate. For example, 'light' halothane (0.5%) anaesthesia did not alter CMR_{glc} or increased it in some regions, but electrical stimulation of halothane-anaesthetized rats evoked either no or much smaller changes than in the conscious rat (Table 4). Chloral hydrate reduced the resting CMR_{glc} by approximately 30–50% in many structures, and apomorphine-induced metabolic changes were either prevented or markedly suppressed by chloral hydrate (Table 4). None of the apomorphine-induced increases in local CMR_{glc} reached the corresponding rate in conscious resting animals. In the whisker-to-barrel field pathway in resting rats, α-chloralose preferentially depressed CMR_{glc} in the thalamus and sensory cortex compared with the spinal and principal sensory trigeminal nuclei, and the metabolic responses of these two structures to whisker stimulation were blunted compared with the two trigeminal nuclei (Table 4). Notably, the absolute increases in CMR_{glc} under α-chloralose were only ~25% of those in conscious rats, the percentage changes were about half of those of conscious rats, and rates in anaesthetized-stimulated rats were lower than those in resting conscious rats (Table 4).

Electrical forepaw stimulation evoked only modest increments in *total* (i.e. flux through the hexokinase step assayed with [^{14}C]DG) or *oxidative* metabolism (i.e. ^{13}C incorporation into glutamate) of glucose in primary sensory cortex of α-chloralose-anaesthetized rats (Table 4; Shulman et al., 1999). Adjustment for the partial volume of activated tissue yielded the highest response to forepaw stimulation, ~1 $\mu mol \cdot g^{-1} \cdot min^{-1}$, approximating resting rates in other cerebral cortical structures (Table 4). Electrical stimulation of the raphe

Table 4 Continued.

CMR_{O2} can be calculated as $6CMR_{glc}$ [see Table 1 in Hyder et al. (1996) and footnote ||, above].
‡‡ Data from Table 2 of Hyder et al. (1997). Assays were carried out as above except that the stimulated TCA cycle rate was corrected for the volume fraction (0.57) of somatosensory cortex that responded to the forepaw electrical stimulation, leading to a larger response to stimulation and higher percent change.
§§ Data from Table 1 of Yang and Shen (2006). MRS assays of incorporation of [1,6-^{13}C]glucose into glutamate C4 were carried out in ventilated (70% N_2O/30%O_2), α-chloralose-anaesthetized rats (80 mg/kg intravenous, and 26.7 mg/kg per h infusion) using forepaw electrical stimulation procedures (5 mA square-wave pulse 0.3 ms at 3 Hz) similar to those of Hyder et al. (1996, 1997). Their calculated V_{TCA} with partial volume correction in the activated tissue was divided by 2 to obtain the tabulated estimate oxidative CMR_{glc}. The CMR_{glc} and percentage change during activation were substantially smaller than those of Hyder et al. (see Discussion by Yang and Shen, 2006). Assay of metabolite levels by the same laboratory (Xu et al., 2005) revealed a 15% decrease in the phosphocreatine/creatine ratio, small changes in concentrations of glutamate, glutamine, and *myo*-inositol, and no rise in lactate level above the low basal value of <0.3 μmol/g.
|| ||Rats were anaesthetized with α-chloralose: 40 mg/kg, subcutaneous, plus 20 mg/kg 2 h later. 2.6 h later, the dorsal raphe nucleus was electrically stimulated during (50 μA, 200 Hz, 1 s on, 1 s off for 50 min) during the glucose utilization assay with [^{14}C]DG.)
¶¶Ventilated (30%O_2/70%N_2O) rats were anaesthetized with α-chloralose (45 $mg \cdot kg^{-1} \cdot h^{-1}$; intravenous) for at least 1 h before data acquisition. Cerebellar climbing fibres were electrically stimulated in the inferior olive (5 Hz, pulses of 200 μs constant current, intensity of 0.15 mA) during metabolic assays. CMR_{glc} was determined with the [^{14}C]DG method, and CMR_{O2} calculated from measurements of CBF and oxygen partial pressure. Mean stimulus-evoked percentage increases in CBF, CMR_{O2}, CMR_{glc}, and extracellular lactate were 46.7, 33.4, 24 and 24% respectively.

nucleus in conscious rats produces widespread increases in CMR_{glc}, whereas under α-chloralose anaesthesia the increases in CMR_{glc} are modest, the rates are much lower than normal resting values in the same structures, and the magnitudes of incremental increases are a small fraction of those in conscious animals (Table 4). Electrical stimulation of climbing fibres to activate cerebellar cortex produces modest increases in the anaesthetized rat, and rates are well below those in conscious rats. To sum up, anaesthetics, including α-chloralose, usually markedly reduce metabolic activity in resting subjects, they restrict the maximal rise of CMR_{glc} during activation to a level either below or somewhat greater than that in the conscious resting state, and they narrow the range of increased CMR_{glc} that otherwise occurs in stimulated conscious subjects (Table 4). An important, unresolved question is whether suppression of consciousness by α-chloralose blocks or substantially reduces the disproportionate rise in glycolytic rate compared with oxidative metabolism during activation.

Anaesthetics are confounding factors in the interpretation of studies of relationships between brain function and neuroenergetics because their actions on different neurotransmitter systems, receptors, and response dynamics after sensory stimulation are complex and not fully understood (Muller et al., 2011). Responses to a fixed stimulus can vary in spatial extent and magnitude with dose, duration, and type of anaesthesia (Austin et al., 2005), and maximal response to a specific stimulus differs among anaesthetics (Kim et al., 2010). When incremental changes (i.e. the difference of stimulated minus baseline relative to baseline) are assayed, the impact of the baseline on percentage change rises with the decrement caused by anaesthesia. Thus, percentage increases in anaesthetized subjects can be misleading because they may exceed those in the conscious state even if the incremental change is smaller. Percentage changes do not reflect overall energetics required supporting brain activity, and they can be inappropriate measures of change (Table 4). The finding of negative increments (i.e. value was lower during the experimental compared with baseline condition) in some studies provoked discussions regarding interpretation of incremental changes in metabolic rate compared with total rates during rest and stimulation and the energy necessary to support a given physiological state; these issues have been reviewed by others (Gusnard and Raichle, 2001; Shulman et al., 2009).

Summary

Metabolic capacities of embryonic rat brain cells are extremely low, and enormous postnatal developmental changes alter enzyme and transporter levels on a daily basis until well after weaning. Weaning involves a fuel shift from ketone bodies, lactate and glucose in immature mammals to glucose in adult brain. Resting oxygen and glucose utilization rates in adult brain vary by 4–5-fold among white and grey matter structures. The physical, physiological and biochemical properties of the brain vasculature and brain cells ensure that fuel supply satisfies energy demand over a very wide range of activity. Despite large local differences in CMR_{glc}, glucose concentrations are maintained at similar levels throughout the brain. Glucose supply exceeds CMR_{glc} by a factor of ~1.5, and can support physiological stimulus-evoked doubling of CMR_{glc}, as well as much higher rates during abnormal conditions. The hyperaemic response to brain activation has a rapid onset, ranging from 350–500 ms to a few seconds, and the brain's capacity for CBF up-regulation is enormous, as high as 9-fold at seizure onset. Glycogen is a supplemental fuel for astrocytes. Presynaptic nerve endings (synaptosomes) isolated from adult brain have a large excess metabolic capacity, and they respond to extremely high metabolic demand arising from intense ion pumping with 5–10-fold increases in glycolysis and glucose-supported respiration. These findings support the conclusion that the brain has a rapid response-high capacity mechanism to supply oxygen and glucose to activated tissue in excess of demand. Fast delivery plus buffering by endogenous glucose and glycogen indicates that brain cells do not need supplementary substrates, such as lactate, to support activation energetics. Some endogenous lactate may be oxidized, but apparent utilization of lactate based on disappearance of extracellular lactate after a single electrical stimulus of hippocampus contributes a trivial amount (4%) to total glucose plus lactate consumption (see Table 7 in Dienel, 2011). Metabolic activities and fuel preferences in cultured astrocytes and neurons, brain slices from immature subjects and adult tissue are unlikely to be equivalent. Model systems using immature cells need not be predictive of fluxes in adult tissue.

Anaesthetics are used to reduce movement artefacts in experimental animals, and they depress brain function, consciousness and metabolic rates. Many anaesthetics block or modulate metabolic responses to various stimuli. Even under α-chloralose, most, but not all, metabolic responses evoked by different stimuli are either well below or similar to the conscious resting value. The large increases in CMR_{glc} in conscious subjects and the more nearly-similar values for total and oxidative CMR_{glc} under α-chloralose, raises the possibility that the functional activities that stimulate glycolysis in the conscious activated state are suppressed by anaesthesia. Data in the following section support the hypothesis that glycolytic flux is enhanced compared with oxidative metabolism during brain activation in conscious subjects and is linked to lactate release.

BRAIN ACTIVATION IN NORMAL, CONSCIOUS SUBJECTS

Non-oxidative metabolism of glucose usually exceeds oxidative metabolism

PET studies of human brain activation in the 1980s revealed that CBF and CMR_{glc} increased disproportionately more than CMR_{O2}, which rose slightly above the resting rate (Fox and

Raichle, 1986; Fox et al., 1988). Also, registration of human brain activation by voluntary hand movements with [^{18}F]FDG was about twice that with [^{11}C]glucose, 23% versus 12% respectively (Blomqvist et al., 1989, 1990, 1994). Hand movements caused a global reduction in the CMR_{O2}/CMR_{glc} ratio and release from brain of ^{11}C-labelled acidic metabolites of [^{11}C]glucose to blood. Blomqvist et al. (1989, 1990, 1994) concluded that [^{18}F]FDG measured total CMR_{glc} whereas rates determined with [^{11}C]glucose approximated the rate of glucose oxidation determined by global CMR_{O2}. Mental activation during a card-sorting test also increased CBF and CMR_{glc} but not CMR_{O2}, causing a fall in the global oxygen/glucose metabolic ratio along with increased lactate release to cerebral venous blood (Madsen et al., 1995).

To assess biochemical changes in brain during aerobic glycolysis, our laboratory developed an animal model using generalized sensory stimulation of conscious rats. The CMR_{O2}/CMR_{glc} ratio fell during stimulation, but it was accompanied by 44% and 30% increases in CMR_{glc} and CMR_{O2} respectively (Madsen et al., 1998, 1999). The blood lactate level increased during sensory stimulation due to muscular activity and caused slight lactate uptake into brain. Brain glucose levels were stable, but brain lactate content doubled, whereas the glycogen level fell. The net rise in brain lactate level accounted for only approximately 5% of the glucose consumed during activation, and for about half of the glucose consumed in excess of oxygen (Madsen et al., 1999). Increased brain-lactate levels during activation have been reported in many biochemical and microdialysis studies in rodent brain, as well as in MRS studies in human brain during visual stimulation (e.g., Prichard et al., 1991; Frahm et al., 1996; Mangia et al., 2007a; Lin et al., 2010b). Metabolic assays with [6-^{14}C]glucose during generalized sensory stimulation revealed a 25% increase in labelling of total brain metabolites during activation, including lactate, GABA, alanine and glutamate; labelling of glycogen was unchanged during activation and doubled during recovery from stimulation (Dienel et al., 2002). Increased glutamate labelling is consistent with the measured increase in CMR_{O2} during activation, as well as higher TCA cycle flux during electrical forepaw stimulation of anaesthetized rats (Hyder et al., 1996, 1997; Yang and Shen, 2006). Increased oxidative metabolism during brain activation has been documented by different methodologies, including a–v (arteriovenous) difference for oxygen (Quistorff et al., 2008), changes in local O_2 concentration with O_2 electrodes (Enager et al., 2009), *in vivo* assays using ^{17}O-MRS (Zhu et al., 2009), and modelling of data obtained from dynamic, calibrated fMRI assays (Buxton, 2010; Hyder et al., 2010). Disproportionate increases in glucose compared with oxygen utilization do not mean that CMR_{O2} cannot or does not increase during activation, but the increases are generally less than approximately 35%. In brain of conscious humans given various stimuli, the mean increase in CMR_{O2} is 20 ± 13% (see tabulation and discussion by Shulman et al., 2001; Mangia et al., 2007b).

To sum up, manifestation of aerobic glycolysis (reflected by a fall in the CMR_{O2}/CMR_{glc} ratio) occurs during the resting state when there is slight efflux of lactate to blood, and it usually, but not always, occurs during brain activation, as well as during and after exhaustive exercise (Shulman et al., 2001; Giove et al., 2003; Rothman et al., 2003; Dienel and Cruz, 2004, 2008; Dalsgaard, 2006; Quistorff et al., 2008; Mangia et al., 2009b). In addition to lactate production and release, increased flux into the pentose phosphate shunt pathway will contribute to the fall in CMR_{O2}/CMR_{glc} due to decarboxylation of carbon one of glucose, which consumes glucose but not oxygen. The magnitude of the CMR_{O2}–CMR_{glc} mismatch in small activated structures will be underestimated by global measurements due to mixing of venous blood from activated and non-activated regions. Also, the CMR_{O2}/CMR_{glc} will be underestimated when there is consumption of glycogen and lactate during activation if CMR_{glc} is based only on glucose a–v differences or on DG/FDG glucose utilization assays. The absolute and relative changes, if any, in fuel utilization are strongly influenced by the physiological state of the subject (conscious or anaesthetized), the stimulus paradigm, the neural pathways involved and other factors.

Underestimation of glucose utilization during brain activation with [6-^{14}C]glucose assays

Visual stimulation and kainate-induced seizures

At about the same time as the PET studies of activation in humans, Collins et al. (1987) and Ackermann and Lear (1989) reported greater registration of functional activation in autoradiographic assays with [^{14}C]DG compared with [6-^{14}C]glucose in rat brain. Higher rates of on-off flash stimuli caused progressive increases in trapping of products of [^{14}C]DG up to approximately 2-fold in the superior colliculus, whereas metabolic registration by [6-^{14}C]glucose did not increase after the initial 20% increment (Figure 4A). Kainate-induced hippocampal seizures also caused discordant results, with the incremental increase in calculated CMR_{glc} for [^{18}F]FDG being about twice that of [6-^{14}C]glucose in the same rat (Figure 4B). Failure of [6-^{14}C]glucose autoradiographic assays to fully register activation-induced increases in total ^{14}C (i.e. autoradiography assays precursor plus products) indicates that labelled metabolites must have been lost from the activated structures. Both research groups ascribed the underestimates of functional activation to increased production and release of [^{14}C]lactate from brain, with strong emphasis on the importance of stimulus-induced glycolysis (Ackermann and Lear, 1989; Lear and Ackermann, 1989; Lear, 1990). Unfortunately, lactate release from small brain structures cannot be assayed, owing to inaccessible venous output. To evaluate the basis for DG-glucose mismatches, our laboratory studied global activation of cerebral cortex and local activation of the inferior colliculus.

Cortical spreading depression

Topical application of K^+ to the dura of conscious rats induces continuous waves of depolarization that increase ion pumping, ATP demand and CMR_{glc} throughout the cerebral

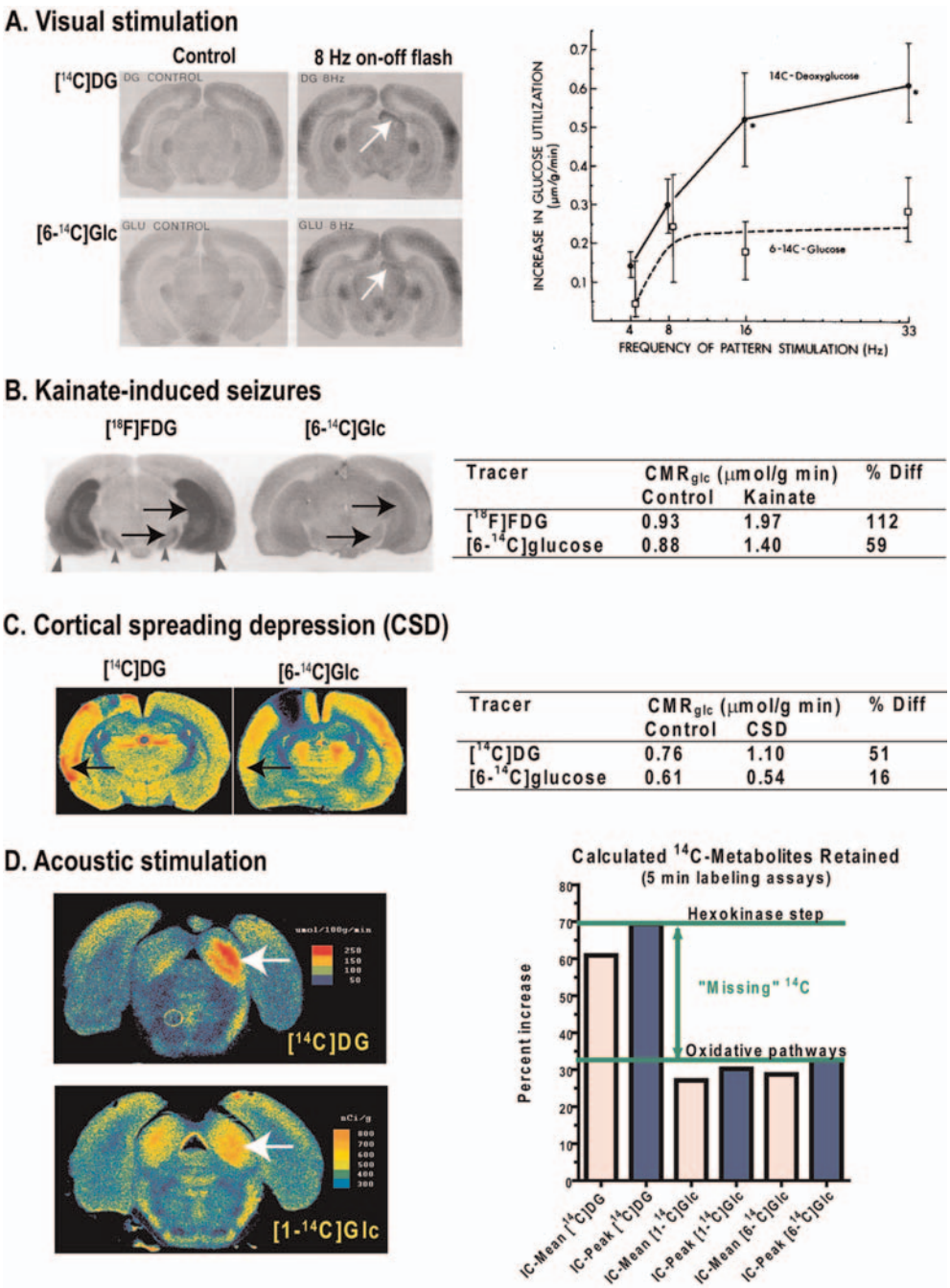

Tracer	CMR_{glc} (μmol/g min) Control	Kainate	% Diff
[18F]FDG	0.93	1.97	112
[6-14C]glucose	0.88	1.40	59

Tracer	CMR_{glc} (μmol/g min) Control	CSD	% Diff
[14C]DG	0.76	1.10	51
[6-14C]glucose	0.61	0.54	16

Figure 4 **Underestimation of metabolic activation in autoradiographic assays of glucose utilization with [1- or 6-^{14}C]glucose compared with [^{14}C]deoxyglucose**

(**A**) Rats were given unilateral visual stimulation with on-off flash to activate metabolic activity in the dorsal superior colliculus of conscious rats (white arrows). Autoradiographs illustrate images obtained from [^{14}C]DG and [6-^{14}C]glucose ([6-^{14}C]$_{Glc}$) at 8 Hz, and the graph shows the incremental increase in calculated glucose utilization above no stimulation as function of stimulus frequency. Figure reprinted from Collins RC, McCandless DW, Wagman IL (1987) Cerebral glucose utilization: comparison of [^{14}C]deoxyglucose and [6-^{14}C]glucose quantitative autoradiography. J Neurochem 49:1564–1570. published by John Wiley and Sons © International Society for Neurochemistry. (**B**) Seizures were induced in conscious rats by kainic acid prior to CMR_{glc} assays with [^{18}F]FDG and [6-^{14}C]glucose in the same rat. Glucose utilization increased in several brain structures (hippocampus, upper horizontal arrows; entorhinal cortex, large arrowheads; substantia nigra, small arrowheads and lower horizontal arrows). Registration of label accumulation by [^{18}F]FDG was much higher than for [6-^{14}C]glucose; the Table shows calculated CMR_{glc} and percentage difference (Diff) for the hippocampus. Reprinted by permission from Macmillan Publishers Ltd: [J Cereb Blood Flow Metab] (Ackermann and Lear (1989), Glycolysis-induced discordance between glucose metabolic rates measured with radiolabeled fluorodeoxyglucose and glucose, J Cereb Blood Flow Metab 9:774–785), copyright (1989). (**C**) Unilateral topical application of KCl to the dorsal left hemisphere of conscious rats increases glucose utilization; metabolic activation is higher in the [^{14}C]DG compared with [6-^{14}C]glucose autoradiographs. Colour scales indicate metabolite rate for

[^{14}C]DG and ^{14}C concentration for [^{14}C]glucose. The scale from low to high CMR_{glc} or ^{14}C concentration is blue, green, yellow and red. Quantitative values are shown in the Table. Data are from (Adachi et al., 1995; Cruz et al., 1999). (**D**) Unilateral (right) acoustic stimulation with an 8 kHz tone increases glucose utilization in groups of cells that preferentially respond to the tone. Tonotopic bands in the inferior colliculus are readily detected with [^{14}C]DG compared with [1- or 6-^{14}C]glucose (horizontal arrows), and right-left differences are also greater with [^{14}C]DG. Colour scales indicate metabolic rate for [^{14}C]DG and ^{14}C concentration for [^{14}C]glucose. The graph shows the percentage increase in labelling in 5 min metabolic assays. IC-mean denotes the mean percentage increase for the entire inferior colliculus, and the IC-peak value is for the major tonotopic band (arrow). Corresponding percentage increases were also determined with [1- or 6-^{14}C]glucose. Since DG assays total glucose utilization at the hexokinase step and glucose registers mainly the oxidative pathways (see Figure 1), the missing label represents loss of diffusible labelled metabolites of glucose. Figure reprinted from Nancy F. Cruz, Kelly K. Ball, Gerald A. Dienel (2007) Functional imaging of focal brain activation in conscious rats: Impact of [^{14}C]glucose metabolite spreading and release, J Neurosci Res 85:3254-3266 published by John Wiley and Sons Copyright © 2007 Wiley-Liss, Inc.

cortex. When autoradiographic assays were used to characterize metabolic activation during unilateral spreading depression, the level of total ^{14}C retained in brain after *in vivo* brief assays with [6-^{14}C]glucose substantially underestimated the increase registered with [^{14}C]DG (Adachi et al., 1995). K^+-activated-to-contralateral differences in various regions of cerebral cortex were $<$12% with [6-^{14}C]glucose compared with 30–60% for [^{14}C]DG (Figure 4C, left panel). Next, biochemical assays were used to separate labelled precursor and products, assay tissue glucose concentration, and calculate CMR_{glc} with each tracer using the appropriate value for the lumped constant for DG (Adachi et al., 1995). Calculated CMR_{glc} with [6-^{14}C]glucose rose only 16% in the K^+-activated hemisphere compared with 51% with [^{14}C]DG (Figure 4C, right panel). Accumulation of labelled metabolites of [6-^{14}C]glucose in tissue was very low compared with those of [^{14}C]DG even though lactate labelling and the level of unlabelled lactate rose proportionately in the K^+-treated tissue. The specific activity of brain lactate was half that of brain [6-^{14}C]glucose, indicating that the lactate was derived from blood-borne glucose and there was no lactate dilution by other carbon sources (e.g., glycogenolysis or exchange labelling with unlabelled blood lactate). As discussed below, lactate release to blood was rapid and substantial.

Acoustic stimulation

The inferior colliculus is a midbrain auditory processing structure that has the highest capillary density, blood flow rate and CMR_{glc} in brain (Gross et al., 1987). Activation of the auditory pathway with a single tone stimulus selectively activates cells that respond to that frequency and increases their metabolic rate (Ryan et al., 1982). For example, unilateral presentation of an 8 kHz tone to conscious rats evoked robust tonotopic bands of metabolic activation with [^{14}C]DG but not with [^{14}C]glucose (Figure 4D, left panel). When assays were carried out with 5 min labelling periods for both tracers and corrections were made for estimates of precursor and product in the stimulated and contralateral tissue (Cruz et al., 2007) the relative labelling by [^{14}C]DG of the activated compared with contralateral structure rose by an average of 60% (70% at the band peak), contrasting with the much lower (~30%) increase in trapping of label derived from either [1-^{14}C]- or [6-^{14}C]glucose (Figure 4D, right panel). [^{14}C]DG registers flux at the hexokinase step and represents total glucose utilization, whereas [^{14}C]glucose labels all downstream metabolites, with label trapping mainly in the amino acids derived from the oxidative pathway. In our study of metabolic labelling by [6-^{14}C]glucose during 5 min of generalized sensory stimulation of conscious rats (Dienel et al., 2002), four TCA cycle-derived amino acids accounted for about half of the label recovered in metabolites, and inclusion of labelled TCA cycle intermediates would increase this fraction further. Based on the higher total glucose utilization determined with [^{14}C]DG compared with trapping of metabolites of [1- or 6-^{14}C]glucose (Figure 4), the rise in non-oxidative metabolism is about twice that of oxidative metabolism of glucose. Furthermore, about half of the additional glucose consumed during acoustic activation was incorporated into diffusible metabolites that left the brain within 5 min. In addition to label loss, lack of prominent tonotopic bands in the [^{14}C]glucose autoradiographs (Figure 4D) suggests spread of diffusible labelled metabolites within the inferior colliculus, reducing detection of focal activation.

To sum up, autoradiographic and biochemical studies of functional metabolic activation during physiological stimulation of the visual and auditory pathways and pathophysiological activation of the hippocampus and cerebral cortex all exhibit large underestimation of brain activation when [6-^{14}C]glucose is used for brain imaging compared with [^{14}C]DG or [^{18}F]FDG.

Rapid release of unlabelled and labelled lactate to blood during brain activation

Lactate efflux from whole brain, cerebral cortex and the eye has been evaluated during rest and metabolic activation by assay of a–v differences and sampling from the jugular vein, superior sagittal sinus or retinal veins respectively.

Mental activation and halothane anaesthesia

As discussed above, small amounts of lactate are released from resting rat and human brain. Lactate release from human brain increases during mental testing (Madsen et al., 1995), and efflux of ^{11}C-labelled acidic metabolites of [^{11}C]glucose from brain during PET assays of finger tapping is consistent with lactate release (Blomqvist et al., 1989, 1990, 1994). Halothane anaesthesia enhances lactate release from resting rat brain (Linde et al., 1999).

Spreading depression and seizures

Since unilateral spreading depression caused disproportionate increases in glycolytic compared with oxidative metabolism of glucose (Figure 4C), a–v differences across the cerebral cortex were assayed during bilateral spreading cortical depression (Cruz et al., 1999). Lactate release to blood was detectable within 2 min after pulse labelling with [6-^{14}C]glucose (Figure 5A, left panel), and lactate was the predominant ^{14}C-labelled metabolite released to blood; release of $^{14}CO_2$ and ^{14}C-labelled amino acids was low and slow. After a 2–4 min lag, lactate efflux corresponded to approximately 20% of the glucose entering the brain in the same a–v pair, for both labelled and unlabelled lactate (Figure 5A, right panel). Since lactate release to blood accounted for only about half of the underestimate of local CMR_{glc} with [6-^{14}C]glucose, spreading of [^{14}C]lactate within brain was also examined. ^{14}C spread within brain was extensive enough to account for loss of laminar labelling patterns in cerebral cortex with [6-^{14}C]glucose that were visible in [^{14}C]DG autoradiographs during spreading depression (Cruz et al., 1999).

The 4–6 min lag from onset of metabolic labelling until high quantities of lactate are lost from brain (Figure 5A) probably explains, in part, apparently discrepant results obtained in assays with ^{14}C-labelled glucose and DG that used different labelling durations (Figure 5B). For example, with 0.5 min labelling assays during seizures, a large increase in metabolic labelling was registered with both ^{14}C-labelled glucose and DG. However, with 5–15 min labelling assays, the quantity of metabolites labelled by [^{14}C]glucose was not much greater than control, sharply contrasting the 1.75–3.25-fold increases registered by [^{14}C]DG (Figure 5B). Since lactate is quickly and highly labelled by glucose, pyruvate and lactate are the first non-phosphorylated, diffusible metabolites of the glycolytic pathway, and the lactate/pyruvate ratio in normal tissue is approximately 10–13 (Siesjo, 1978), enhanced lactate production and release from brain are strongly implicated as underlying causes for underestimation of CMR_{glc} with 1-^{14}C- and 6-^{14}C-labelled glucose.

Ammonia-evoked lactate release

An acute ammonia challenge increases glucose and oxygen uptake into brain and enhances release of unlabelled lactate from brain to blood, from a resting value of 4% of the glucose entering the brain to 15% after ammonia loading (Hawkins et al., 1973) (Figure 5A, right panel, green lines). The ammonia-evoked lactate efflux is particularly interesting, because the total brain lactate level was lower than arterial-blood lactate concentration. Since lactate transport is passive and concentration-gradient driven, there must have been compartmentation of brain lactate. Ammonia is detoxified by astrocytes within seconds after entering the brain due to its fixation into glutamine via the ATP-requiring glutamine synthase reaction (Cooper et al., 1979, 1985). Thus, glycolysis may have been preferentially up-regulated in perivascular astrocytic endfeet, with lactate release to blood.

Lactate efflux from the resting and stimulated eye

Lactate release from eyes of the rabbit, pig and cat is very high, ranging from approximately 20 to 100% of glucose influx, and it increases during activation compared with rest (reviewed by Dienel, 2011). In the rabbit, lactate efflux represented approximately 40–50% of glucose influx. In the pig and cat, the outer retina was more highly glycolytic than the inner retina, and lactate release increased in the dark (activation). Krebs (1972) noted that aerobic glycolysis in the retina is exceptionally high compared with other organs, particularly in avian species with high visual acuity. The cellular origin of the lactate produced by the retina remains to be unequivocally established, but, based on widespread labelling by [^{3}H]DG throughout all retinal layers, both retinal neurons and Müller cells probably consume glucose and may produce and release lactate (Winkler et al., 2003).

Summary

The above studies demonstrate that metabolic activation is not registered by labelled glucose to the same extent as DG or FDG, whether using PET, autoradiographic or biochemical methods. DG-glucose mismatches occur in cerebral cortex, hippocampus, superior colliculus and inferior colliculus under normal or pathophysiological conditions. All four of these brain regions have glutamatergic signalling pathways. The magnitude of increased trapping of labelled glucose metabolites during activation ranges from ~15% to 60%. The increment is smallest for physiological stimulation of visual and auditory pathways and highest during seizures (Figures 4 and 5). Label from glucose is rapidly incorporated into highly labelled diffusible metabolites, mainly lactate that quickly carry substantial amounts of label out of activated tissue to blood.

Lactate release and models for neuron–astrocyte energetics during brain activation

High lactate release

The robust nature of the discordant DG-glucose autoradiographs and the rapid, substantial loss of lactate from activated brain strongly contradict the notion that lactate generated within the brain is an important neuronal fuel during activation. As illustrated in Figure 5(C), pyruvate can be directly oxidized in the cell that phosphorylated the glucose, or it can be converted into lactate and released to extracellular fluid. Extracellular lactate can be released from the tissue and locally oxidized. Lactate release reduces the amount of trapped label. Local uptake and oxidative metabolism of extracellular labelled lactate, regardless of its cellular origin and cellular fate, should be accompanied by label incorporation into TCA cycle-derived amino acids

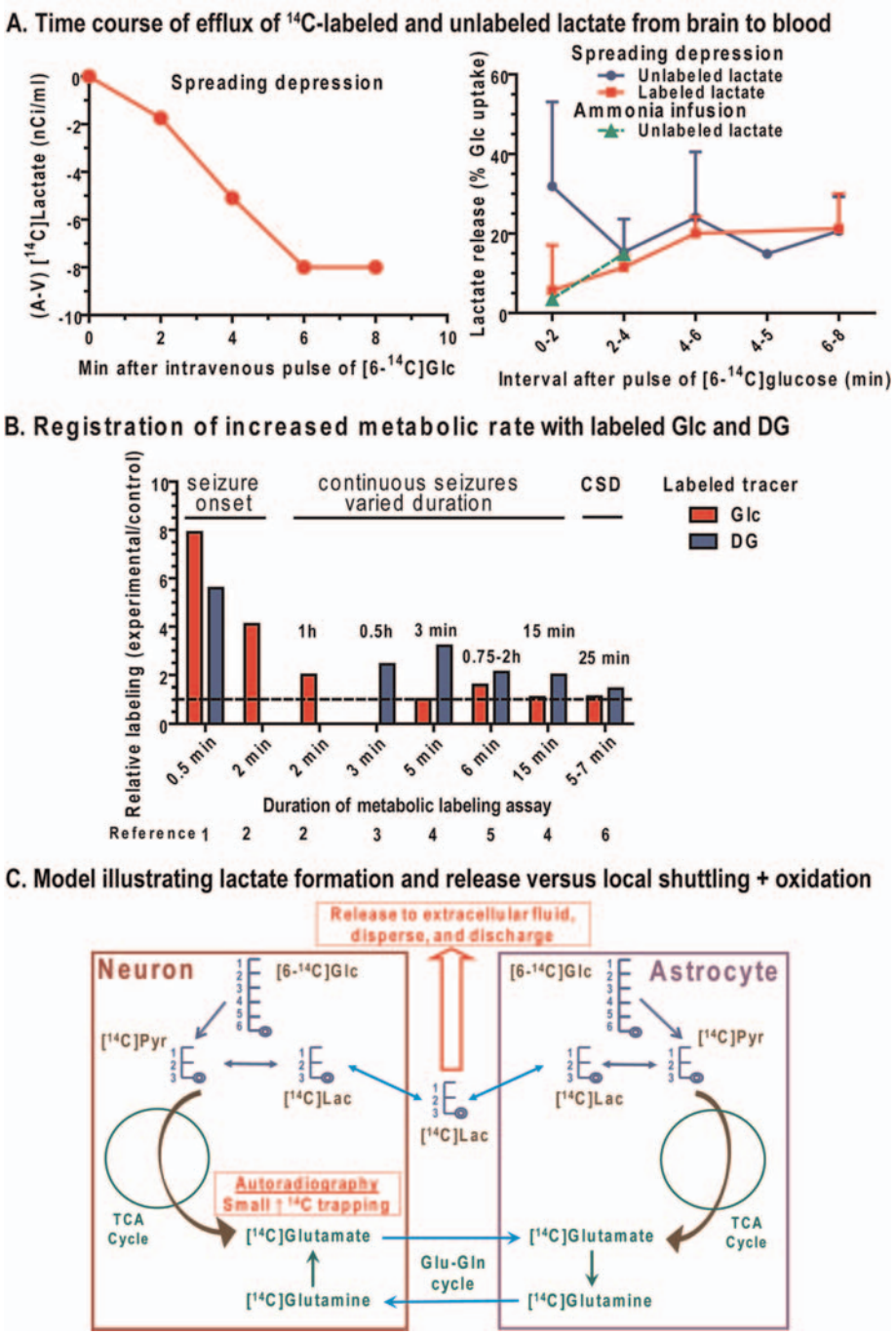

Figure 5 **Lactate efflux from brain and dependence of underestimation of metabolic activation with [^{14}C]glucose on duration of labelling assay**

(**A**) Left panel: time course of release of [^{14}C]lactate from brain at intervals after pulse labelling with [6-^{14}C]glucose during bilateral cortical spreading depression. Each point represents the a–v difference during a 2-min sampling interval plotted at the time of the end of the interval. Lactate was the predominant labelled compound released to blood; release of ^{14}C-labelled amino acids and $^{14}CO_2$ into venous blood was very low and slow (not shown). Reprinted by permission from Macmillan Publishers Ltd: (J Cereb Blood Flow Metab] (Cruz NF, Adachi K, Dienel GA (1999), Rapid efflux of lactate from cerebral cortex during K+ -induced spreading cortical depression., J Cereb Blood Flow Metab 19:380-392), copyright (1999). Right panel: time courses of release of labelled and unlabelled lactate from brain at intervals after pulse labelling during spreading cortical depression [reprinted by permission from Macmillan Publishers Ltd: (J Cereb Blood Flow Metab) (Cruz NF, Adachi K, Dienel GA (1999), Rapid efflux of lactate from cerebral cortex during K+ -induced spreading cortical depression., J Cereb Blood Flow Metab 19:380-392), copyright (1999)] or after an acute intravenous ammonia injection where the values plotted at 2–4 min are actually at 4–5 min (data from Hawkins et al., (1973). Values are expressed as percentage of glucose entering the brain in the same a–v sample pair. (**B**) Labelled glucose registers large increases in metabolic activation with very short (0.2–2 min), but not longer (5–15 min) assay intervals. Data are expressed relative to the

control value in each study. Duration of seizures or CSD (cortical spreading depression) is indicated above the respective data sets. Data are from the following references: (1) (Miller et al., 1982); (2) (Borgstrom et al., 1976); (3) (Cremer et al., 1988); (4) (Van den Berg and Bruntink, 1983); (5) (Ackermann and Lear, 1989); (6) (Adachi et al., 1995). **(C)** Glucose is metabolized in neurons and astrocytes, and autoradiographic studies indicate that a large fraction of the label derived from glucose is not retained in the cell (Figure 4). If lactate were produced by either neurons or astrocytes and shuttled to another cell where it is oxidized, the label should be diluted into the large amino acid pools due to the action of the MAS (Figure 1) and trapped in the activated tissue. Lack of trapping indicates rapid release of labelled metabolites, mainly lactate. Reprinted from Neurochem Int, 45, Dienel GA and Cruz NF, Nutrition during brain activation: does cell-to-cell lactate shuttling contribute significantly to sweet and sour food for thought? 321–351, Copyright (2004), with permission from Elsevier.

(mainly glutamate), followed by dilution in the large amino acid pools and retention of label in activated tissue (Figure 5C). If cell-to-cell lactate production and shuttling coupled to its local oxidation and label trapping were quantitative, the relative increase in label during activation would be similar for [^{14}C]DG (total glucose utilization) and for [^{14}C]glucose (mainly oxidative glucose utilization) because label in lactate would be retained in the activated region. However, this was not the case. Relative increases during activation were substantially smaller for [^{14}C]glucose compared with [^{14}C]DG (Figures 4 and 5), and large amounts of lactate are released. These findings are relevant to several models for the cellular basis of neuroenergetics.

Astrocyte-to-neuron lactate shuttle model

On the basis of tissue culture experiments in which glutamate exposure evoked an increase in DG phosphorylation and lactate efflux to the culture medium, Pellerin and Magistretti (1994) proposed that astrocytic uptake of glutamate plus Na^+ from the synaptic cleft stimulates astrocytic glycolysis to satisfy the energy demand for two ATP associated with Na^+ extrusion and glutamine synthesis from glutamate. The lactate is stated to be transferred to nearby neurons, where it serves as an important oxidative fuel during excitatory glutamatergic neurotransmission. This model predicts predominant cellular compartmentation of glycolytic (astrocytic) and oxidative (neuronal) metabolism during activation and it links lactate shuttling to glutamatergic neurotransmission and to glutamate-glutamine cycling between neurons and astrocytes (Magistretti et al., 1999; Pellerin and Magistretti, 2004, 2011; Pellerin, 2005, 2008, 2010; Hyder et al., 2006; Pellerin et al., 2007; Jolivet et al., 2010). The data described above (Figures 4 and 5) do not fulfil a central prediction of the astrocyte-to-neuron lactate shuttle model, that is, the rise in total glucose utilization during brain activation of normal conscious subjects *in vivo* would be accompanied by a corresponding increase of similar magnitude in trapping of labelled products of glucose via the oxidative pathways.

Redox shuttle model

Cerdan et al. (2006) proposed a different shuttle process that is also based on astrocytic production of lactate and its transfer to neurons where it is oxidized to pyruvate. However, this pyruvate is then released from neurons and transported back to astrocytes for oxidation or conversion into lactate to facilitate astrocytic glycolysis. This redox shuttle mechanism transfers reducing equivalents (NADH) from astrocytes to neurons and by-passes the astrocytic MAS; neurons oxidize the NADH and thereby can generate more ATP (Figure 1). In principle, a small fraction of the pyruvate-lactate in activated cells could sustain this redox shuttle system by cycling between adjacent cells, in contrast with net transfer of lactate from astrocytes to neurons in the Pellerin–Magistretti model. Redox shuttling and lactate release are compatible concepts.

Neuron-to-astrocyte lactate shuttle

The predicted direction and magnitude of cell-to-cell lactate shuttling is governed by model assumptions. Modelling of lactate carbon flow during brain activation has a novel outcome when based mainly on nutrient transporter levels and two assumptions: (i) more rapid glucose transport into neurons compared with astrocytes and (ii) up-regulation of glycolysis in both neurons and astrocytes. In this model, neuronal glucose uptake is posited to be predominant, neurons produce and release lactate to extracellular fluid, and lactate is taken up by astrocytes; the magnitude of neuron-to-astrocyte lactate shuttling is calculated to be quite small, of the order of 10% of ΔCMR_{glc} (Simpson et al., 2007; Mangia et al., 2009a, 2011; DiNuzzo et al., 2010a). An extension of this model (DiNuzzo et al., 2010b, 2011) includes contributions of astrocytic glycogenolysis. Glycogen utilization is predicted to maintain astrocytic Glc-6-P levels high enough to inhibit hexokinase, thereby reducing astrocytic utilization of extracellular and blood-borne glucose. Glycogen would serve to fuel astrocytes and also provide a mechanism to reduce glucose use by astrocytes and increase its availability to neurons during activation. This model raises the possibility that lactate released from brain during activation may be comprised of blood glucose-derived lactate mainly from neurons plus glycogen-derived lactate from astrocytes. The fate of pyruvate derived from glycogen in brain *in vivo* is not known, but in our previous studies, the specific activity of brain lactate was half that of blood and brain [6-^{14}C]glucose (i.e. it was not diluted by other sources of unlabelled lactate; see below: lactate exchange), raising the possibility that the glycolytic pathways for glucose and glycogen may be segregated.

Maximal contribution of cell-to-cell lactate shuttling

Since lactate metabolism requires oxidation, the rise in trapping of products of labelled glucose or the incremental

increase in CMR_{O2} during brain activation represents the maximal contribution for lactate shuttling during activation compared with rest. In other words, if all of the additional glucose consumed during brain activation compared with rest were phosphorylated and converted into lactate in one cell type, then transferred to another cell type for oxidation, the rise in product trapping or CMR_{O2} reflects the maximal magnitude of this process, which ranges from approximately 0 to 35% above rest in most studies of normal conscious human and animal subjects. The contribution of shuttling is, however, likely to be much lower than that represented by increases in product trapping or CMR_{O2}. For example, the contribution of lactate shuttling must be reduced by the proportion that (i) the 'glycolytic' cell type (that releases the lactate) also oxidizes pyruvate and (ii) the lactate recipient cell also phosphorylates glucose. Both neurons and astrocytes phosphorylate and oxidize glucose, but the proportions during brain activation are not known. If one assumes that astrocytes directly oxidize approximately 25–30% of the glucose via the pyruvate carboxylase and PDH reactions (reviewed by Hertz, 2011a) and that astrocytes and neurons each phosphorylate about half of the glucose (Nehlig et al., 2004), then the maximal contribution of any cell-to-cell lactate shuttling coupled to local lactate oxidation falls to a quite low level, of the order of $<$10%.

Astrocyte glycogenolytic and oxidative metabolism rises during activation and abnormal conditions

Brain activation stimulates fluxes in many pathways in astrocytes. The fact that oxidative metabolism increases indicates that astrocytes have significant, unidentified energy demands that stimulate consumption of minor or alternative substrates during brain activation, including glycogen (Table 3) (Hertz et al., 2007; Dienel, 2011). In tissue culture, glutamate taken up from extracellular fluid is readily oxidized by astrocytes, and the proportion increases with extracellular glutamate level (McKenna et al., 1996). Na^+-dependent glutamate uptake stimulates astrocytic oxygen consumption by 55% with 100 μmol/l extracellular glutamate (Eriksson et al., 1995), which would provide much more ATP than a rise in glycolysis reflected by the 100% increase DG metabolism evoked by 500 μmol/l glutamate (Pellerin and Magistretti, 1994). It is not known how much neurotransmitter glutamate is oxidized during activation *in vivo*, but small increases in oxidative metabolism will generate more ATP in astrocytes than large increases in glycolysis (Table 2). Acetate is preferentially oxidized by astrocytes *in vitro* and *in vivo*, and labelled acetate is used to measure astrocytic oxidative activity in resting (Lebon et al., 2002; Deelchand et al., 2009; Patel et al., 2010) and activated brain. Acetate oxidation increases during acoustic activation (Cruz et al., 2005), visual stimulation (Dienel et al., 2007b), spreading cortical depression (Dienel et al., 2001a), and other conditions in rats and humans (Wyss et al., 2009). Acetate oxidation also increases after behavioural training (Dienel et al., 2003), in reactive cells responding to stab wound injury (Cetin et al., 2003), in gliotic brain tumours (Dienel et al., 2001b), in experimental epilepsy (Hosoi et al., 2010), and is altered after ischaemia (Hosoi et al., 2007) and by NMDA (*N*-methyl-D-aspartate) receptor activity (Hirose et al., 2009). Elevated extracellular $[K^+]$ enhances acetate oxidation in brain slices (Schweigert et al., 2004), suggesting that uptake of K^+ released during neuronal activity stimulates astrocytic respiration in adult brain. Thus, astrocytic energetics during excitatory neurotransmission is not described solely by glycolytic metabolism of blood-borne glucose, and the astrocyte-to-neuron lactate shuttle is incomplete because it does not include astrocytic oxidative or glycogenolytic metabolism during activation. Astrocytic metabolism can be regulated by complex mechanisms and integrated with amino acid shuttling (Brookes, 1997, 2000). The functions of ATP derived from glycolytic, glycogenolytic and oxidative pathways in astrocytes in adult brain need to be established.

To sum up, results obtained from *in vivo* brain activation studies in many laboratories provide strong evidence against local oxidation of large amounts of lactate generated from glucose in brain (Figures 4 and 5). It is therefore necessary to elucidate details of the biochemical and physiological processes that take place during activation. Our laboratory took the approach of 'following the money', that is, the fate of lactate and glucose label during brain activation in normal conscious rats.

Routes for loss of labelled lactate and other labelled metabolites

My laboratory has a long-standing interest in understanding the basis of metabolic brain images and the reasons for the large underestimation of CMR_{glc} when assayed with [^{14}C]glucose during brain activation. The following sections summarize our assessment of biochemical and physiological processes underlying images obtained with [^{14}C]DG and [1- and 6-^{14}C]glucose during acoustic stimulation of the inferior colliculus of conscious rats. Major pathways involved in metabolite trapping or release are illustrated in Figure 6(A). The numbers identify pathways that were evaluated in experiments described in Figures 6(B)–6(D). For reference, Figure 6 also shows: (i) a [^{14}C]DG autoradiograph with tonotopic bands in the right inferior colliculus characterized by two peaks of high metabolic activity (black) and a 'valley' between peaks with lower but elevated activity (red); and (ii) a [1-^{14}C]glucose autoradiograph that lacks prominent tonotopic bands. DG is trapped as DG-6-P (pathway 1), whereas label from glucose is contained in all downstream compounds and it accumulates mainly in TCA cycle-derived amino acids (pathway 2). Pathway 7 denotes net metabolite release (see Figure 4). Note that it is extremely difficult to quantitatively account for all of the label delivered to and metabolized by the brain during *in vivo* studies for two major reasons. (i) Living brain is an 'open system'. Substrates and metabolites can enter and leave a region of interest by various routes. (ii) The vascular supply of most brain regions is

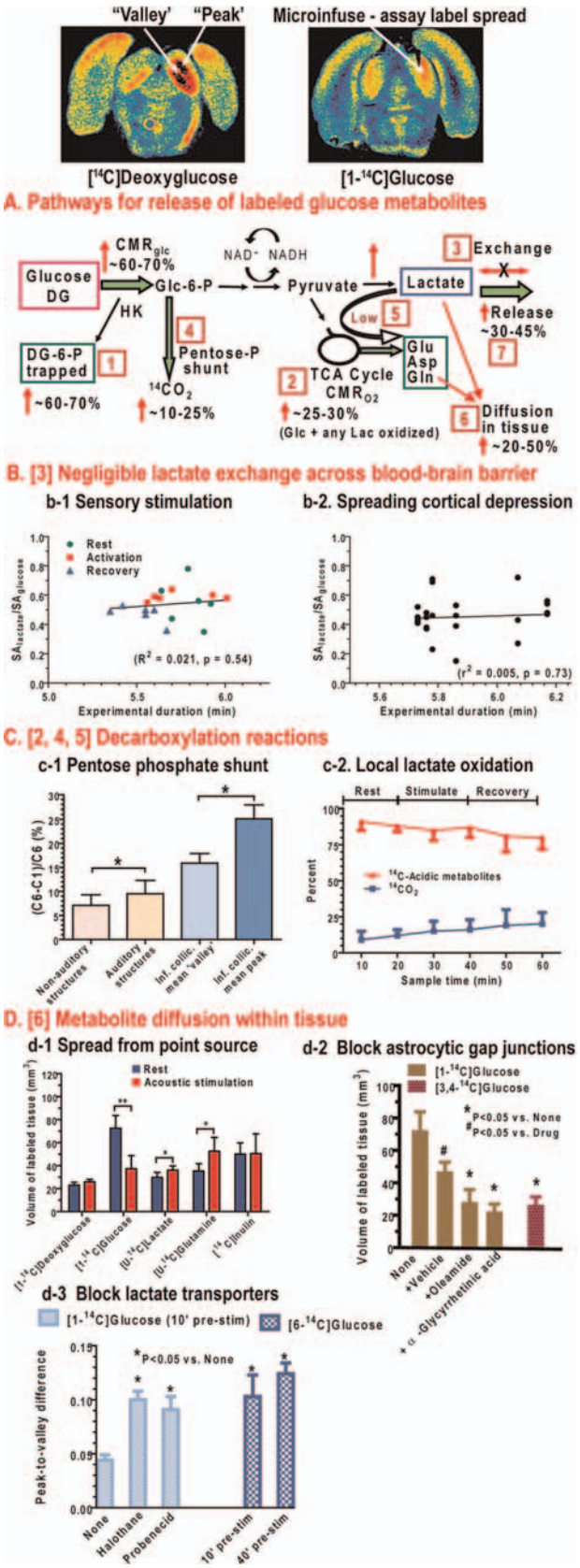

Figure 6 Assessment of pathways and routes for release of label from activated tissue

For reference, autoradiographs from conscious rats given unilateral single-tone acoustic stimulation show the patterns of metabolic labelling with ^{14}C-labelled DG and glucose (From Cruz et al., 2007; see Figure 4D). The tonotopic bands with the highest rates of glucose utilization in the [^{14}C]DG autoradiograph (black) are denoted as 'peaks' and the region between the two peaks as 'valley' (see Figure 6D, d-3). In some studies labelled tracers were microinfused into the inferior colliculus of the conscious rat to evaluate lactate oxidation (Figure 6C, c-2) or label spreading (Figure 6D). (**A**) Diagram illustrating major sites for trapping or release of metabolic tracers. The numbers in boxes represent pathways that are assessed in (**B–D**) and identified in brackets in the titles. The difference in trapping of metabolites of DG (**A**, pathway 1) and retention of labelled metabolites of glucose (**A**, pathway 2) reflects loss of label from activated tissue (**A**, pathway 7). (**B**) Ratio of specific activity of brain lactate to that of brain glucose as function of experimental duration before, during, and after generalized sensory stimulation (b-1) and during spreading depression (b-1). The mean relative specific activity (SA) of lactate is half that of [6-^{14}C]glucose, that is, equal the theoretical maximum, because [6-^{14}C]glucose produces one labelled and one unlabelled lactate, reducing the specific activity in half. These data rule out exchange (**A**, pathway 3) as a major factor in label loss, because release of labelled lactate and uptake of unlabelled lactate would reduce lactate specific activity. Figure reprinted from Dienel and Cruz, 2009 Exchange-mediated dilution of brain lactate specific activity: implications for the origin of glutamate dilution and the contributions of glutamine dilution and other pathways. J Neurochem 109 Suppl 1:30-37 published by John Wiley and Sons © 2009 The Authors. Journal Compilation © 2009 International Society for Neurochemistry. (**C**, **c–1**) C1 of glucose is lost by decarboxylation via the pentose-phosphate shunt pathway. Pentose shunt pathway flux was calculated from data in the study of (Cruz et al., 2007) from differential labelling of the total metabolite pool by [1- and 6-^{14}C]glucose, expressed as a percentage: 100*([6-^{14}C]glucose–[1-^{14}C]glucose)/[6-^{14}C]glucose. These values mainly represent the percentage of oxidative metabolism of glucose, which would be higher than the percentage of total glucose utilization. These results demonstrate that loss of label from C1 of glucose increases to approximately 25% of the level of glucose oxidation during acoustic activation (**A**, pathway 4). (**c–2**) Local oxidation of lactate generated from [3,4-^{14}C]glucose microinfused into the inferior colliculus of conscious rats. ^{14}C from C3,4-labelled glucose is released at the PDH step, and if lactate is formed and rapidly, locally oxidized the level of $^{14}CO_2$ in extracellular fluid should be similar to that of [^{14}C]lactate. However, lactate accounted for approximately 80% of the ^{14}C in extracellular fluid, ruling out high rates of local oxidation of lactate generated from glucose in brain (**A**, pathway 5). Reprinted with permission from Kelly K Ball, Nancy F Cruz, Robert E Mrak and Gerald A Dienel (2010), Trafficking of glucose, lactate, and amyloid-beta from the inferior colliculus through perivascular routes, J Cereb Blood Flow Metab 30:162-176. (**D**, **d–1**) Different tracers were microinfused into the inferior colliculus of conscious rats during rest and acoustic stimulation, and the volume of labelled tissue measured. The volume labelled by DG did not change during activation. The higher volume labelled by glucose compared with DG during rest indicates that metabolites downstream of Glc-6-P diffused from the site of phosphorylation, and the fall in labelled volume during activation indicates product loss or restricted movement of metabolites. Spreading of lactate and glutamine increased during acoustic stimulation, whereas that of the extracellular marker, inulin, did not. (**d–2**) Microinfusion of two gap junction inhibitors into the unstimulated inferior colliculus before [^{14}C]glucose significantly reduced label spread, consistent with metabolite diffusion through astrocytic gap junctions. If label spread were mainly due to lactate, the volume of labelled tissue should be high for [3, 4-^{14}C]glucose because label would be retained in lactate; the low volume suggests diffusion of TCA cycle-derived compounds (e.g., glutamate, glutamine). (**d–3**) The peak-to-valley ratio is a measure of focal activation. The higher the ratio, the greater the rise in local CMR_{glc} in the peak compared with an adjacent region, the valley. The ratio doubled when assayed in halothane-anaesthetized rats (halothane can block gap junctions) and with probenecid treatment to block lactate transport. Changing the position of the label to C6 of glucose also doubled the ratio, which was the same at the beginning or end of the routine DG assay (indicating no change in metabolic response during the 45 min interval). Plotted from data of Cruz et al. (2007). Together, these findings demonstrate that spreading of metabolites within activated tissue is mediated, in part, by lactate transporters and astrocytic gap junctions, and it contributes to loss of registration of focal activation when [^{14}C]glucose is the tracer (**A**, pathway 6).

not accessible for cannulation and input and output cannot be determined along with blood flow and metabolic rates. Even when a–v differences across the whole brain or cerebral cortex are assayed, activation is difficult to evaluate because the structures cannot be uniformly activated, and a–v differences are the combined result of contributions from activated and non-stimulated regions.

Lactate exchange

Label loss can arise from exchange of labelled lactate in brain for unlabelled lactate in blood (pathway 3). Exchange reactions would cause the specific activity of brain lactate (i.e. the quantity of label in lactate divided by the quantity of unlabelled lactate) to fall due to dilution of labelled brain lactate by unlabelled blood lactate. This process is high in immature rats due to >10-fold higher levels of MCTs at the blood–brain barrier than in adults (Cremer and Heath, 1974; Cremer et al., 1979). However, at 5–7 min after pulse labelling with [6-^{14}C]glucose, the mean specific activity of rat brain lactate equalled the theoretical maximum (i.e. 0.5 due to formation of one labelled and one unlabelled pyruvate) during rest, sensory stimulation, and recovery from sensory stimulation (Figure 6B–b1) and during spreading cortical depression (Figure 6B–b2). These data rule out significant label loss by lactate exchange in 5–10 min experiments in normal adult rat brain (Dienel and Cruz, 2009).

Pentose-phosphate shunt pathway

Entry of Glc-6-P into the pentose shunt pathway (Figures 1A and 6A, pathway 4) leads to oxidative decarboxylation of C1 and generation of NADPH and ribulose-5-P. When CMR_{glc} is assayed with C1-labelled glucose, the pentose pathway will cause label loss and underestimation of CMR_{glc}. Up-regulation of this pathway will also reduce the CMR_{O2}/CMR_{glc} ratio because glucose is consumed without involving respiration. For every six glucose molecules entering the pentose pathway, one glucose equivalent (16.6%) is converted into CO_2. The ribulose-5-P from the other five glucose molecules enters the non-oxidative branch of the pentose pathway and undergoes a series of transketolase–transaldolase reactions to produce glyceraldehyde-3-P and fructose-6-P that then re-enter the glycolytic pathway upstream of the ATP generating reactions (Figure 1A). This means that when the pentose shunt pathway is up-regulated and nucleotide biosynthesis is negligible, 83% of the glucose carbon that entered the pathway is re-cycled to glycolysis. If phosphorylated pentose-phosphate shunt intermediates did not re-enter the glycolytic pathway, phosphate would be trapped in these intermediates and reduce its availability for synthesis of ATP. Since most of glucose carbon returns to energy-producing pathways, the emphasis by Jolivet et al. (2010) and Pellerin and Magistretti (2011) on the inability of neurons to increase glycolytic flux and the requirement for cultured embryonic cortical neurons to direct glucose into the pentose pathway at the expense of glycolysis (Herrero-Mendez et al., 2009) is misleading and incorrect. In fact, many laboratories have shown that neuronal cultures can increase glucose transport and utilization (Dienel, 2011).

The flux through the pentose shunt pathway during rest and acoustic stimulation was calculated from data obtained in our previous studies (Cruz et al., 2007) by taking advantage of the differential loss of $^{14}CO_2$ from [1-^{14}C]glucose compared with [6-^{14}C]glucose when Glc-6-P enters the pentose shunt pathway (Figure 6A). In non-auditory structures, pentose shunt flux was ~7% of the total label recovered in metabolites of [6-^{14}C]glucose (i.e. trapped via the oxidative pathways), a value similar to the ~2–8% of glucose metabolism obtained in previous studies in rat brain (Ben-Yoseph et al., 1995 and cited references). Pentose shunt activity increased to ~10% in auditory structures during acoustic stimulation, to 15% in the 'valley' between the two tonotopic bands in the activated inferior colliculus (Figure 6, top left), and to 25% in the major tonotopic band (Figure 6C-c1). Thus, biochemical and MRS metabolic assays that use C1-labelled glucose are subject to significant label loss and underestimates of CMR_{glc} when the pentose shunt pathway is activated. This activity also contributes to the fall in CMR_{O2}/CMR_{glc} ratio.

Local oxidation of lactate

Labelling studies showed that lactate is quickly and highly labelled by glucose (Adachi et al., 1995; Cruz et al., 1999; Dienel et al., 2002), and microdialysis studies during acoustic activation showed that extracellular lactate level in the inferior colliculus approximately doubled, whereas glucose level was stable (Cruz et al., 2007). Glucose-derived label could be lost from activated domains by local uptake of extracellular lactate and its oxidation in small compartments that do not readily equilibrate with the large pools of unlabelled amino acids (Figure 6A, pathway 5). For example, isolated pools may be located in pre- and post-synaptic neuronal structures and in filopodial perisynaptic astrocytic processes. Synaptosomes and dendritic shafts (but not spines) are known to contain mitochondria, and perisynaptic astrocytic processes were recently shown to contain mitochondria (Lovatt et al., 2007; Lavialle et al., 2011; Pardo et al., 2011). To test the possibility of local lactate oxidation, [3,4-^{14}C]lactate was microinfused into the inferior colliculus of conscious rats, and ^{14}C-labelled CO_2 and acidic compounds (pyruvate/lactate) were assayed in microdialysate that was simultaneously collected via combination infusion-dialysis probes (Ball et al., 2010). If lactate were produced from [3,4-^{14}C]glucose, taken up into nearby cells and rapidly oxidized, $^{14}CO_2$ would be released by PDH, and quantities of [^{14}C]lactate and $^{14}CO_2$ in the microdialysate would be similar. This was not observed. Lactate accounted for ~80% of the label and CO_2 ~20% (Figure 6C-c2). These findings rule out rapid, substantial local oxidation of lactate generated in brain from microinfused glucose. Cell-to-cell lactate shuttling

coupled to local oxidation is low in the inferior colliculus of conscious resting and stimulated rats.

Metabolite spreading during activation versus rest

Spreading of labelled metabolites within tissue can disperse locally high metabolite levels, reduce registration of focal activation and contribute to release from brain (Figure 6A, pathway 6). Our initial studies (Cruz et al., 1999) showed that label from [^{14}C]lactate diffused within brain when supplied by a point source. To further evaluate this process, labelled compounds were microinfused into the inferior colliculus of conscious rats during rest and acoustic stimulation (Cruz et al., 2007). The volume of tissue labelled by [^{14}C]DG was equivalent during rest and activation, indicating the activity state did not alter the number of cells that took up and metabolized the infused DG (and glucose) (Figure 6D-d1). In sharp contrast, [1-^{14}C]glucose labelled a volume approximately 3-times greater than that of DG during rest and the labelled volume was lower during activation. This indicates that metabolites downstream of Glc-6-P diffused into the larger volume and that there was label loss during activation or conversion into metabolites that did not spread readily. Lactate and glutamine are known to be released to extracellular fluid, and the volumes labelled by these compounds and their metabolites increased during acoustic stimulation. Spreading of [^{14}C]inulin, an extracellular space marker, was unaffected by activation, suggesting that glutamine and lactate may have diffused, in part, through intracellular routes.

Astrocytic gap junctional trafficking

Astrocytes are known to be coupled by gap junctional channels that permit transcellular diffusion of small molecules within the syncytium. A role for astrocytic gap junctional communication in metabolite spreading *in vivo* was tested by first microinfusing a gap junction inhibitor, α-glycyrrhetinic acid or oleamide, into inferior colliculus of non-stimulated, conscious rats, then infusing labelled glucose (Cruz et al., 2007). These drugs markedly reduced spreading of label derived from [1-^{14}C]glucose compared with control or vehicle-infused animals (Figure 6D-d2), implicating diffusion within the astrocytic syncytium as a route for dispersal of glucose metabolites. Label derived from [3,4-^{14}C]glucose is retained in pyruvate and lactate, but it is lost via decarboxylation by PDH. If lactate diffusion were responsible for the large volume labelled by [1-^{14}C]glucose in the non-stimulated inferior colliculus, then [3,4-^{14}C]glucose should also label a large volume, like [1-^{14}C]glucose. However, the volume labelled by [3,4-^{14}C]glucose in non-stimulated tissue was very low, suggesting that decarboxylation reduced its ability to spread. Thus, TCA cycle-derived compounds may have contributed to the large volume labelled by [1-^{14}C]glucose under resting conditions.

Lactate transporters

Lactate is diffusible, and inhibition of its transport with probenecid enhanced registration of tonotopic bands in autoradiographs generated from metabolism of [1-^{14}C]glucose. The 'peak-to-valley' difference reflects tonotopic band contrast (Figure 6, top left panel), and this value doubled when assayed after probenecid treatment (Figure 6D-d3). The peak-to-valley difference also increased in halothane-anaesthetized rats (see Discussion in Cruz et al., 2007) and when the position of the label in glucose was changed from the C1–C6 position to prevent label loss via the pentose shunt pathway. The same values were obtained when the 5-min labelling assays were carried out with C6 glucose at the onset and at the end of the routine 45 min DG labelling period (Figure 6D-d3), indicating that glucose metabolism did not 'adapt' to prolonged stimulation during the longer period of the DG assay. Together, these findings link loss of focal registration of metabolic activation to lactate efflux from activated cells, increased diffusion of lactate and other metabolites during activation, and astrocytic trafficking of labelled metabolites (Ball et al., 2007; Cruz et al., 2007).

Extensive astrocytic gap junctional coupling and restricted transfer of hexose-6-P

Small molecules $<$1 kDa are generally permeable to gap junctional channels. If [^{14}C]DG were metabolized mainly in astrocytes during activation as proposed by the lactate shuttle model, then the [^{14}C]DG-6-P would be expected to spread among coupled astrocytes in the inferior colliculus during the 45 min experimental period of the routine DG method. Intercellular diffusion of DG-6-P should diminish registration of tonotopic bands with long experimental intervals, yet this did not occur (Figures 4 and 6). This observation raised several possibilities: (i) neurons metabolize most of the DG and glucose; (ii) astrocytes in the inferior colliculus are poorly coupled; and (iii) DG-6-P did not go through gap junctions. Since quantitative assay of cellular metabolic activity has not yet been achieved in any laboratory, we evaluated the number of dye-coupled cells in the inferior colliculus and hexose-6-P permeability of astrocytic gap junctions.

The size of the astrocytic syncytium in acute slices of adult rat inferior colliculus was evaluated by impaling a single astrocyte located in the middle of the slice with a Lucifer Yellow-filled micropipette and allowing the dye to diffuse into that cell for 5 min, that is, the same duration of the [^{14}C]glucose assay (Ball et al., 2007). Lucifer Yellow spread radially from the centre of the slice toward the meningial border, and heterogeneously labelled up to approximately 10 000 astrocytes (Figure 7A-a). At about a millimetre from the injection site there was strong labelling of astrocytic soma (Figure 7A–b) and perivascular structures (Figure 7A-c) that represent dye-coupled endfeet (Simard et al., 2003). Astrocytes in the inferior colliculus are extensively coupled, and dye spreading demonstrates that material from a single

cell can be rapidly and widely dispersed to astrocytic soma and perivascular endfeet.

Gap junctional permeability of three hexose-6-Ps was tested directly using radioactive, fluorescent and microenzymatic methods (Gandhi et al., 2009b). In brief, Glc-6-P, DG-6-P and NBDG-6-P were demonstrated to be very poorly gap-junction permeant, whereas the parent non-phosphorylated hexoses, glyceraldehyde-3-P, NADH, NADPH and three anionic fluorescent dyes used as internal standards for the transfer assays readily diffused among coupled astrocytes (Figure 7B). DG-6-P and NBDG-6-P can provide cellular resolution of metabolism because their diffusion among astrocytes is highly restricted. The hexokinase regulator, Glc-6-P, is also restricted to the cell where generated, facilitating feedback control of glycolysis. In contrast, downstream metabolites and redox compounds do spread from cell to cell, and trafficking may include glutamate and glutamine. A previous report of gap junctional transfer of [U-^{14}C]Glc-6-P, [U-^{14}C]glutamate, and [U-^{14}C]glutamine (Giaume et al., 1997) measured ^{14}C spread without identifying the compounds transferred. Diffusion of label derived from Glc-6-P must have arisen from downstream metabolites, and amino acid metabolism is not ruled out.

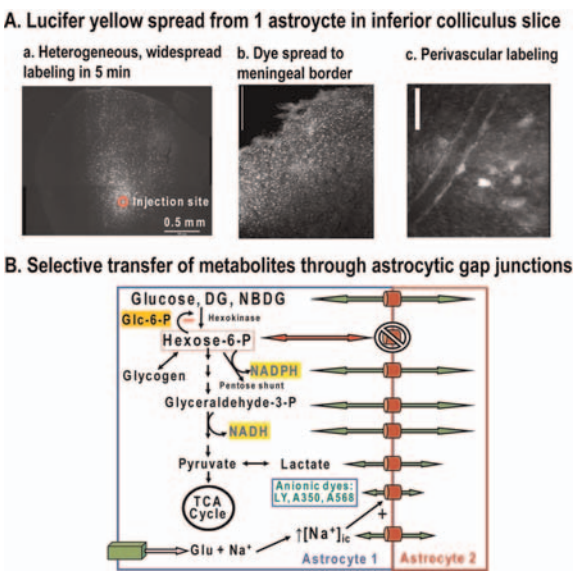

Figure 7 Gap junctional communication among astrocytes in the inferior colliculus

(**A**) Astrocytes in the adult rat inferior colliculus are highly coupled by gap junctions. Diffusion of Lucifer Yellow VS into a single astrocyte for 5 min labels up to approximately 10 000 cells (left panel), with high labelling of soma at the dorsal border of the inferior colliculus (middle panel, scale bar, 100 μm) and their perivascular endfeet (scale bar=25 μm). Figure re-printed from Gautam K. Gandhi, Nancy F. Cruz, Kelly K. Ball, Gerald A. Dienel (2009) Astrocytes are poised for lactate trafficking and release from activated brain and for supply of glucose to neurons, Journal of Neurochemistry 111:522–536. published by John Wiley and Sons © 2009 The Authors. Journal Compilation © 2009 International Society for Neurochemistry. (**B**) Model illustrating highly restricted passage of three hexose-6-Ps, Glc-6-P, DG-6-P and NBDG-6-P, through astrocytic gap junctions compared with the parent sugars and to downstream metabolites, redox compounds and anionic fluorescent dyes. Schematic based on data of Gandhi et al. (2009b). Exposure of astrocytes to extracellular glutamate and K^+ increases gap junctional coupling (Enkvist and McCarthy, 1994; De Pina-Benabou et al., 2001). Retention of Glc-6-P in the cell where it is phosphorylated may be necessary to ensure feedback regulation of glucose utilization in each astrocyte. Since glyceraldehyde-3-P, NADH and NADPH are all gap junction permeant, the presence of a phosphate moiety is not the sole basis for retention of hexose-6-P. Abbreviations: Glc, glucose; Glu, glutamate; ic, intracellular; P, phosphate; LY, Lucifer Yellow.

Astrocytic gap junctions are known to be permeant to energy metabolites, signalling molecules and electrolytes (Giaume et al., 1997; Giaume et al., 2010). Diffusion of material through gap junctions is stimulated by high intracellular sodium (Gandhi et al., 2009b), extracellular glutamate, quisqualate and kainate (Enkvist and McCarthy, 1994), and elevated levels of extracellular K^+ (Enkvist and McCarthy, 1994; De Pina-Benabou et al., 2001). These findings indicate that excitatory neurotransmission and Na^+-linked glutamate uptake into astrocytes are likely to increase the effective syncytial volume of coupled astrocytes and enhance their capacity to reduce focal energy demand by dispersal and sharing of small molecules. This notion is supported by demonstration that astrocytic gap junctions mediate intercellular spread of sodium during electrical stimulation of hippocampal slices to stimulate glutamatergic pathways (Langer et al., 2012). The long-lasting intracellular sodium gradients in astrocytes (Langer et al., 2012 and cited references) indicate that sodium extrusion is slower than its uptake along with glutamate, so there must be a considerable initial mismatch between Na^+ influx during excitatory neurotransmission and rates of Na^+-K^+-ATPase activity to extrude Na^+. If so, the hypothesized temporal-spatial linkage of putative astrocytic ATP demand, lactate generation and lactate shuttling to neurons related to excitatory transmission (Magistretti et al., 1999; Hyder et al., 2006) needs revision to accommodate astrocytic trafficking of metabolites, transmitters and electrolytes. To sum up, compounds and electrolytes associated with glutamatergic excitatory neurotransmission and energetics are readily dispersed among gap junction-coupled astrocytes and they enhance spreading of material among more coupled astrocytes, thereby reducing demands on perisynaptic astrocytic processes.

Lactate uptake from extracellular fluid and transcellular shuttling of lactate and glucose

Since extracellular lactate level doubled (from approximately 1 to 2 mmol/l) during acoustic activation and most extracellular lactate was not locally oxidized *in vivo* (Figure 6), we sought to identify the cell type(s) that can preferentially take up lactate in adult brain tissue. We, therefore devised a single-cell fluorescent enzymatic assay (Gandhi et al., 2009a) in which a reporter cell is impaled with a micropipette containing an enzyme assay mixture comprised of Amplex Red plus lactate oxidase and HRP (horseradish peroxidase). Lactate uptake causes a 1:1 stoichiometric formation of fluorescent resorufin in the reporter cell, and *in situ* calibrations of resorufin fluorescence as function of concentration

enabled quantitative cellular assays of lactate uptake and trafficking. Initial uptake and net uptake were first assayed from an extracellular point source, that is, a micropipette containing lactate that was placed ~2 μm from the reporter cell. Then lactate shuttling from one astrocyte to another astrocyte or to a neuron was assayed by impaling a donor astrocyte with lactate and recording lactate levels in the recipient cell by means of the enzyme assay system.

Uptake was first assayed at 2 mmol/l extracellular lactate, which approximates total lactate level during brain activation. Then higher concentrations were used so that estimates of maximal transport rate could be calculated for astrocytes and neurons. The initial uptake rate of lactate into astrocytes at 2 mmol/l lactate was 2.4 times that into neurons (Figure 8A), and over the concentration range tested, the slope of initial uptake rate was 4.3-times faster than into neurons (Figure 8B). Astrocytic capacity for lactate uptake, reflected by net uptake of lactate, was also twice that into neurons at 2 mmol/l lactate (Figure 8C), and the slope of the net uptake into astrocytes as function of lactate level was 2.3-fold higher than into neurons (Figure 8D). Thus, initial rate and capacity for lactate uptake into astrocytes greatly exceeds that into neurons, even at 2 mmol/l lactate, where neuronal transporters are operating at a near-maximal rate (K_m of the neuronal MCT2 for lactate is ~ 0.7 mmol/l; Manning Fox et al., 2000).

Next, transfer of lactate from one astrocyte to another astrocyte via gap junctions was assessed and compared with transfer from an astrocyte to a neuron located at the same distance from the lactate-donor astrocyte. Astrocyte-astrocyte lactate shuttling was much faster and far greater than astrocyte-neuron shuttling (Figures 8E–H). When the intracellular lactate level in the donor astrocyte was 2 mmol/l, both the initial rate and net transfer of lactate that was shuttled between gap junction-coupled astrocytes was twice that from an astrocyte to an equidistant neighbouring neuron (Figures 8E–G). There was no change in the initial rate of astrocyte-to-neuron shuttling over the concentration range tested, whereas shuttling to a coupled astrocyte rose several fold when intracellular lactate level in the donor astrocyte was elevated (Figure 8F). Furthermore, the slope of the net transfer of lactate from one astrocyte to another astrocyte as a function of lactate level was almost five times higher than that to a nearby neuron.

Similar experiments using glucose oxidase to assay astrocyte-to-neuron glucose transfer demonstrated that glucose inserted into an astrocyte diffused down its concentration gradient to a nearby neuron, indicating that astrocytes can supply glucose contained within the syncytium to activated neurons that have lower glucose levels (Gandhi et al., 2009a).

Estimates of maximal transport capacity calculated using measured lactate uptake data obtained at different lactate concentrations and zero trans Michaelis–Menten kinetics indicated that the astrocytic maximal transport capacity may be as high as 8–30 times the capacity of neurons, depending on the relative amounts of MCT1 and MCT4. Thus, astrocytes have the capacity to take up most of the extracellular lactate during brain activation and approximately 45–75% of the lactate during resting conditions (Gandhi et al., 2009a). These data emphasize: (i) the much higher lactate uptake and intercellular shuttling capacities of astrocytes compared with neurons over a very wide range of lactate concentrations; (ii) 200% greater astrocytic lactate uptake and dispersal among coupled astrocytes compared with neuronal uptake and shuttling to neurons at 2 mmol/l lactate; and (iii) saturation of MCT2, the neuronal lactate transporter, at much lower lactate levels than the astrocyte transporters, MCT1 and MCT4 (K_m values of ~4 and 28 mmol/l respectively; Manning Fox et al., 2000). It is important to recognize that the low K_m of the neuronal transporter, MCT2, not only limits lactate entry, it also restricts lactate efflux from neurons, thereby helping to retain glucose-derived pyruvate for oxidation (Chih et al., 2001; Chih and Roberts Jr, 2003). These properties support a major role for astrocytes in lactate dispersal and discharge from functionally activated domains and also allow for some neuronal lactate uptake and release that are governed by local lactate concentration gradients.

Perivascular drainage of interstitial fluid: a link to the lymphatic system

Our dye-labelling studies demonstrated that Lucifer Yellow diffusion from a single astrocyte produced strong perivascular labelling throughout the astrocytic syncytium (Figure 7). Astrocytic endfeet are gap junction-coupled (Simard et al., 2003) and contain lactate transporters (Gerhart et al., 1998; Hanu et al., 2000), suggesting that lactate may be released from endfeet directly to perivascular fluid that flows along the vasculature. Extracellular lactate is a vasodilator (Gordon et al., 2008), and its continuous release from endfeet during activation may be necessary for a sustained role as a blood flow regulator. If so, this lactate would probably be washed out of activated tissue. Perivascular, interstitial and CSF (cerebrospinal) fluids communicate with lymphatic drainage systems that deliver proteins and small molecules from brain to cervical and spinal lymph nodes (Bradbury and Cserr, 1985; Koh et al., 2005; Carare et al., 2008; Ball et al., 2010). The quantity of material distributed within brain via perivascular flow and released via lymphatic drainage is influenced by cardiac pulsations, intracerebral pressure and head position (Bradbury and Cserr, 1985; Rennels et al., 1985; Ball et al., 2010) and cited references). This novel pathway is involved in metabolite clearance from brain, in addition to metabolite discharge to blood.

Since quantitative analysis of metabolic labelling by [6-^{14}C]glucose and [^{14}C]DG during cortical spreading depression (Figures 4 and 5) accounted for only about half of the 'missing' glucose-derived ^{14}C-metabolites (Adachi et al., 1995; Cruz et al., 1999), we assessed metabolite release via the lymphatic pathway drainage system. Three tracers, Evans

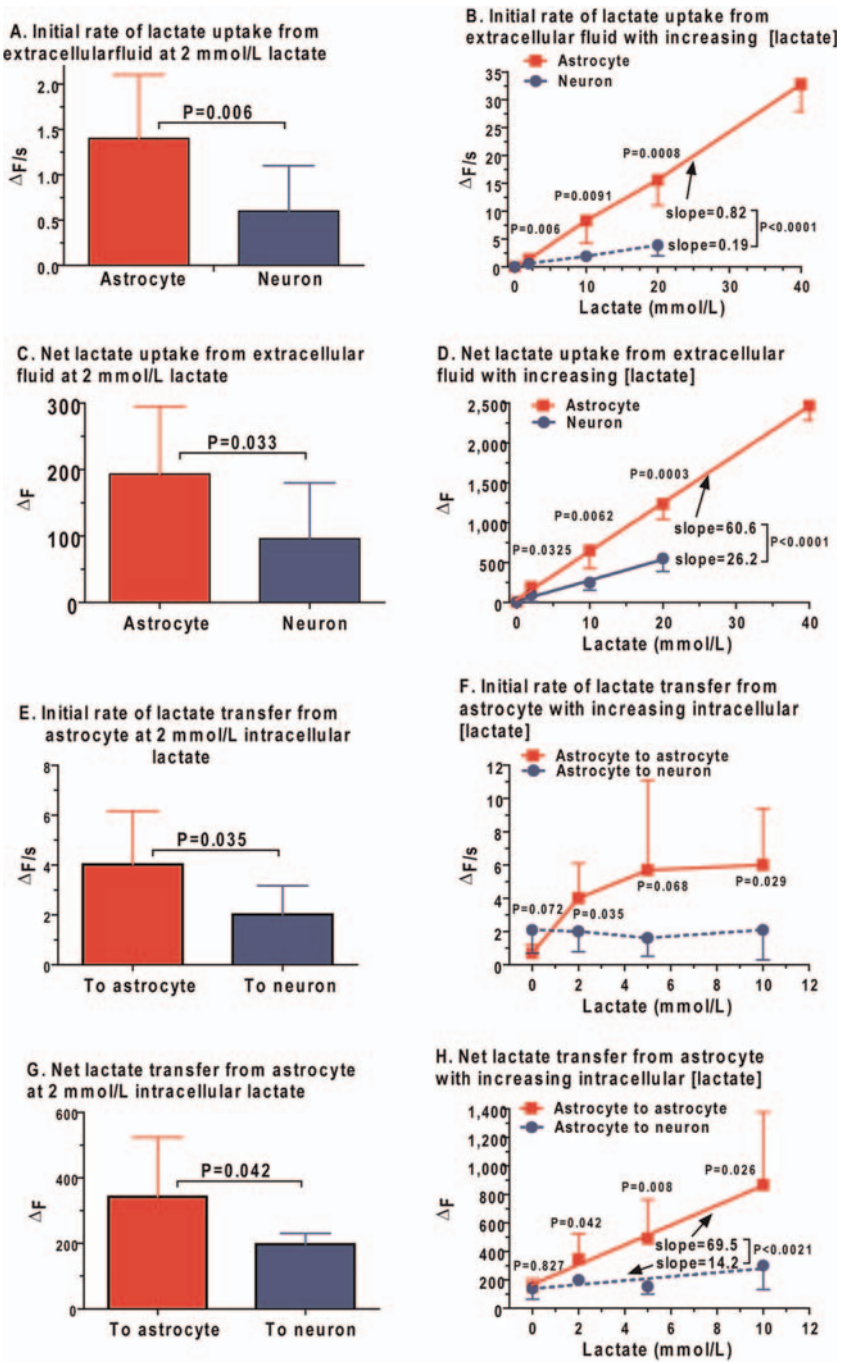

Figure 8 **Astrocytes have high capacity for rapid lactate uptake and lactate dispersal to other gap junction-coupled astrocytes compared with neuronal lactate uptake and astrocyte-to-neuron lactate shuttling**

Initial (**A**, **B**) and net (**C**, **D**) rates of lactate uptake from an extracellular point source into astrocytes and neurons at different lactate concentrations. Initial (**E**, **F**) and net (**G**, **H**) rates of lactate transfer from an astrocyte to another astrocyte or to a neuron located the same distance from the donor astrocyte as the gap junction-coupled recipient astrocyte. Figure re-printed from Gautam K. Gandhi, Nancy F. Cruz, Kelly K. Ball, Gerald A. Dienel (2009) Astrocytes are poised for lactate trafficking and release from activated brain and for supply of glucose to neurons, Journal of Neurochemistry 111:522–536. published by John Wiley and Sons © 2009 The Authors. Journal Compilation © 2009 International Society for Neurochemistry. When the extracellular lactate level approximates the mean tissue lactate level during brain activation (2 mmol/l), lactate uptake into astrocytes and lactate shuttling among astrocytes is about twice that of neurons, and the difference is larger as the lactate level rises. Astrocyte-to-neuron lactate shuttling does not change with increasing lactate level, even as high as 10 mmol/l in the donor astrocyte. Shuttling of lactate to neurons is much less than that dispersed to another astrocyte, and thousands of astrocytes are gap junction coupled.

Blue-bound albumin, [1-^{14}C]glucose and the non-metabolizable D-[^{14}C]lactate were microinfused into the inferior colliculus of conscious rats (Ball et al., 2010). Evans Blue verified localized infusion into the inferior colliculus (Figure 9A-a) and enabled visualization of perivascular routes from the inferior colliculus (Figure 9A-b). Evans Blue labelling involved the leptomeninges at the ventral surface of the brain, small and large vessels including the circle of Willis and middle cerebral arteries, and the vasculature under the olfactory bulbs that drains through the cribriform plate to the cervical lymph nodes (Bradbury and Cserr, 1985; Koh et al., 2005). Evans Blue labelling was most prominent on the ipsilateral hemisphere and removal of the leptomeninges eliminated nearly all of the visible blue dye from the brain surface. Next, ^{14}C tracers were infused, the brains dissected, and tissue solubilized and radioactivity counted. ^{14}C-label derived from [1-^{14}C]glucose was recovered mainly in the infused inferior colliculus (60%) and in the meningial membranes (34%), but small amounts were recovered throughout the brain (Figure 9B), indicative of some long-distance intracerebral spreading. Labelled compounds in the membranes were separated by HPLC, and ~40% of the label was recovered in glucose, ~20% in lactate, and the rest in three other fractions (Figure 9C). Since some of the lactate was probably generated by post-mortem metabolism, D-[^{14}C]lactate was infused, and label was also recovered in the meningial membranes (Figure 9D). Recovery of ~35% of the total [^{14}C]glucose-derived label in meningial membranes after microinfusion suggests sufficient capacity of lymphatic drainage to make a major contribution to lactate disposal during brain activation. The *in vivo* flux through the perivascular-lymphatic drainage system remains to be established, but it accounts, in part, for the missing label in the assays with [^{14}C]glucose.

Impact of unrecognized drainage systems from brain

Involvement of lymphatic systems in metabolite clearance suggests that a–v difference assays may not accurately register the quantities actually released or consumed by brain tissue. For example, if some of the labelled and unlabelled lactate generated during activation were released downstream of the sampling site for a–v difference assays, lactate efflux would be underestimated. On the other hand, when a fraction of the glucose and lactate taken up from blood into brain is washed out of brain via perivascular fluid flow before it is used by brain cells, then uptake and metabolic rates calculated by the Fick principle (i.e. CBF[A-V]) will be overestimated. The latter phenomenon is anticipated to be most prominent during extreme exercise that evokes high blood flow, vigorous arterial pulsations, and transient increases in intracerebral pressure due to strong exertion with breath holding. Strenuous muscular activity increases blood lactate levels above those in brain, reverses the lactate gradients illustrated in Figure 9(E), and drives lactate into brain. During exhaustive exercise, perivascular-lymphatic washout of some glucose and lactate taken up across the blood–brain barrier before it enters interstitial fluid and brain cells probably contributes to the 'missing carbohydrate' that leaves blood but cannot be accounted for by oxidative metabolism or accumulation in brain (Quistorff et al., 2008).

'Syncytial synapse' model: gap junction-coupled astrocytes share the workload of activation: networks between neurons and vasculature for support, dispersal and discharge

The following data from studies in conscious adult rat brain *in vivo* and in adult brain slices support the notion of rapid lactate dispersal and release: large underestimation of CMR_{glc} with labelled glucose (Figure 4), rapid efflux of labelled and unlabelled lactate from brain to blood (Figure 5), contributions of lactate transporters and gap junctions to local label spreading (Figure 6), extensive gap-junctional connectivity involving up to 10 000 astrocytes and perivascular labelling (Figure 7), faster and higher capacity to take up lactate and disperse lactate among gap junction-coupled astrocytes (Figure 8), and drainage of glucose, lactate and other molecules from interstitial fluid to meningial membranes via the perivascular routes that ultimately flow into the lymphatic system (Figures 9A–9D). Together, these findings support our model for the 'syncytial synapse' (Figure 9E) in which coupled astrocytes have a prominent role in lactate trafficking regardless of which cells produce lactate. This model extends the notion of the tripartite synapse that is comprised of pre-and postsynaptic neuronal elements plus surrounding astrocytic processes (Araque et al., 1999) to include all astrocytes coupled to these processes via gap junctions. The large astrocytic syncytial volume can serve as a source for transcellular diffusion of fuel, neurotransmitter precursors, redox compounds and signalling compounds, as well as a sink for dispersal of Na^+, K^+, lactate and glutamate to disperse their immediate perisynaptic concentrations and facilitate lactate discharge from endfeet to perivascular fluid and blood.

Rapid metabolite diffusion among gap junction-coupled astrocytes can reduce the focal energetic burden on perisynaptic astrocytic compartments during excitatory neurotransmission. For example, glucose, lactate, NADH, NADPH and sodium diffuse among coupled astrocytes according to intracellular concentration gradients, thereby supplying fuel and relieving limitations imposed by local energy demands, redox changes, and lactate and Na^+ accumulation. In contrast, Glc-6-P generated from glucose or glycogen is restricted to the cell of origin, where it serves as fuel, pentose-phosphate shunt pathway precursor, and regulator of hexokinase activity by feedback inhibition. Restricted diffusion of Glc-6-P from the cell of origin enables strong metabolic control of the first irreversible step of glycolysis in each astrocyte, whereas downstream metabolites can be shared. Neurotransmitter compounds, glutamate and

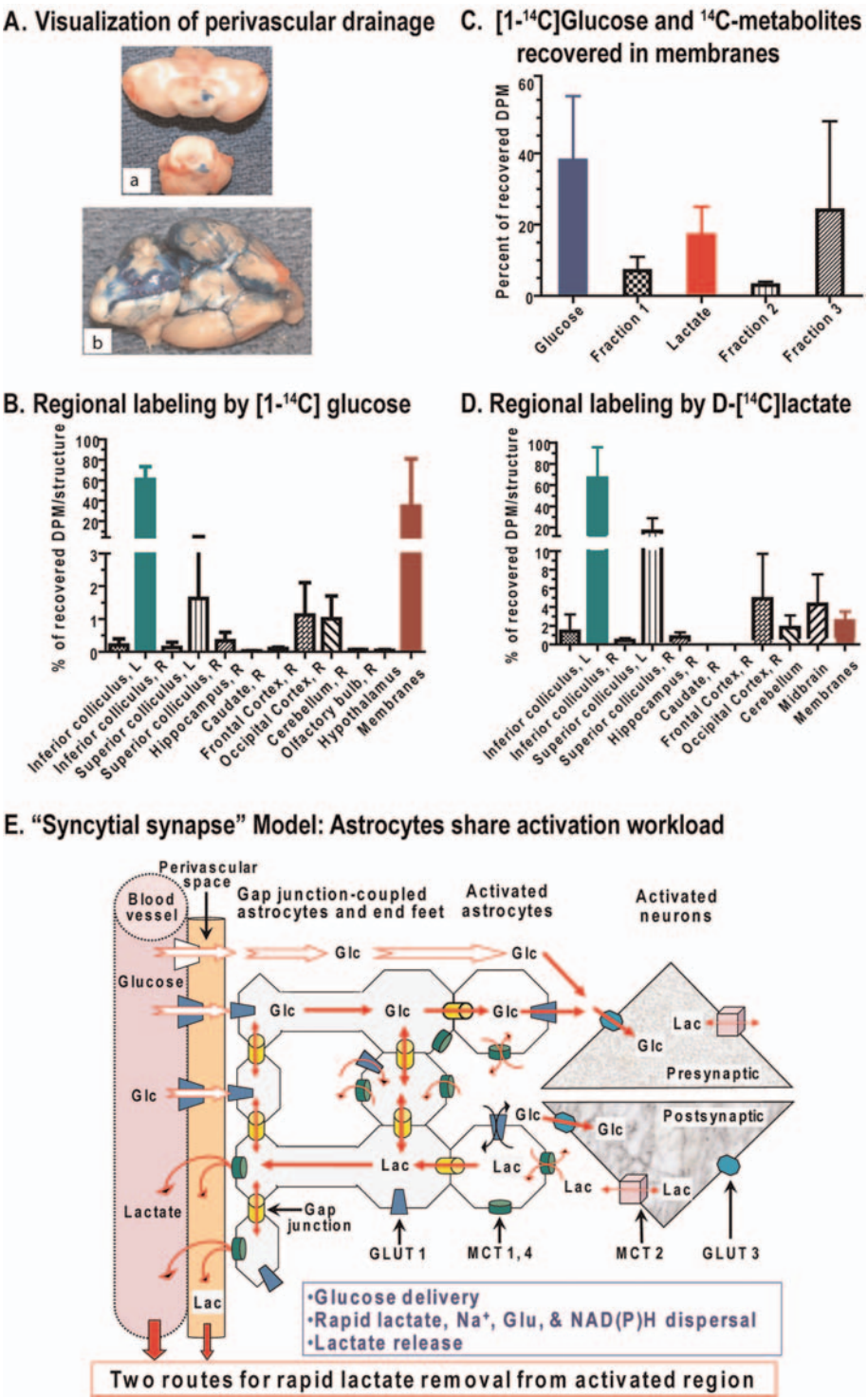

Figure 9 **Labelling of perivascular drainage systems by tracer microinfusion, and a model for roles of astrocytes in metabolite trafficking during brain activation**

(A) Microinfusion of Evans Blue albumin into the inferior colliculus of conscious rats (**a**) labels the perivascular space in the meningial membranes (**b**). **(B)** Microinfusion of [1-^{14}C]glucose into the inferior colliculus of conscious rats predominantly labels the infused inferior colliculus and meningial membranes (about 60 and 35% of recovered ^{14}C respectively), with low-level spreading of label throughout the brain. **(C)** Extraction of the membranes and separation of labelled compounds revealed the presence of glucose, lactate and other unidentified compounds in three other fractions. **(D)** Microinfusion of non-metabolizable D-[^{14}C]lactate also labelled many brain structures plus the meningial membranes. Data from Ball et al. (2010). **(E)** A model emphasizing diffusion and transporter-mediated pathways for (i) uptake of glucose from blood into brain and distribution within tissue and (ii) clearance of

lactate from glycolytic domains via intracellular and extracellular routes *during brain activation* of relatively sedentary subjects with low blood-lactate levels. Figure re-printed from Gautam K. Gandhi, Nancy F. Cruz, Kelly K. Ball, Gerald A. Dienel (2009) Astrocytes are poised for lactate trafficking and release from activated brain and for supply of glucose to neurons, Journal of Neurochemistry 111:522-536. published by John Wiley and Sons © 2009 The Authors. Journal Compilation © 2009 International Society for Neurochemistry. The model reflects experimental findings in Figures 4–9, and emphasizes potential roles of the astrocytic syncytium to supply nutrients and disperse compounds associated with excitatory neurotransmission. Gap junctional communication can reduce the workload on individual astrocytes or their processes and form a large network to share membrane-impermeant compounds. Gap junction-coupled endfeet can direct lactate along the vasculature for discharge into perivascular fluid, where it can modulate vascular diameter. Lactate can be cleared by perivascular-lymphatic drainage systems and by release to venous blood. Abbreviations: Glc, glucose; Lac, lactate; Glu, glutamate.

glutamine, probably also diffuse among astrocytes, but this likelihood needs experimental verification. Cytoplasmic redox molecules can diffuse from cell to cell, contrasting with their mitochondrial counterparts that cannot cross the mitochondrial membrane. NADH and NADPH are commonly assessed by fluorescence or two-photon microscopy, and cytoplasmic mobility must be taken into account with interpreting results.

The 'syncytial synapse' model emphasizes lactate release and a minor role for lactate as fuel during brain activation in normal, normoglycaemic sedentary subjects. It does contradict findings of substantial lactate usage by brain under other physiological or pathophysiological conditions or roles for lactate in specialized brain cells involved in food intake regulation. The notion that experimental and physiological paradigms are very important is stressed. Context needs to be taken into account when analysing and interpreting data. One size (metabolic model) does not fit all (situations). Metabolic and functional activities of brain cells during disease states and progressively changing pathophysiological states are much more complicated than the energetics of brain activation in the normal adult.

Lactate release versus local oxidation during activation: Some apparent controversies

The evidence-based lactate release model in Figure 9(E) does not support substantial astrocyte-to-neuron lactate shuttling linked to local neuronal lactate oxidation (Giaume et al., 2010; Jolivet et al., 2010; Pellerin and Magistretti, 2011). Release of large amounts of lactate and small maximal contributions of lactate shuttling to overall glucose utilization during activation argue strongly against lactate as a major neuronal fuel in normal, relatively sedentary subjects. Lactate shuttling has been controversial for many reasons that were previously assessed in detail (Dienel, 2011). In short, astrocyte-to-neuron lactate shuttling and use of glucose-derived lactate as a major neuronal fuel during activation lack strongly supportive *in vivo* data. Also, selective citation of a few *in vitro* studies to support their claim that neurons cannot up-regulate glycolysis and, therefore depend on lactate (Jolivet et al., 2010; Pellerin and Magistretti, 2011) does not take into account a very extensive literature (Dienel, 2011). Many laboratories have shown that cultured neurons and synaptosomes isolated from adult brain can markedly up-regulate glycolysis and glucose-supported respiration. Recent discussions in the literature give the appearance of a data-based controversy, but examination of the data can reveal sources of perplexity.

Pellerin and Magistretti (2011) commented on the Gandhi et al. (2009a) report describing astrocytic predominance of lactate uptake and shuttling, and they directed readers' attention to an outlying fact by stating "...Gandhi et al. (2009a) have shown that when raising artificially extracellular lactate concentrations up to 40 mmol/l in brain slices, astrocytes display a higher transport and distribution capacity for lactate compared with neurons". Their commentary is misleading, because they do not present the context that a large lactate concentration range was used to span the K_m values for astrocytic MCTs so that *maximal* transport *capacity* could be estimated. Notably, they also omit mention of the 2-fold higher *rates and capacities* for astrocytes compared with neurons for lactate uptake from extracellular fluid and of cell-cell shuttling when lactate level was 2 mmol/l, the concentration equivalent to the mean tissue lactate level during activation (Figure 8). Even when astrocyte-to-neuron lactate shuttling was assayed with 10 mmol/l lactate inserted into a donor astrocyte, the initial rate of transfer to a neuron was not higher than with 2 mmol/l in the donor astrocyte, and net transfer to a neuron was only approximately 1/3 that to a *single* coupled astrocyte (Figure 8). Trans-astrocytic dispersal capacity is very high, and lactate has the potential to diffuse to thousands of coupled astrocytes. Gandhi et al. (2009a) demonstrated that the *capacity* for lactate uptake and transfer to other astrocytes is much higher than that to neurons over a wide range of lactate levels that probably exceed those produced in microdomains during brain activation. Details of how that capacity functions *in vivo* remain established, but the amount of lactate generated in brain and *locally* oxidized during activation has not been shown to be more than a small fraction of glucose oxidation in normal conscious subjects; most is released. Furthermore, the cells that generate lactate in brain *in vivo* and the processes that up-regulate glycolysis *in vivo* have not yet been identified. These unknowns contribute to confusion in the literature.

Pellerin and Magistretti (2011) also emphasized results of the Boumezbeur et al. (2010) study that reported that the contribution of infused blood-borne [^{13}C]lactate to total oxidation in brain of normal, conscious adult humans was $<$10%, with a calculated upper limit of 60% during extreme conditions when the transporters are saturated. They cited Figley (2011) for an extensive discussion of: (i) the relevance of these data to the astrocyte-to-neuron lactate shuttle

hypothesis; and (ii) ''the fact that Boumezbeur's *in vivo* data were in contradiction with Gandhi et al. (2009a) *ex vivo* results.'' Pellerin and Magistretti (2011) and Figley (2011) appear to equate (i) brain lactate oxidation arising from intravenous lactate infusion that increases the lactate level in the *entire brain* with (ii) glutamate-induced astrocyte-to-neuron lactate shuttling during *local activation* of specific functional pathways. An inference of an apparent 'contradiction' in the above two data sets is that neuronal oxidation of lactate may be the same when brain lactate level is maintained at the elevated mean concentration of <2 mmol/l by either lactate influx from blood or by focal activation of glycolytic metabolism. If this were true, the small measured 2–8% contribution of blood lactate oxidation to total TCA cycle flux over the range of brain lactate level studied by Boumezbeur et al. (2010) defines a situation where lactate is a minor, supplementary fuel compared with blood-borne glucose that accounted for 92–98% of TCA cycle flux. The metabolic studies described above in support of the 'syncytial synapse' model can readily accommodate this magnitude of local lactate oxidation by any brain cells. In fact, the lactate trafficking studies by Gandhi et al. (2009a) did show some astrocyte to neuron trafficking *in situ*. An important element in the comparison of the above two studies is that brain activation and lactate infusion generate lactate gradients in opposite directions. Activation produces local brain-to-blood lactate concentration gradients, whereas exercise- or infusion-induced inward flooding of the entire brain with lactate will dissipate internally generated lactate gradients in brain. The physiological context of the two studies is different, as discussed in the next section.

In sharp contrast with the so-called 'contradiction' discussed above, there is an enormous, unexplained discrepancy between the results of Boumezbeur et al. (2010) and those of Pellerin-Magistretti group (Bouzier-Sore et al., 2003, 2006). The two Bouzier-Sore studies were cited by Pellerin and Magistretti (2011) as evidence that lactate is a preferential oxidative substrate for neurons. They reported that the relative contribution of lactate compared with glucose for oxidation by short-time cultures of neurons derived from newborn brain was 75–79% for lactate compared with 21–25% for glucose when the medium concentrations of both substrates were the same and fixed at either 1.1 or 5.5 mmol/l. These data are quite different than the 2–8% in human brain, and the discordant results were not addressed by either Pellerin and Magistretti (2011) or Figley (2011). The basis for the very high lactate usage in immature cultured neurons compared with normal adult human brain remains to be established, but culture conditions and developmental programs that are not equivalent to the brain's environment, maturation, and function *in vivo* are among the likely possibilities.

Pellerin and Magistretti (2011) also made the following statement: ''Curiously, a long-held view considered lactate (and more specifically lactic acid) as a toxic waste for brain cells that must be evacuated by all means from the brain parenchyma despite the fact that it is an important energy source (Dienel and Hertz, 2001).'' This sentence is an exaggerated interpretation that is the opinion of Pellerin and Magistretti. Dienel and Hertz (2001) did not make this statement. Instead, they emphasized that, when lactate is produced by a glycolytic cell, the lactate must leave the cell so that glycolytic flux can be maintained. The LDH reaction is equilibrative and lactate accumulation would impair regeneration of NAD^+ from NADH. Based on quantitative *in vivo* and *in vitro* data sets presented in Figures 4–9, a large fraction of lactate generated within brain is quickly released from activated brain structures, implying that maintaining high glycolytic flux is much more important than local oxidation of lactate under these conditions. Lactate can be a supplemental brain fuel, but none of the eight pictorial model descriptions and supporting data included by Pellerin and Magistretti (2011) in their summary of the 16-year-old astrocyte-neuron lactate shuttle model establishes experimentally the *in vivo* magnitude and duration of two essential model elements: glutamate-evoked astrocyte-to-neuron transfer of lactate coupled to local neuronal lactate oxidation.

Figley (2011) also made note of the 60% maximal oxidative contribution of lactate, as well as the use of lactate as fuel during hypoglycaemia. However, neither of these conditions is relevant to the usual activation studies nor to astrocyte-to-neuron lactate shuttling during brain activation of normal, normoglycaemic conscious subjects. Maximal lactate oxidation occurs during exhaustive exercise when blood lactate levels rise to 15–20 mmol/l (Quistorff et al., 2008), during supranormal lactate infusion *in vivo*, and during high-lactate flooding assays *in vitro* (reviewed by Dienel, 2011). Glucose supply in normoglycaemic subjects generally greatly exceeds demand, whereas insulin-induced hypoglycaemia is an abnormal state associated with strict glycaemic control in diabetic patients. When glucose supply to brain is inadequate, other available substrates, including endogenous amino acids, are consumed by brain, as shown by many previous studies in experimental animals (Siesjo, 1978). The distinction between the physiology of sedentary compared with modestly, vigorously physically active subjects and between normoglycaemic and modestly or severely hypoglycaemic subjects emphasizes a danger of generalization beyond the scope of a paradigm: incorrect conclusions can be drawn.

Figley (2011) cited Caesar et al. (2008) for *in vivo* evidence that extracellular lactate level rises at onset of brain activation. He did not, however, mention that the same study showed that (i) inhibition of *postsynaptic glutamate receptors completely blocked* the activation-evoked increase in CMR_{O2}, CMR_{glc}, and the increase in extracellular lactate level, and (ii) inhibition of *glutamate transport* into astrocytes had *no effect* on *metabolic stimulation* or increased *lactate levels*. Thus, Caesar et al. (2008) rule out detectable contributions of astrocytic glutamate uptake to increases in extracellular lactate levels, CMR_{glc}, or CMR_{O2} in their *in vivo* activation paradigm. These *in vivo* findings do not support the notion of

glutamate uptake-induced glycolysis that is the basis for the astrocyte-neuron lactate shuttle model (Pellerin and Magistretti, 1994, 2011). In fact, glutamate-evoked glycolysis is not a robust property of many cultured astrocyte preparations (reviewed in Dienel, 2011). A likely explanation for these discordant results is that glutamate is oxidized by the astrocytes that do not increase CMR_{glc} and that glutamate oxidation supports the associated energy demands in these cells (Hertz et al., 1998; Peng et al., 2001).

Summary

Brain imaging during sensory stimulation of normal conscious rats and under pathophysiological conditions reveals substantial increases in total glucose utilization with [^{14}C]deoxyglucose and much smaller increases in trapping of products of [1- or 6-^{14}C]glucose via the oxidative pathways. In conjunction with a fall in the CMR_{O2}/CMR_{glc} ratio during brain activation, these findings indicate increased formation and release of labelled and unlabelled lactate from activated brain. During acoustic stimulation of conscious rats, about half of the additional glucose consumed during activation is not retained in the tissue during 5 min experiments, and tonotopic bands of activation are poorly registered with [^{14}C]glucose. Total and extracellular lactate levels rise during brain activation. Lactate release from cerebral cortex was directly demonstrated by a–v difference assays during spreading depression and ammonia loading, but cannot be directly assayed during activation of small, inaccessible structures. Analysis of pathways for label loss ruled out lactate exchange across the blood–brain barrier and high rates of local oxidation of lactate generated from glucose microinfused into brain. The studies implicated increased pentose phosphate shunt pathway flux in loss of label from C1-labelled glucose, and metabolite spreading via MCTs and astrocytic gap junctions in loss of registration of focal activation. Direct single-cell transport assays in slices of adult rat brain showed lactate uptake into astrocytes greatly exceeds that into neurons when the extracellular lactate is 2 mmol/l or higher. Shuttling of lactate among gap junction-coupled astrocytes is also much greater than transfer to nearby neurons, even when the intracellular lactate is 10 mmol/l. Dye transfer among coupled astrocytes produces high labelling of perivascular endfeet, suggesting that astrocytes may discharge lactate to perivascular fluid for release to blood and to the lymphatic drainage system. When labelled glucose was microinfused into extracellular fluid, meningial membranes accounted for approximately 35% of the label recovered in brain tissue; D-lactate was also recovered in these membranes. Together, these findings support the conclusion that lactate is generated in increased amounts during brain activation and that it quickly spreads and is released to blood and lymphatic drainage systems, contributing to underestimation of total glucose utilization rate when assayed with [1- or 6-^{14}C]glucose.

PHYSIOLOGICAL CONTEXT: INFLUENCE OF BLOOD LACTATE LEVEL ON DIRECTION OF FLUX

Arterial plasma and brain lactate levels are major determinants of the direction of labelled and unlabelled lactate movement. Early studies using intravenous or intracarotid injections of tracer doses of ^{14}C-labelled glucose, pyruvate, and lactate showed that more label was incorporated into glutamate compared with glutamine (O'Neal and Koeppe, 1966; Cremer et al., 1978). These data are interpreted as predominant neuronal oxidation that exceeds calculated astrocytic glucose oxidation rates in rat and human brain (i.e. ~18–35% of the total; Oz et al., 2004; Hyder et al., 2006; Hertz, 2011a; Rothman et al., 2011). After insertion of substrates into interstitial fluid of adult rats by microdialysis astrocytes oxidize ~50% of lactate and 35% of glucose (Zielke et al., 2007). Interestingly, intracisternal injection of pyruvate and glucose favours their metabolism in astrocytes, reflected by label incorporation into glutamine via the small glutamate pool (Tucek and Cheng, 1974). Astrocytic oxidation of interstitial pyruvate (versus neuronal oxidation of blood-borne pyruvate) supports the redox shuttle hypothesis formulated by Cerdan et al. (2006). These studies suggest that delivery route may influence cellular and subcellular utilization of brain fuel. Exit routes may also govern metabolic fate, and we hypothesize that lactate channelling to astrocytic endfeet favours its release during activation in normal, conscious subjects (Figure 9E).

In vivo brain activation studies in conscious humans and rats have been carried out when blood-lactate levels are low (normal, normoglycaemic, relatively-sedentary subjects) and when blood-lactate levels are elevated (during muscular activity and lactate infusions). The general characteristics of these two situations are illustrated in Figure 10(A). Arterial plasma glucose levels are normal and stable in both conditions. Quiescent subjects can exhibit slight lactate fluxes into or out of brain. If subjects move around, arterial plasma lactate level may rise from ~0.5–1 mmol/l to ~1–3 mmol/l and slightly exceed that in brain, causing lactate uptake instead of efflux (see Tables 6 and 8 in Dienel, 2011). In contrast, during vigorous exercise to exhaustion, plasma lactate levels rise enormously, up to 15–20 mmol/l (Dalsgaard, 2006; Quistorff et al., 2008). CBF, CMR_{glc}, and CMR_{lac} increase more than CMR_{O2}, causing the oxygen-glucose and oxygen-carbohydrate indices to fall (Figure 10A); these decrements are underestimated when glycogen is consumed.

Outward lactate gradient–lactate exit

Many forms of physiological or mental stimulation or pathophysiological conditions have minimal involvement of the musculature, and arterial plasma lactate levels are

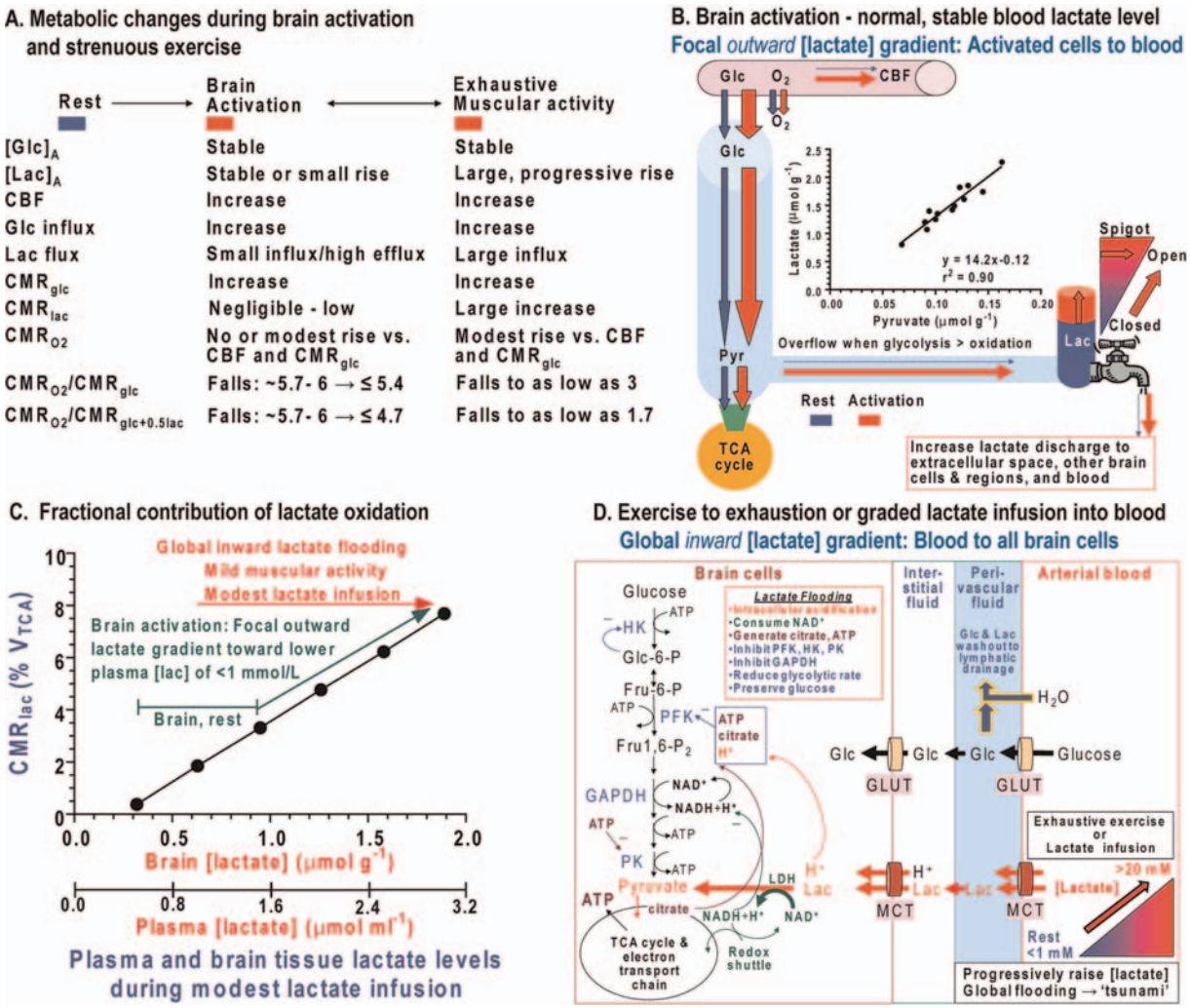

Figure 10 **Lactate gradients influence direction of lactate diffusion**

(**A**) Typical metabolic changes reported during brain activation in normal, conscious, relatively sedentary subjects and during exhaustive exercise. Data compiled from reviews (Dienel and Cruz, 2004, 2008; Quistorff et al., 2008). (**B**) *Lactate 'overflow' model* illustrates an outward lactate concentration gradient from brain to blood from activated brain structures. The disproportionate rise in glycolysis compared with oxidative metabolism during brain activation increases intracellular pyruvate level, causing lactate levels to rise proportionately in accordance with the equilibrium of the LDH reaction (Siesjo, 1978). The inset shows measured pairs of lactate and pyruvate levels in brain of control animals; data are from (Folbergrova et al., 1972; Ponten et al., 1973; Ljunggren et al., 1974; Veech and Hawkins, 1974; Duffy et al., 1975; MacMillan, 1975; Miller et al., 1975; Veech, 1980). These plotted values span the range of lactate in normal and activated brain that is, approximately 0.5–2 µmol/g; the mean pyruvate and lactate concentrations were 0.11 and 1.48 µmol/g respectively, and the mean lactate/pyruvate ratio was 13.1. Intracellular lactate exceeds the extracellular level, and lactate diffuses down its concentration gradient to extracellular fluid from which it can be cleared by various routes (see Figure 9). (**C**) *Lactate infusions*. Infusion of lactate into normal conscious subjects increases the lactate concentration in arterial plasma above that measured in brain, causing lactate to diffuse into the entire brain and dissipate lactate gradients within brain. Boumezbeur et al. (2010) infused [^{13}C]lactate into human subjects and measured its oxidation rate. The linear regressions from their Figure 6 were used to calculate human brain lactate levels from arterial plasma lactate levels at 0.5 mmol/l intervals using their equation $[lactate]_{brain}=0.63\ [lactate]_{plasma}$. These data were plotted against the corresponding calculated values for $CMR_{lactate}$, calculated with their equation, $CMR_{lac}=0.019[lac]_{plasma}-0.007$. CMR_{lac} is expressed as % V_{TCA}, where $V_{TCA}=0.65$ mmol/g min and represents the total oxidation rate in neurons plus glia (Boumezbeur et al., 2010). The plotted points illustrate the approximate fractional rates of lactate oxidation at plasma and brain lactate levels arising from the infusion schedule. Actual values measured by Boumezbeur et al. would be distributed around this regression line. Note that lactate contributes approximately 2–8% to total oxidation, and glucose the remaining 92–98%. For reference, the green text indicates the range of brain lactate levels in normal activated brain in subjects with lower arterial plasma lactate levels and an outward, brain-to-blood lactate gradient. The red text denotes the point above which arterial plasma levels rise during progressively increasing intensity of exercise or of higher lactate infusion schedules causing an inward, blood-to-brain lactate gradient. (**D**) *Lactate flooding model* illustrates effects of a large, global inward lactate gradient from blood to brain during extreme physical activity or infusion of large amounts of lactate. Plasma lactate levels rise above approximately 4–5 mmol/l, that is, approximately 2–4 times higher than those observed during normal brain activation of relatively sedentary subjects, and lactate floods into the *entire* brain. Under the most extreme condition of exercise to exhaustion, blood lactate rises to 15–20 mmol/l, and lactate influx resembles a 'tsunami' flood that would eliminate all local lactate gradients arising from glycolytic metabolism. Some of the lactate and glucose leaving

blood might be washed out via perivascular-lymphatic drainage (see Figure 9), causing a–v differences to be overestimated. Entry of lactate into brain cells can decrease availability of NAD^+ for glycolysis and cause acidification and generate ATP and citrate. Together, these regulators can inhibit phosphofructokinase activity, reduce glucose utilization and spare glucose (see text for more details).

relatively low (<1–2 mmol/l). Brain lactate level in resting control rats is directly proportional to pyruvate concentration over the range observed during normal brain activation that is, up to ~2 μmol/g (inset, Figure 10B). Increases in intracellular lactate content during activation probably arise from its equilibration with higher pyruvate levels caused by increased glycolytic flux. Lactate then diffuses down its concentration gradients to other intracellular domains, disperses via gap junctions and MCTs, then discharges to perivascular fluid and blood (i.e. the 'spigot opens', Figure 10B). The large, rapid efflux of lactate and discordant images obtained with [1- or 6-^{14}C]glucose and [^{14}C]DG (Figures 4 and 5) represent overflow conditions. The hyperaemic response to activation not only delivers glucose and oxygen in excess of demand (Figure 3), it also washes out lactate. Lactate will be 'pulled' out of perivascular fluid (and also endfeet and nearby cells) due to its equilibrative transport and dilution in a larger, higher-flow blood volume that contains lower levels of lactate. Increased CMR_{glc} and rapid elimination of lactate from activated brain indicates that NAD^+ regeneration and maintenance of high glycolytic flux is a higher priority than lactate oxidation. Return of lactate to blood under surplus conditions provides fuel for other body tissues, it does not compromise neuroenergetics, and it does not waste fuel, just as feeding table scraps to the dog does not deprive a sated person of calories.

Some lactate released from activated cells and retained in tissue may be used as oxidative fuel for neurons and astrocytes. Unfortunately, current analytical methods cannot distinguish between oxidation of pyruvate generated from glucose within a cell versus pyruvate formed from lactate that was produced by other cells. CMR_{O2} reflects oxidation of all substrates, and ΔCMR_{O2} puts a ceiling on the magnitude of lactate shuttling. For example, if CMR_{O2} increases by 30% during activation, this rise is the upper limit for lactate shuttling, that is, when the entire increment is due to oxidation of lactate produced by another cell. However, if neurons directly oxidize half of the additional glucose, the maximal shuttle contribution is 15%, if astrocytes oxidize 30% of the pyruvate and if other substrates are oxidized, this fraction falls further, consistent with results obtained from mathematical modelling (<10%) (DiNuzzo et al., 2010a; Mangia et al., 2011).

Small inward lactate gradient–lactate flooding will blunt intracerebral lactate gradients

Lactate levels rise in blood during muscular activity and hypoxic conditions, and elevated lactate represents a physiological condition in which whole-body non-oxidative glucose utilization exceeds its oxidation. Modest increases in arterial plasma lactate level above that in brain cause lactate to diffuse down its concentration gradient into the entire brain. Global lactate influx can dissipate local tissue lactate gradients associated with aerobic glycolysis and provide a supplemental fuel that can spare glucose for glycolytic metabolism. However, despite an overall inward gradient, Hawkins et al. (1973) showed that lactate efflux occurs during an ammonia challenge, providing evidence for compartmentation of lactate metabolism and release.

Boumezbeur et al. (2010) infused [3-^{13}C]lactate into human subjects and produced plasma lactate levels ranging from ~0.7 to 3 mmol/l. Corresponding brain lactate levels in these subjects were approximately 60% of those in plasma and were below 2 μmol/g, that is, within the range commonly observed in brain activation studies in sedentary subjects. The contribution of blood lactate oxidation to total TCA cycle activity ranged from ~2 to 8% over the range measured, with glucose providing 92–98% of the total substrate for oxidative metabolism (Figure 10C). This percentage is similar to that calculated for resting conditions by van Hall (2009) during infusion of [1-^{13}C]lactate to produce a blood lactate level of 0.9 mmol/l. Thus, modest flooding of the entire brain with lactate by raising the blood level makes a small contribution to neuroenergetics, slightly supplementing glucose as the predominant fuel.

Lactate 'muscles its way into consciousness' – large inward gradient, a 'lactate tsunami'

Biochemical regulation evoked by elevated lactate

Progressive increases in the intensity of physical activity produce large amounts of lactate that are released from muscle. Exhaustive exercise raises arterial plasma lactate levels up to 15–20 mmol/l (Dalsgaard, 2006; Quistorff et al., 2008) and drives lactate into the entire brain, thereby eliminating most or all endogenous lactate gradients (Figure 10D). Massive lactate influx into cells with co-transport of a proton can cause intracellular acidification. The extent and duration of a fall in pH depends on relative intracellular and extracellular pH, extracellular lactate level, buffering capacity and proton extrusion mechanisms (Nedergaard and Goldman, 1993; Carpenter and Halestrap, 1994; Jackson and Halestrap, 1996). Cultured astrocytes and neurons exposed to 5 mmol/l extracellular L-lactate acidify at similar rate, with a transient, maximal fall of 0.1–0.2 pH unit (Nedergaard and Goldman, 1993). In medullary slices from adult mouse brain that were exposed to 5 mmol/l lactate in the perfusate, the intracellular pH fell by 0.08 pH unit in astrocytes and by 0.11 unit in neurons (Erlichman et al., 2008). Phosphofructokinase, a major regulator of glycolysis (Figure 10D), is extremely sensitive to small changes in pH

and, although the pH profile is influenced in a complex manner by levels of other compounds, a decrease of 0.1 pH unit can nearly eliminate its activity in skeletal muscle extracts (Trivedi and Danforth, 1966). High pH sensitivity of glycolysis is also evident when glycolytic rate is assayed as lactate production in intact leucocytes or cellular extracts; the rate falls markedly as pH is reduced from 7.2 to 6.5 (Halperin et al., 1969). Blockade of lactate efflux from tumour cells inhibits glycolysis due to reduction of intracellular pH (Belt et al., 1979). Build-up of intracellular lactate level will also, by mass action, convert available NAD^+ to $NADH+H^+$, thereby producing another proton and depriving the glycolytic pathway of NAD^+ for the glyceraldehyde-3-P dehydrogenase reaction (Figure 10D). These regulatory processes could also be expected to occur when MCT levels are reduced by treatment with antisense oligonucleotides or 4-CIN, complicating interpretation of results of transport studies.

Utilization of lactate as an oxidative fuel requires operation of the MAS for re-oxidation of NADH generated by its conversion into pyruvate (McKenna et al., 1993; Figure 10D). Cell-type differences in lactate oxidation can arise from redox shuttle capacity, which is higher in neurons than astrocytes in adult brain (Ramos et al., 2003; Pardo et al., 2011), but sufficient for astrocytic needs (Hertz, 2011b). Entry of lactate-derived pyruvate into the TCA cycle will maintain citrate level and generate ATP. Taken together, three inhibitors of phosphofructokinase, H^+, ATP, and citrate, will be produced by a large inward lactate gradient and lactate oxidation (Figure 10D). These regulators, along with competition for NAD^+ availability, can depress glycolytic rate, raise Glc-6-P levels, and reduce glucose utilization. These actions preserve glucose when a large supply of an 'opportunistic' fuel generated by intense muscular activity is available (Figure 10D).

Human studies

Relationships between blood and brain lactate concentration, lactate oxidation and extent of inhibition of glycolysis are complex and difficult to establish *in vivo*. Infusion of lactate into resting human subjects to raise plasma level by 6.5-fold, from 0.6 to 4.1 mmol/l reduced whole brain glucose utilization assayed by [^{18}F]FDG-PET by 17% (Smith et al., 2003). A complicated experimental paradigm involving graded exercise for 80 min caused global CMR_{glc} to fall by approximately 32%, or approximately 4–5% per 1 mmol/l increase in blood lactate level (Kemppainen et al., 2005). More recently, van Hall et al. (2009) established that graded infusions of [1-^{13}C]lactate contributed 8, 19 and 27% to oxidative metabolism when blood lactate levels were 0.9, 3.9 and 6.9 mmol/l during rest or moderate exercise. Nearly all of the lactate was oxidized and recovered as $^{13}CO_2$. Net glucose uptake into brain fell by ~20% during lactate infusion at rest, but glucose uptake was not reduced further during exercise when lactate levels were higher. In other studies by the Secher–Quistorff group, net glucose uptake increased substantially during exhaustive exercise, along with lactate uptake. However, the oxygen/carbohydrate utilization ratio fell from approximately 5.7 to 5.9 during rest to as low as 1.7 during exhaustive exercise even though oxygen supply was not limiting (Dalsgaard, 2006; Quistorff et al., 2008; Volianitis et al., 2008). The fate of carbohydrate taken up in excess of oxygen is not known, and washout of some of the incoming glucose and lactate via perivascular-lymphatic drainage may cause a–v differences and calculated metabolic rates to be overestimated.

To summarize, when lactate is infused into conscious humans to produce small increases in their blood level, lactate accounts for ~4–8% of oxidative metabolism and glucose 92–96%. Higher blood lactate levels (4–9 mmol/l) arising from infusion or exercise contributed ~15–30% of the brain's energy demands, with glucose providing 70–85% and serving as the predominant fuel.

Rat studies

Rats subjected to running exercise at approximately 85% of maximal oxygen uptake increased CMR_{glc} in grey and white matter by a mean of 38%, with local increases as high as 164% (Vissing et al., 1996). Largest responses were in structures involved with motor, sensory and autonomic functions. Some structures showed no change, but there was *no decrease* in CMR_{glc} in any brain structure. Unfortunately, blood lactate levels were not determined. Raising plasma lactate from ~1 to ~6 mmol/l in α-chloralose-anaesthetized rats by lactate infusion caused a 38% decrement in CMR_{glc} (Wyss et al., 2011). These discordant findings emphasize the need for cautious interpretative generalization of data obtained under different conditions and anaesthesia.

Experimental context is essential for interpretation of physiological roles of lactate

Physiological and biochemical status

The physiology of lactate utilization, the experimental system and experimental conditions must be taken into account when comparing results from different studies. Context is especially important to minimize 'interpretations gone wild' when trying to integrate results into a single conceptual model. Metabolic demands and responses under one experimental system need not apply to others. For example, (i) short-term cultures of brain cells derived from embryonic or newborn animals may have incomplete development. When grown in media containing pathophysiological levels of glucose (10–50 mmol/l) they acquire abnormal phenotypes that may be related to diabetes (Abe et al., 2006; Gandhi et al., 2010; Takahashi et al., 2012; Wang et al., 2012). (ii) Brain slices from immature and mature rats are not metabolically equivalent (Figure 2). (iii) Anaesthetized or conscious sedentary subjects do not have same metabolic activities at rest or during activation (Table 4).

(iv) Plasma lactate levels rise with extent of physical activity and drive lactate down its concentration gradient into the brain (Figure 10). (v) Abnormal or pathophysiological conditions have unique physiology. At a first approximation, metabolic models applied to all brain structures and systems are useful tools as long as the limits of generalization and the likelihood of contextual differences are taken into account. Further development and refinement of neuroenergetics models is essential.

Supplemental fuel

Brain fuel usage is governed by developmental stage, fuel availability, physiological state and biochemical regulatory mechanisms, as well as disease state. The brain normally depends on blood glucose that is maintained at near-constant levels by many complex pathways involving various organs and endocrine systems. As long as brain hexokinase is saturated, raising glucose concentration does not increase its metabolism in brain, and local energy demand (i.e. generation of ADP) governs glucose utilization. As discussed in detail (Chih et al., 2001; Chih and Roberts Jr, 2003; Roberts, 2007), utilization of glucose is highly regulated at many steps, whereas lactate utilization is not; lactate use is governed by equilibrative reactions. The brain consumes more lactate and ketone bodies when available because physiological conditions that produce lactate (physical activity, hypoxia) or ketone bodies (starvation) evoke regulatory situations that spare glucose. Lactate is regarded by some investigators as a 'preferred' fuel compared with glucose (Jolivet et al., 2010; Pellerin and Magistretti, 2011; and cited references). However, lactate-evoked biochemical regulation of metabolic fluxes is not the same as 'choosing or preferring' one fuel over another (see discussion in Dienel, 2011). Are isocaloric amounts of glucose and lactate chosen by brain cells in the same way as a person might prefer to eat isocaloric amounts of chocolate or vanilla candies? If lactate were truly 'preferred' over glucose, why is any lactate released from brain during rest or activation? Lactate is also considered an important fuel to support evoked potentials in brain slices and during recovery from an ischaemic energy crisis (Schurr and Gozal, 2011). However, others have shown that technical aspects of brain slice experiments have a very strong influence on the ability of lactate and other alternative substrates to support and preserve neuronal function; evoked potentials and other functions can fail in the absence of glucose, even when ATP concentration is maintained at normal levels by various alternative substrates (Dienel and Hertz, 2005; Okada and Lipton, 2007; Roberts, 2007). Apparent contradictions in lactate use do not rule in or rule out use of lactate. Each case needs to be examined in its own right.

Signalling, gene expression, neuroprotection and neurological disorders

Most attention is directed toward lactate as an oxidative fuel, but lactate can have other interesting roles in brain function. For example, lactate spreading from activated cells is proposed to serve as a 'volume transmitter' to co-ordinate redox state and energy metabolism in many cells, as well as influence neurovascular coupling (Bergersen and Gjedde, 2012). Lactate level and redox status can also influence gene expression and astrocytic calcium signalling (Garriga-Canut et al., 2006; Bergersen and Gjedde, 2012; Requardt et al., 2012; Wilhelm and Hirrlinger, 2012). Lactate flooding will increase intracellular pyruvate concentration as long as the MAS is functional (Figures 1A–10D). Pyruvate is neuroprotective due to detoxification of hydrogen peroxide, which reacts non-enzymatically with α-ketoacids (Desagher et al., 1997). Also, infusion of sodium lactate into susceptible humans can provoke panic or anxiety attacks (Maddock, 2001; Wemmie, 2011).

Summary: some unresolved issues related to physiological context, astrocyte–neuron interactions and functional metabolic activities, and lactate metabolism

Lactate concentration gradients and the source(s) of lactate are key elements related to its utilization. Three central issues are the quantitative cellular contributions to glycolytic and oxidative metabolism during rest and activation, the cellular source(s) of lactate generated within brain, and the fate(s) of brain lactate. Since data relevant to neuroenergetics are derived from very diverse developmental, experimental, and physiological systems, many issues need to be considered when evaluating evidence in terms of theoretical models. For example.

What is the experimental context and strengths/weaknesses of an experimental system? Is the developmental stage of the model system (e.g., fuel usage, enzyme and transporter levels, cell–cell interactions, neurotransmitter systems) equivalent to the adult brain *in vivo*? Culture systems are best suited to assess mechanisms and pathways that, once understood, can be evaluated in adult tissue. How do culture conditions and regional development influence outcome?

Does anaesthesia preferentially suppress stimulus-evoked glycolysis compared with oxidative metabolism? Translation of results from anaesthetized subjects to the conscious, activated condition requires a better understanding of cellular activities suppressed by anaesthesia and of the metabolic pathways that support those activities. If α-chloralose suppresses activation-induced glycolysis, does concomitant lactate infusion suppress it further?

Are relevant pathways taken into account? What pathways are differentially activated in neurons and astrocytes and to what extent? What functions do the rise in glycolysis, serve? How is the ATP generated from different pathways utilized? Does dispersion of workload influence temporal-spatial demands of excitatory neurotransmission? How does subcellular compartmentation influence energetics and

lactate channelling? What is the magnitude of perivascular drainage and its influence on metabolic assays?

What is the cellular basis of neuroenergetics? Interpretation of results with DG and 2-NBDG in terms of cellular glucose utilization requires determination of the 'lumped constant' in (adult) neurons, astrocytes and oligodendrocytes. Supply-demand relationships at different glucose concentrations must be established for 2-NBDG and 6-NBDG in each experimental system due to the influence of glucose transport and metabolism on fates of glucose analogues.

Do MCT transporter inhibition or knockdown experiments adequately test the hypothesis and its alternatives? Cell-to-cell transfer of lactate cannot be directly assessed *in vivo*, and transporter inhibition or knockdown may be used to assess putative lactate trafficking. For example, 4-CIN (100 μmol/l) was used to preferentially inhibit neuronal MCT2 (Erlichman et al., 2008), but impairment of neuronal mitochondrial pyruvate transport and effects on lactate release from neurons were not assessed and ruled out. Higher 4-CIN doses (250, 500, 1000 μmol/l) markedly inhibit lactate and glucose oxidation in cultured neurons and astrocytes (McKenna et al., 2001). Mitochondrial pyruvate transport is inhibited by low micromolar concentrations of 4-CIN (Halestrap, 1975; Halestrap and Denton, 1975). If a small fraction of extracellular 4-CIN enters cells, it can impair glucose oxidation and may cause compensatory increases in glycolysis independent of any effects on exogenous lactate influx and oxidation. Also, if neurons are a source of lactate during activation, inhibition of lactate efflux from neurons by 4-CIN or MCT2 knockdown may interfere with neuronal glucose utilization due to intracellular acidification (Belt et al., 1979) and inhibition of phosphofructokinase (Figure 10D). Experimental manipulation of MCT activity or level requires many controls plus parallel assays of transport and metabolism. Questions related to effects of MCT knockdown or inhibition and lactate supplementation in memory studies (Newman et al., 2011; Suzuki et al., 2011) have been discussed above. For further discussion of potential complications with use of 4-CIN and related references, see Table 10 and related text in Dienel (2011).

What are the absolute values of the magnitudes of lactate shuttling, release and local use as an oxidative fuel? Flux through the increased size of the brain lactate pool during activation is not known, rates of release and shuttling cannot be directly assayed, and contributions of lactate to functional metabolism during activation of normal sedentary subjects remain to be established.

Do percentage changes in metabolite concentrations and pathway fluxes give appropriate portrayals of metabolic changes and pathway relationships? Percentage changes are a convenient way to normalize data and compare results from different studies and paradigms. Many studies have analysed incremental changes in concentration changes or rates during brain activation (e.g. Hu and Wilson, 1997a, b; Lin et al., 2010a, 2010b; Newman et al., 2011), but fractional changes subtract out total metabolic activity at baseline and it is essential to include quantitative data describing the actual magnitude of metabolite levels and pathway fluxes (Shulman et al., 2009). Furthermore, interpretative reliance on percentage changes, particularly of concentration, can be very misleading and sometimes wrong unless absolute concentrations and related fluxes are known and taken into account. The following examples illustrate this point. (i) Metabolite levels are the result of net input and output to and from the pool, and changes can arise from either or both fluxes. (ii) Lactate concentrations can rise by as much as 150% during brain activation. This seems like a large change but, in fact, corresponds to a very small amount of glucose carbon, on the order of $<2\%$ of the glucose metabolized to pyruvate during the same interval of sensory stimulation of conscious rats (see Table 8 and related text in Dienel, 2011). (iii) Percentage changes in extracellular glucose and lactate levels are generally small at onset of activation, the concentration changes move in opposite directions, and the metabolite levels probably correspond to very different fluxes through these pools, as discussed above and in Table 7 in Dienel (2011). The flow of glucose from blood to brain cells through the extracellular glucose pool is not taken into account by net changes in its concentration. (iv) Direction of metabolite concentration change can be misleading. During sensory stimulation studies of non-fasted conscious rats, the animals move around, causing arterial plasma glucose levels to rise due to glycogenolysis. Elevated plasma glucose caused passive 20–30% increases in regional brain glucose levels, which also occurs during anaesthesia and suppression of function and metabolism. Without parallel metabolic assays, the increase in glucose level might be incorrectly interpreted as reduced CMR_{glc}, when, in fact, CMR_{glc} increased by 25–50% (i.e. supply exceeded demand; see Table 8 in Dienel, 2011). (v) Changes in NAD(P)H fluorescence ($\Delta F/F$) are generally very small ($<10\%$) and reflect small changes against a low background. To my knowledge, the relationships between redox changes and pathway fluxes are not known, but they are often interpreted in terms of shifts in oxidative or glycolytic metabolism or even in terms of lactate shuttling, when, in fact, there is no direct evidence to support many such conclusions. Perhaps the most reliable interpretation is the brief, oxidative shift at onset of a stimulus that is associated with BOLD signal changes, but fluxes remain to be established. To sum up, percentage changes represent a useful starting point for analysis, not an endpoint.

Are there activation-induced shifts in how the total ATP generated is used? A focus on fractional increases in energy metabolism infers that the incremental rise represents the cost of the activated state. However, re-partitioning of ATP usage derived from the much larger component of overall energetics (the 100% at baseline) could also help support the activated state. Some processes may be transiently down-regulated (e.g., 'housekeeping chores'), whereas others may be temporarily up-regulated to support increased signalling during the activated state. Substantial 're-assignment' of ATP

from one process to another would limit the usefulness of analysis of percentage changes to understand the activated state. This topic has received little experimental attention.

Rigorous analytical and interpretive analysis is needed in the field of brain energetics. The astrocyte-to-neuron lactate shuttle model is simple to explain, easy to understand, and has garnered wide, but often non-critical, acceptance. However, it has also generated considerable controversy because it does not fully describe astrocytic energetics during brain activation (e.g., oxidative and glycogenolytic metabolism are neglected), and strong supportive evidence for the quantitative importance of lactate shuttling during brain activation *in vivo* is still lacking after 16 years. Selective citation of specific studies in support of the model by its proponents without concomitant inclusion and discussion of many studies that provide strong *in vivo* and *in vitro* data against this model (Dienel, 2011) does not advance the field. Brain activation is not as simple as it may seem to be.

CONCLUDING PERSPECTIVE

Infrastructure and metabolic assays

The high capacity of adult rat brain to increase glucose and oxygen utilization rates is acquired through developmental programs that mainly occur throughout the first postnatal month and govern large regional changes in enzyme and transporter levels and neurotransmitter networks. Fuel is supplied to adult brain in excess of its demand, and upon activation, hyperaemic responses rapidly increase delivery of glucose and oxygen to activated structures. Surplus fuel delivery and buffering by endogenous glucose and glycogen suggests that brain does not need lactate to supplement glucose, but may use small amounts, depending on the situation and availability. Most of the brain's energy is derived from oxidative metabolism of glucose, but activation of normal conscious subjects preferentially increases glycolytic metabolism. Glycogen is an active, endogenous supplemental fuel stored in astrocytes, and blood lactate is an opportunistic, glucose-sparing fuel that is consumed in greatest quantities during intense physical activity. Anaesthetics must be used in some experimental situations, but they suppress consciousness and they differentially reduce the magnitude of increase in total glucose utilization during activation in brain regions involved in the same functional pathway. Suppression of activation-induced glycolysis by α-chloralose is a possibility that needs to be addressed in future experiments. Modelling assumptions influence predicted cellular origin of lactate and the direction of lactate shuttling. Kinetic differences between glucose, DG, and methylglucose and their relationships to glucose supply-demand have been established over a wide range of plasma and brain glucose levels. Similar studies are required to use 2-NBDG and 6-NBDG to evaluate phosphorylation and transport within a cell type and between cell types in each preparation.

Lactate release and uptake

Brain imaging with labelled glucose and deoxyglucose reveals large underestimates of calculated CMR_{glc} during activation due, in part, to rapid release of labelled and unlabelled lactate to blood. Reduced registration of focal activation arises from upregulation of the pentose phosphate shunt pathway and diffusion of labelled metabolites from activated cells via MCTs and astrocytic gap junctions that link thousands of astrocytes into a large, heterogeneous syncytium. Most extracellular lactate derived from microinfused glucose is not locally oxidized *in vivo*. In slices, extracellular lactate is more rapidly taken up into astrocytes and dispersed to other astrocytes compared with neuronal lactate uptake and astrocyte-to-neuron shuttling. Lactate released from astrocytic endfeet to perivascular space can alter vascular diameter and blood flow throughout a large volume of tissue that contains the astrocytic syncytium. This process may contribute to surplus fuel delivery to a larger tissue volume than that of the activated cells and to lactate washout. Metabolite clearance via perivascular and lymphatic drainage systems can contribute to lactate efflux to blood and to 'missing metabolites' extracted from blood in a–v difference studies. Low arterial plasma lactate levels are associated with lactate release from resting and activated brain, whereas high lactate levels that accompany muscular activity increase lactate oxidation and glucose-sparing responses. Local blood-brain lactate gradients govern the direction and magnitude of lactate release and utilization.

Models for cellular signals and experimental context

Metabolic activity in neurons and astrocytes generates signals used for brain imaging and spectroscopic studies, and major advances have been made in studies of brain cells *in vitro* and *in vivo*. However, technical limitations of current methodology have held back elucidation of the cellular basis of neuroenergetics. No one will dispute the findings in many laboratories that lactate is oxidized by brain when delivered in tracer or loading doses. Label from lactate is incorporated into the large glutamate compartment and interpreted as neuronal. However, there are many critical, unresolved issues related to the role lactate in normal brain activation, including cellular origin, the direction of lactate shuttling, pathways for dispersal and release of lactate, and the magnitude of the fraction that is actually consumed in brain during activation. Controversy arises when results from non-comparable developmental and experimental systems are selectively lumped together. Hopefully, some of these issues have been identified and clarified in this and the preceding (Dienel, 2011) reviews, and that this material stimulates future incisive

experiments to critically evaluate the role of lactate in brain activation. Specific conditions, for example, physical activity and lactate flooding, where lactate is oxidized to a greater extent, must be distinguished from those involving activation and low plasma lactate levels. Fuel availability and pathway regulatory mechanisms are important determinants of outcome. Lactate concentration gradients and experimental context are also critical issues. The predominance of glucose as the major brain fuel and lactate release from activated domains in normal conscious adult brain is strongly supported by *in vivo* evidence. Lactate oxidation during flooding conditions is also supported by strong *in vivo* evidence. All models for lactate dynamics are plausible to some extent, and they may vary in importance with experimental system, brain region, and condition. However, data cited in support of a *large* astrocyte-to-neuron lactate shuttle in normal brain of normoglycaemic, sedentary subjects *in vivo* are far from compelling. Estimates in support of lactate oxidation during activation of normal brain tissue are on the order of $<10\%$, with glucose more than 90%. Technological advances are required for elucidation of cellular contributions to brain images and the cellular basis of disorders that diminish brain function, including diabetes, stroke, AD (Alzheimer's disease) and mitochondrial dysfunction.

ACKNOWLEDGEMENTS

The content is solely the responsibility of the author and does not necessarily represent the official views of the National Institute Of Diabetes And Digestive And Kidney Diseases, National Institute of Neurological Diseases and Stroke, or the National Institutes of Health.

FUNDING

This work was supported by the National Institutes of Health [grant numbers DK081936 and NS038230].

REFERENCES

Abe T, Takahashi S, Suzuki N (2006) Oxidative metabolism in cultured rat astroglia: effects of reducing the glucose concentration in the culture medium and of D-aspartate or potassium stimulation. J Cereb Blood Flow Metab 26:153–160.

Ackermann RF, Lear JL (1989) Glycolysis-induced discordance between glucose metabolic rates measured with radiolabeled fluorodeoxyglucose and glucose. J Cereb Blood Flow Metab 9:774–785.

Adachi K, Cruz NF, Sokoloff L, Dienel GA (1995) Labeling of metabolic pools by [6–14C]glucose during K(+)-induced stimulation of glucose utilization in rat brain. J Cereb Blood Flow Metab 15:97–110.

Araque A, Parpura V, Sanzgiri RP, Haydon PG (1999) Tripartite synapses: glia, the unacknowledged partner. Trends Neurosci 22:208–215.

Attwell D, Laughlin SB (2001) An energy budget for signaling in the grey matter of the brain. J Cereb Blood Flow Metab 21:1133–1145.

Attwell D, Buchan AM, Charpak S, Lauritzen M, Macvicar BA, Newman EA (2010) Glial and neuronal control of brain blood flow. Nature 468:232–243.

Austin VC, Blamire AM, Allers KA, Sharp T, Styles P, Matthews PM, Sibson NR (2005) Confounding effects of anesthesia on functional activation in rodent brain: a study of halothane and alpha-chloralose anesthesia. NeuroImage 24:92–100.

Bachelard HS (1967) The subcellular distribution and properties of hexokinases in the guinea-pig cerebral cortex. Biochem J 104:286–292.

Bak LK, Walls AB, Schousboe A, Ring A, Sonnewald U, Waagepetersen HS (2009) Neuronal glucose but not lactate utilization is positively correlated with NMDA-induced neurotransmission and fluctuations in cytosolic Ca^{2+} levels. J Neurochem 109(Suppl. 1):87–93.

Bak LK, Obel LF, Walls AB, Schousboe A, Faek SA, Jajo FS, Waagepetersen HS (2012) Novel model of neuronal bioenergetics: post-synaptic utilization of glucose but not lactate correlates positively with Ca^{2+} signaling in cultured mouse glutamatergic neurons. ASN NEURO 4(3):art:e00083. doi:10.1042/AN20120004

Ball KK, Cruz NF, Mrak RE, Dienel GA (2010) Trafficking of glucose, lactate, and amyloid-beta from the inferior colliculus through perivascular routes. J Cereb Blood Flow Metab 30:162–176.

Ball KK, Gandhi GK, Thrash J, Cruz NF, Dienel GA (2007) Astrocytic connexin distributions and rapid, extensive dye transfer via gap junctions in the inferior colliculus: implications for [(14)C]glucose metabolite trafficking. J Neurosci Res 85:3267–3283.

Baquer NZ, McLean P, Greenbaum AL (1975) Systems relationships and the control of metabolic pathways in developing brain. In: Normal and Pathological development of energy metabolism (Hommes FA, Van den Berg CJ, eds), pp 109–131. London: Academic Press.

Belt JA, Thomas JA, Buchsbaum RN, Racker E (1979) Inhibition of lactate transport and glycolysis in Ehrlich ascites tumor cells by bioflavonoids. Biochemistry 18:3506–3511.

Ben-Yoseph O, Camp DM, Robinson TE, Ross BD (1995) Dynamic measurements of cerebral pentose phosphate pathway activity *in vivo* using [1,6–13C2,6,6–2H2]glucose and microdialysis. J Neurochem 64:1336–1342.

Bergersen LH, Gjedde A (2012) Is lactate a volume transmitter of metabolic states of the brain? Front Neuroenerg 4:5, doi:10.3389/fnene.2012.00005

Blennow G, Folbergrova J, Nilsson B, Siesjo BK (1979) Cerebral metabolic and circulatory changes in the rat during sustained seizures induced by DL-homocysteine. Brain Res 179:129–146.

Blomqvist G, Seitz RJ, Sjogren I, Halldin C, Stone-Elander S, Widen L, Solin O, Haaparanta M (1994) Regional cerebral oxidative and total glucose consumption during rest and activation studied with positron emission tomography. Acta Physiol Scand 151:29–43.

Blomqvist G, Stone-Elander S, Halldin C, Roland PE, Widen L, Lindqvist M, Swahn CG, Langstrom B, Wiesel FA (1990) Positron emission tomographic measurements of cerebral glucose utilization using [1–11C]D-glucose. J Cereb Blood Flow Metab 10:467–483.

Blomqvist G, Widén L, Stone-Elander S, Halldin C, Roland PE, Swahn CG, Haaparanta M, Solin O, Lindqvist M, Långström B, Wiesel FA (1989) Comparison between (1-^{11}C)-D-glucose, (U-^{11}C)-D-glucose, and (^{18}F)2-fluoro-deoxy-D-glucose as tracers for PET measurements of cerebral glucose utilization In: Positron emission tomography in clinical research and clinical diagnosis: Tracer modeling and radioreceptors (Beckers C, Goffinet A, Bol A, eds), pp. 182–193. Kluwer Academic Publishers, Dordrecht.

Bonvento G, Lacombe P, MacKenzie ET, Seylaz J (1991) Effects of dorsal raphe stimulation on cerebral glucose utilization in the anaesthetized rat. Brain Res 567:325–327.

Borgstrom L, Chapman AG, Siesjo BK (1976) Glucose consumption in the cerebral cortex of rat during bicuculline-induced status epilipticus. J Neurochem 27:971–973.

Borowsky IW, Collins RC (1989) Metabolic anatomy of brain: a comparison of regional capillary density, glucose metabolism, and enzyme activities. J Comp Neurol 288:401–413.

Boumezbeur F, Petersen KF, Cline GW, Mason GF, Behar KL, Shulman GI, Rothman DL (2010) The contribution of blood lactate to brain energy metabolism in humans measured by dynamic 13C nuclear magnetic resonance spectroscopy. J Neurosci 30:13983–13991.

Bouzier-Sore AK, Voisin P, Canioni P, Magistretti PJ, Pellerin L (2003) Lactate is a preferential oxidative energy substrate over glucose for neurons in culture. J Cereb Blood Flow Metab 23:1298–1306.

Bouzier-Sore AK, Voisin P, Bouchaud V, Bezancon E, Franconi JM, Pellerin L (2006) Competition between glucose and lactate as oxidative energy substrates in both neurons and astrocytes: a comparative NMR study. Eur J Neurosci 24:1687–1694.

Bradbury MWB, Cserr HF (1985) Drainage of cerebral interstitial fluid and of cerebrospinal fluid into lymphatics. In: Experimental Biology of the Lymphatic Circulation (Johnston MG, ed), pp 355–394. New York: Elsevier.

Bradford HF, Ward HK, Thomas AJ (1978) Glutamine–a major substrate for nerve endings. J Neurochem 30:1453–1459.

Brondsted HE, Gjedde A (1988) Measuring brain glucose phosphorylation with labeled glucose. Am J Physiol 254:E443–448.

Brookes N (1997) Intracellular pH as a regulatory signal in astrocyte metabolism. Glia 21:64–73.

Brookes N (2000) Functional integration of the transport of ammonium, glutamate and glutamine in astrocytes. Neurochem Int 37:121–129.

Brown AM, Ransom BR (2007) Astrocyte glycogen and brain energy metabolism. Glia 55:1263–1271.

Brown AM, Tekkok SB, Ransom BR (2003) Glycogen regulation and functional role in mouse white matter. J Physiol 549:501–512.

Buchweitz-Milton E, Weiss HR (1990) Effect of salbutamol on regional cerebral oxygen consumption, flow and capillary and arteriolar perfusion. Neurol Res 12:169–175.

Buschiazzo PM, Terrell EB, Regen DM (1970) Sugar transport across the blood–brain barrier. Am J Physiol 219:1505–1513.

Buxton RB (2010) Interpreting oxygenation-based neuroimaging signals: the importance and the challenge of understanding brain oxygen metabolism. Front Neuroenerg 2:8.

Caesar K, Hashemi P, Douhou A, Bonvento G, Boutelle MG, Walls AB, Lauritzen M (2008) Glutamate receptor-dependent increments in lactate, glucose and oxygen metabolism evoked in rat cerebellum *in vivo*. J Physiol 586:1337–1349.

Carare RO, Bernardes-Silva M, Newman TA, Page AM, Nicoll JA, Perry VH, Weller RO (2008) Solutes, but not cells, drain from the brain parenchyma along basement membranes of capillaries and arteries: significance for cerebral amyloid angiopathy and neuroimmunology. Neuropathol Appl Neurobiol 34:131–144.

Carlsson C, Hagerdal M, Siesjo BK (1976) The effect of nitrous oxide on oxygen consumption and blood flow in the cerebral cortex of the rat. Acta Anaesthesiol Scand 20:91–95.

Carpenter L, Halestrap AP (1994) The kinetics, substrate and inhibitor specificity of the lactate transporter of Ehrlich-Lettre tumour cells studied with the intracellular pH indicator BCECF. Biochem J 304 (Pt 3):751–760.

Cerdan S, Rodrigues TB, Sierra A, Benito M, Fonseca LL, Fonseca CP, Garcia-Martin ML (2006) The redox switch/redox coupling hypothesis. Neurochem Int 48:523–530.

Cetin N, Ball K, Gokden M, Cruz NF, Dienel GA (2003) Effect of reactive cell density on net [2–14C]acetate uptake into rat brain: labeling of clusters containing GFAP+- and lectin+-immunoreactive cells. Neurochem Int 42:359–374.

Cheeseman AJ, Clark JB (1988) Influence of the malate-aspartate shuttle on oxidative metabolism in synaptosomes. J Neurochem 50:1559–1565.

Chih CP, Roberts EL Jr (2003) Energy substrates for neurons during neural activity: a critical review of the astrocyte-neuron lactate shuttle hypothesis. J Cereb Blood Flow Metab 23:1263–1281.

Chih CP, Lipton P, Roberts EL, Jr. (2001) Do active cerebral neurons really use lactate rather than glucose? Trends Neurosci 24:573–578.

Choi IY, Seaquist ER, Gruetter R (2003) Effect of hypoglycemia on brain glycogen metabolism *in vivo*. J Neurosci Res 72:25–32.

Choi IY, Tkac I, Ugurbil K, Gruetter R (1999) Noninvasive measurements of [1-(13)C]glycogen concentrations and metabolism in rat brain *in vivo*. J Neurochem 73:1300–1308.

Choi IY, Lee SP, Kim SG, Gruetter R (2001) *In vivo* measurements of brain glucose transport using the reversible Michaelis–Menten model and simultaneous measurements of cerebral blood flow changes during hypoglycemia. J Cereb Blood Flow Metab 21:653–663.

Choi SW, Gerencser AA, Nicholls DG (2009) Bioenergetic analysis of isolated cerebrocortical nerve terminals on a microgram scale: spare respiratory capacity and stochastic mitochondrial failure. J Neurochem 109:1179–1191.

Choi SW, Gerencser AA, Lee DW, Rajagopalan S, Nicholls DG, Andersen JK, Brand MD (2011) Intrinsic bioenergetic properties and stress sensitivity of dopaminergic synaptosomes. J Neurosci 31:4524–4534.

Chuquet J, Quilichini P, Nimchinsky EA, Buzsaki G (2010) Predominant enhancement of glucose uptake in astrocytes versus neurons during activation of the somatosensory cortex. J Neurosci 30:15298–15303.

Clark JB, Bates TE, Cullingford T, Land JM (1993) Development of enzymes of energy metabolism in the neonatal mammalian brain. Dev Neurosci 15:174–180.

Cloherty EK, Sultzman LA, Zottola RJ, Carruthers A (1995) Net sugar transport is a multistep process. Evidence for cytosolic sugar binding sites in erythrocytes. Biochemistry 34:15395–15406.

Collins RC (1997) Red and white brain. Ann NY Acad Sci 835:250–254.

Collins RC, McCandless DW, Wagman IL (1987) Cerebral glucose utilization: comparison of [14C]deoxyglucose and [6–14C]glucose quantitative autoradiography. J Neurochem 49:1564–1570.

Contreras L, Satrustegui J (2009) Calcium signaling in brain mitochondria: interplay of malate aspartate NADH shuttle and calcium uniporter/mitochondrial dehydrogenase pathways. J Biol Chem 284:7091–7099.

Cooper AJ, Mora SN, Cruz NF, Gelbard AS (1985) Cerebral ammonia metabolism in hyperammonemic rats. J Neurochem 44:1716–1723.

Cooper AJ, McDonald JM, Gelbard AS, Gledhill RF, Duffy TE (1979) The metabolic fate of 13N-labeled ammonia in rat brain. J Biol Chem 254:4982–4992.

Crane PD, Pardridge WM, Braun LD, Oldendorf WH (1983) Kinetics of transport and phosphorylation of 2-fluoro-2-deoxy-D-glucose in rat brain. J Neurochem 40:160–167.

Cremer JE (1982) Substrate utilization and brain development. J Cereb Blood Flow Metab 2:394–407.

Cremer JE, Heath DF (1974) The estimation of rates of utilization of glucose and ketone bodies in the brain of the suckling rat using compartmental analysis of isotopic data. Biochem J 142:527–544.

Cremer JE, Teal HM, Heath DF (1975) Regulatory factors in glucose and ketone body utilization in the developing brain. In: Normal and Pathological Development of Energy Metabolism (Hommes FA, Van den Berg CJ, eds), pp 133–142. London: Academic Press.

Cremer JE, Cunningham VJ, Seville MP (1983) Relationships between extraction and metabolism of glucose, blood flow, and tissue blood volume in regions of rat brain. J Cereb Blood Flow Metab 3:291–302.

Cremer JE, Seville MP, Cunningham VJ (1988) Tracer 2-deoxyglucose kinetics in brain regions of rats given kainic acid. J Cereb Blood Flow Metab 8:244–253.

Cremer JE, Sarna GS, Teal HM, J CV (1978) Amino acid precursors: their transport into brain and initial metabolism. In: Amino Acids as Chemical Transmitters (Fonnum F, ed), pp 669–689. New York: Plenum Press.

Cremer JE, Ray DE, Sarna GS, Cunningham VJ (1981) A study of the kinetic behaviour of glucose based on simultaneous estimates of influx and phosphorylation in brain regions of rats in different physiological states. Brain Res 221:331–342.

Cremer JE, Cunningham VJ, Pardridge WM, Braun LD, Oldendorf WH (1979) Kinetics of blood–brain barrier transport of pyruvate, lactate and glucose in suckling, weanling and adult rats. J Neurochem 33:439–445.

Cruz NF, Dienel GA (2002) High glycogen levels in brains of rats with minimal environmental stimuli: implications for metabolic contributions of working astrocytes. J Cereb Blood Flow Metab 22:1476–1489.

Cruz NF, Adachi K, Dienel GA (1999) Rapid efflux of lactate from cerebral cortex during K^+-induced spreading cortical depression. J Cereb Blood Flow Metab 19:380–392.

Cruz NF, Ball KK, Dienel GA (2007) Functional imaging of focal brain activation in conscious rats: impact of [(14)C]glucose metabolite spreading and release. J Neurosci Res 85:3254–3266.

Cruz NF, Lasater A, Zielke HR, Dienel GA (2005) Activation of astrocytes in brain of conscious rats during acoustic stimulation: acetate utilization in working brain. J Neurochem 92:934–947.

Cudennec A, Duverger D, Nishikawa T, McRae-Degueurce A, MacKenzie ET, Scatton B (1988) Influence of ascending serotonergic pathways on glucose use in the conscious rat brain. I. Effects of electrolytic or neurotoxic lesions of the dorsal and/or median raphe nucleus. Brain Res 444:214–226.

Cunningham VJ, Cremer JE (1981) A method for the simultaneous estimation of regional rates of glucose influx and phosphorylation in rat brain using radiolabeled 2-deoxyglucose. Brain Res 221:319–330.

Cunningham VJ, Hargreaves RJ, Pelling D, Moorhouse SR (1986) Regional blood–brain glucose transfer in the rat: a novel double-membrane kinetic analysis. J Cereb Blood Flow Metab 6:305–314.

Dalsgaard MK (2006) Fuelling cerebral activity in exercising man. J Cereb Blood Flow Metab 26:731–750.

de Graaf RA, Pan JW, Telang F, Lee JH, Brown P, Novotny EJ, Hetherington HP, Rothman DL (2001) Differentiation of glucose transport in human brain gray and white matter. J Cereb Blood Flow Metab 21:483–492.

De Pina-Benabou MH, Srinivas M, Spray DC, Scemes E (2001) Calmodulin kinase pathway mediates the K+-induced increase in gap junctional communication between mouse spinal cord astrocytes. J Neurosci 21:6635–6643.

Deelchand DK, Shestov AA, Koski DM, Ugurbil K, Henry PG (2009) Acetate transport and utilization in the rat brain. J Neurochem 109 Suppl 1:46–54.

Desagher S, Glowinski J, Prémont J (1997) Pyruvate protects neurons against hydrogen peroxide-induced toxicity. J Neurosci 17:9060–9067.

Devor A, Sakadzic S, Saisan PA, Yaseen MA, Roussakis E, Srinivasan VJ, Vinogradov SA, Rosen BR, Buxton RB, Dale AM, Boas DA (2011) 'Overshoot' of O is required to maintain baseline tissue oxygenation at locations distal to blood vessels. J Neurosci 31:13676–13681.

Dienel GA (2009) Energy metabolism in the brain. In: From Molecules to Networks. An Introcution to Cellular and Molecular Neuroscience 2nd Edition (Byrne JH, Roberts JL, eds), pp 49–110. Academic Press, San Diego.

Dienel GA (2011) Brain lactate metabolism: the discoveries and the controversies. J Cereb Blood Flow Metab 32:1107–1138.

Dienel GA, Cruz NF (1993) Synthesis of deoxyglucose-1-phosphate, deoxyglucose-1,6-bisphosphate, and other metabolites of 2-deoxy-D-[14C]glucose in rat brain *in vivo*: influence of time and tissue glucose level. J Neurochem 60:2217–2231.

Dienel GA, Hertz L (2001) Glucose and lactate metabolism during brain activation. J Neurosci Res 66:824–838.

Dienel GA, Cruz NF (2004) Nutrition during brain activation: does cell-to-cell lactate shuttling contribute significantly to sweet and sour food for thought? Neurochem Int 45:321–351.

Dienel GA, Hertz L (2005) Astrocytic contributions to bioenergetics of cerebral ischemia. Glia 50:362–388.

Dienel GA, Cruz NF (2008) Imaging brain activation: simple pictures of complex biology. Ann NY Acad Sci 1147:139–170.

Dienel GA, Cruz NF (2009) Exchange-mediated dilution of brain lactate specific activity: implications for the origin of glutamate dilution and the contributions of glutamine dilution and other pathways. J Neurochem 109 Suppl 1:30–37.

Dienel GA, Cruz NF, Sokoloff L (1993) Metabolites of 2-deoxy-[14C]glucose in plasma and brain: influence on rate of glucose utilization determined with deoxyglucose method in rat brain. J Cereb Blood Flow Metab 13:315–327.

Dienel GA, Liu K, Cruz NF (2001a) Local uptake of (14)C-labeled acetate and butyrate in rat brain *in vivo* during spreading cortical depression. J Neurosci Res 66:812–820.

Dienel GA, Wang RY, Cruz NF (2002) Generalized sensory stimulation of conscious rats increases labeling of oxidative pathways of glucose metabolism when the brain glucose-oxygen uptake ratio rises. J Cereb Blood Flow Metab 22:1490–1502.

Dienel GA, Ball KK, Cruz NF (2007a) A glycogen phosphorylase inhibitor selectively enhances local rates of glucose utilization in brain during sensory stimulation of conscious rats: implications for glycogen turnover. J Neurochem 102:466–478.

Dienel GA, Schmidt KC, Cruz NF (2007b) Astrocyte activation *in vivo* during graded photic stimulation. J Neurochem 103:1506–1522.

Dienel GA, Cruz NF, Mori K, Sokoloff L (1990) Acid lability of metabolites of 2-deoxyglucose in rat brain: implications for estimates of kinetic parameters of deoxyglucose phosphorylation and transport between blood and brain. J Neurochem 54:1440–1448.

Dienel GA, Cruz NF, Mori K, Holden JE, Sokoloff L (1991) Direct measurement of the lambda of the lumped constant of the deoxyglucose method in rat brain: determination of lambda and lumped constant from tissue glucose concentration or equilibrium brain/plasma distribution ratio for methylglucose. J Cereb Blood Flow Metab 11:25–34.

Dienel GA, Cruz NF, Adachi K, Sokoloff L, Holden JE (1997) Determination of local brain glucose level with [14C]methylglucose: effects of glucose supply and demand. Am J Physiol 273:E839–849.

Dienel GA, Nelson T, Cruz NF, Jay T, Crane AM, Sokoloff L (1988) Overestimation of glucose-6-phosphatase activity in brain *in vivo*. Apparent difference in rates of [2–3H]glucose and [U-14C]glucose utilization is due to contamination of precursor pool with 14C-labeled products and incomplete recovery of 14C-labeled metabolites. J Biol Chem 263: 19697–19708.

Dienel GA, Popp D, Drew PD, Ball K, Krisht A, Cruz NF (2001b) Preferential labeling of glial and meningial brain tumors with [2-(14)C]acetate. J Nucl Med 42:1243–1250.

Dienel GA, Cruz NF, Ball K, Popp D, Gokden M, Baron S, Wright D, Wenger GR (2003) Behavioral training increases local astrocytic metabolic activity but does not alter outcome of mild transient ischemia. Brain Res 961:201–212.

DiNuzzo M, Maraviglia B, Giove F (2011) Why does the brain (not) have glycogen? Bioessays 33:319–326.

DiNuzzo M, Mangia S, Maraviglia B, Giove F (2010a) Changes in glucose uptake rather than lactate shuttle take center stage in subserving neuroenergetics: evidence from mathematical modeling. J Cereb Blood Flow Metab 30:586–602.

DiNuzzo M, Mangia S, Maraviglia B, Giove F (2010b) Glycogenolysis in astrocytes supports blood-borne glucose channeling not glycogen-derived lactate shuttling to neurons: evidence from mathematical modeling. J Cereb Blood Flow Metab 30:1895–1904.

Dringen R, Gebhardt R, Hamprecht B (1993) Glycogen in astrocytes: possible function as lactate supply for neighboring cells. Brain Res 623:208–214.

Dringen R, Hoepken HH, Minich T, C R (2007) Pentose phosphate pathway and NADPH metabolism. In: Brain Energetics. Integration of Molecular and Cellular Processes, 3rd Edition (Gibson GE, Dienel GA, eds), pp 41–62. Berlin: Springer-Verlag.

Duarte JM, Morgenthaler FD, Lei H, Poitry-Yamate C, Gruetter R (2009) Steady-state brain glucose transport kinetics re-evaluated with a four-state conformational model. Front Neuroenerg 1:6.

Duffy TE, Howse DC, Plum F (1975) Cerebral energy metabolism during experimental status epilepticus. J Neurochem 24:925–934.

Duncan GE, Stumpf WE, Pilgrim C, Breese GR (1987) High resolution autoradiography at the regional topographic level with [14C]2-deoxyglucose and [3H]2-deoxyglucose. J Neurosci Methods 20:105–113.

Enager P, Piilgaard H, Offenhauser N, Kocharyan A, Fernandes P, Hamel E, Lauritzen M (2009) Pathway-specific variations in neurovascular and neurometabolic coupling in rat primary somatosensory cortex. J Cereb Blood Flow Metab 29:976–986.

Enkvist MO, McCarthy KD (1994) Astroglial gap junction communication is increased by treatment with either glutamate or high K+ concentration. J Neurochem 62:489–495.

Eriksson G, Peterson A, Iverfeldt K, Walum E (1995) Sodium-dependent glutamate uptake as an activator of oxidative metabolism in primary astrocyte cultures from newborn rat. Glia 15:152–156.

Erlichman JS, Hewitt A, Damon TL, Hart M, Kurascz J, Li A, Leiter JC (2008) Inhibition of monocarboxylate transporter 2 in the retrotrapezoid nucleus in rats: a test of the astrocyte-neuron lactate-shuttle hypothesis. J Neurosci 28:4888–4896.

Esposito RU, Porrino LJ, Seeger TF, Crane AM, Everist HD, Pert A (1984) Changes in local cerebral glucose utilization during rewarding brain stimulation. Proc Natl Acad Sci USA. 81:635–639.

Figley CR (2011) Lactate transport and metabolism in the human brain: implications for the astrocyte-neuron lactate shuttle hypothesis. J Neurosci 31:4768–4770.

Fitzpatrick SM, Cooper AJ, Duffy TE (1983) Use of beta-methylene-D,L-aspartate to assess the role of aspartate aminotransferase in cerebral oxidative metabolism. J Neurochem 41:1370–1383.

Fitzpatrick SM, Cooper AJ, Hertz L (1988) Effects of ammonia and beta-methylene-DL-aspartate on the oxidation of glucose and pyruvate by neurons and astrocytes in primary culture. J Neurochem 51:1197–1203.

Folbergrova J, MacMillan V, Siesjo BK (1972) The effect of moderate and marked hypercapnia upon the energy state and upon the cytoplasmic NADH-NAD+ ratio of the rat brain. J Neurochem 19:2497–2505.

Folbergrova J, Ingvar M, Siesjo BK (1981) Metabolic changes in cerebral cortex, hippocampus, and cerebellum during sustained bicuculline-induced seizures. J Neurochem 37:1228–1238.

Fox PT, Raichle ME (1986) Focal physiological uncoupling of cerebral blood flow and oxidative metabolism during somatosensory stimulation in human subjects. Proc Natl Acad Sci USA 83:1140–1144.

Fox PT, Raichle ME, Mintun MA, Dence C (1988) Nonoxidative glucose consumption during focal physiologic neural activity. Science 241: 462–464.

Frahm J, Kruger G, Merboldt KD, Kleinschmidt A (1996) Dynamic uncoupling and recoupling of perfusion and oxidative metabolism during focal brain activation in man. Magn Reson Med 35:143–148.

Frey KA, Agranoff BW (1983) Barbiturate-enhanced detection of brain lesions by carbon-14-labeled 2-deoxyglucose autoradiography. Science 219:879–881.

Fuglsang A, Lomholt M, Gjedde A (1986) Blood–brain transfer of glucose and glucose analogs in newborn rats. J Neurochem 46:1417–1428.

Gandhi GK, Cruz NF, Ball KK, Dienel GA (2009a) Astrocytes are poised for lactate trafficking and release from activated brain and for supply of glucose to neurons. J Neurochem 111:522–536.

Gandhi GK, Ball KK, Cruz NF, Dienel GA (2010) Hyperglycaemia and diabetes impair gap junctional communication among astrocytes. ASN Neuro 2:e00030.

Gandhi GK, Cruz NF, Ball KK, Theus SA, Dienel GA (2009b) Selective astrocytic gap junctional trafficking of molecules involved in the glycolytic pathway: impact on cellular brain imaging. J Neurochem 110:857–869.

Garriga-Canut M, Schoenike B, Qazi R, Bergendahl K, Daley TJ, Pfender RM, Morrison JF, Ockuly J, Stafstrom C, Sutula T, Roopra A (2006) 2-Deoxy-D-glucose reduces epilepsy progression by NRSF-CtBP-dependent metabolic regulation of chromatin structure. Nat Neurosci 9:1382–1387.

Gatfield PD, Lowry OH, Schulz DW, Passonneau JV (1966) Regional energy reserves in mouse brain and changes with ischaemia and anaesthesia. J Neurochem 13:185–195.

Gerhart DZ, Enerson BE, Zhdankina OY, Leino RL, Drewes LR (1998) Expression of the monocarboxylate transporter MCT2 by rat brain glia. Glia 22: 272–281.

Ghajar JB, Plum F, Duffy TE (1982) Cerebral oxidative metabolism and blood flow during acute hypoglycemia and recovery in unanesthetized rats. J Neurochem 38:397–409.

Giaume C, Tabernero A, Medina JM (1997) Metabolic trafficking through astrocytic gap junctions. Glia 21:114–123.

Giaume C, Koulakoff A, Roux L, Holcman D, Rouach N (2010) Astroglial networks: a step further in neuroglial and gliovascular interactions. Nat Rev Neurosci 11:87–99.

Gibbs ME, Hutchinson D, Hertz L (2008) Astrocytic involvement in learning and memory consolidation. Neurosci Biobehav Rev 32:927–944.

Gibson GE, Dienel GA, eds (2007) Brain energetics. Integration of molecular and cellular processes, 3 Edition. Berlin: Springer-Verlag.

Giove F, Mangia S, Bianciardi M, Garreffa G, Di Salle F, Morrone R, Maraviglia B (2003) The physiology and metabolism of neuronal activation: *in vivo* studies by NMR and other methods. Magn Reson Imaging 21:1283–1293.

Gjedde A, Marrett S (2001) Glycolysis in neurons, not astrocytes, delays oxidative metabolism of human visual cortex during sustained checker-board stimulation *in vivo*. J Cereb Blood Flow Metab 21:1384–1392.

Gjedde A, Marrett S, Vafaee M (2002) Oxidative and nonoxidative metabolism of excited neurons and astrocytes. J Cereb Blood Flow Metab 22:1–14.

Gordon GR, Choi HB, Rungta RL, Ellis-Davies GC, MacVicar BA (2008) Brain metabolism dictates the polarity of astrocyte control over arterioles. Nature 456:745–749.

Gotoh J, Itoh Y, Kuang TY, Cook M, Law MJ, Sokoloff L (2000) Negligible glucose-6-phosphatase activity in cultured astroglia. J Neurochem 74:1400–1408.

Grome JJ, McCulloch J (1983) The effects of apomorphine upon local cerebral glucose utilization in conscious rats and in rats anesthetized with chloral hydrate. J Neurochem 40:569–576.

Gross PM, Sposito NM, Pettersen SE, Panton DG, Fenstermacher JD (1987) Topography of capillary density, glucose metabolism, and microvascular function within the rat inferior colliculus. J Cereb Blood Flow Metab 7:154–160.

Gross RA, Ferrendelli JA (1980) Mechanisms of cyclic AMP regulation in cerebral anoxia and their relationship to glycogenolysis. J Neurochem 34:1309–1318.

Grossbard L, Schimke RT (1966) Multiple hexokinases of rat tissues. Purification and comparison of soluble forms. J Biol Chem 241:3546–3560.

Gruetter R, Ugurbil K, Seaquist ER (1998) Steady-state cerebral glucose concentrations and transport in the human brain. J Neurochem 70: 397–408.

Grunwald F, Schrock H, Theilen H, Biber A, Kuschinsky W (1988) Local cerebral glucose utilization of the awake rat during chronic administration of nicotine. Brain Res 456:350–356.

Gusnard DA, Raichle ME (2001) Searching for a baseline: functional imaging and the resting human brain. Nature Reviews. Neuroscience 2: 685–694.

Halestrap AP (1975) The mitochondrial pyruvate carrier. Kinetics and specificity for substrates and inhibitors. Biochem J 148:85–96.

Halestrap AP, Denton RM (1975) The specificity and metabolic implications of the inhibition of pyruvate transport in isolated mitochondria and intact tissue preparations by alpha-cyano-4-hydroxycinnamate and related compounds. Biochem J 148:97–106.

Halperin ML, Connors HP, Relman AS, Karnovsky ML (1969) Factors that control the effect of pH on glycolysis in leukocytes. J Biol Chem 244: 384–390.

Hanu R, McKenna M, O'Neill A, Resneck WG, Bloch RJ (2000) Monocarboxylic acid transporters, MCT1 and MCT2, in cortical astrocytes *in vitro* and *in vivo*. Am J Physiol Cell Physiol 278:C921–930.

Hargreaves RJ, Planas AM, Cremer JE, Cunningham VJ (1986) Studies on the relationship between cerebral glucose transport and phosphorylation using 2-deoxyglucose. J Cereb Blood Flow Metab 6:708–716.

Harris JJ, Attwell D (2012) The energetics of CNS white matter. J Neurosci 32:356–371.

Hawkins RA, Miller AL, Nielsen RC, Veech RL (1973) The acute action of ammonia on rat brain metabolism *in vivo*. Biochem J 134:1001–1008.

Henry PG, Adriany G, Deelchand D, Gruetter R, Marjanska M, Oz G, Seaquist ER, Shestov A, Ugurbil K (2006) *In vivo* 13C NMR spectroscopy and metabolic modeling in the brain: a practical perspective. Magn Reson Imaging 24:527–539.

Herrero-Mendez A, Almeida A, Fernandez E, Maestre C, Moncada S, Bolanos JP (2009) The bioenergetic and antioxidant status of neurons is controlled by continuous degradation of a key glycolytic enzyme by APC/C-Cdh1. Nat Cell Biol 11:747–752.

Hertz L (2011a) Astrocytic energy metabolism and glutamate formation–relevance for 13C-NMR spectroscopy and importance of cytosolic/mitochondrial trafficking. Magn Reson Imaging 29:1319–1329.

Hertz L (2011b) Brain glutamine synthesis requires neuronal aspartate: a commentary. J Cereb Blood Flow Metab 31:384–387.

Hertz L, Gibbs ME (2009) What learning in day-old chickens can teach a neurochemist: focus on astrocyte metabolism. J Neurochem 109 Suppl 1:10–16.

Hertz L, Peng L, Dienel GA (2007) Energy metabolism in astrocytes: high rate of oxidative metabolism and spatiotemporal dependence on glycolysis/glycogenolysis. J Cereb Blood Flow Metab 27:219–249.

Hertz L, Swanson RA, Newman GC, Marrif H, Juurlink BH, Peng L (1998) Can experimental conditions explain the discrepancy over glutamate stimulation of aerobic glycolysis? Dev Neurosci 20:339–347.

Herzog RI, Chan O, Yu S, Dziura J, McNay EC, Sherwin RS (2008) Effect of acute and recurrent hypoglycemia on changes in brain glycogen concentration. Endocrinology 149:1499–1504.

Hevner RF, Liu S, Wong-Riley MT (1995) A metabolic map of cytochrome oxidase in the rat brain: histochemical, densitometric and biochemical studies. Neuroscience 65:313–342.

Hirano Y, Stefanovic B, Silva AC (2011) Spatiotemporal evolution of the functional magnetic resonance imaging response to ultrashort stimuli. J Neurosci 31:1440–1447.

Hirose S, Momosaki S, Hosoi R, Abe K, Gee A, Inoue O (2009) Role of NMDA receptor upon [14C]acetate uptake into intact rat brain. Ann Nucl Med 23:143–147.

Hokfelt T, Smith CB, Peters A, Norell G, Crane A, Brownstein M, Sokoloff L (1983) Improved resolution of the 2-deoxy-D-glucose technique. Brain Res 289:311–316.

Hokfelt T, Smith CB, Norell G, Peters A, Crane A, Goldstein M, Brownstein M, Sokoloff L (1984) Attempts to combine 2-deoxyglucose autoradiography and tyrosine hydroxylase immunohistochemistry. Neuroscience 13: 495–512.

Holden JE, Mori K, Dienel GA, Cruz NF, Nelson T, Sokoloff L (1991) Modeling the dependence of hexose distribution volumes in brain on plasma glucose concentration: implications for estimation of the local 2-deoxyglucose lumped constant. J Cereb Blood Flow Metab 11:171–182.

Hosoi R, Kashiwagi Y, Tokumura M, Abe K, Hatazawa J, Inoue O (2007) Sensitive reduction in 14C-acetate uptake in a short-term ischemic rat brain. J Stroke Cerebrovasc Dis 16:77–81.

Hosoi R, Kitano D, Momosaki S, Kuse K, Gee A, Inoue O (2010) Remarkable increase in 14C-acetate uptake in an epilepsy model rat brain induced by lithium-pilocarpine. Brain Res 1311:158–165.

Howarth C, Peppiatt-Wildman CM, Attwell D (2010) The energy use associated with neural computation in the cerebellum. J Cereb Blood Flow Metab 30:403–414.

Howse DC, Duffy TE (1975) Control of the redox state of the pyridine nucleotides in the rat cerebral cortex. Effect of electroshock-induced seizures. J Neurochem 24:935–940.

Howse DC, Caronna JJ, Duffy TE, Plum F (1974) Cerebral energy metabolism, pH, and blood flow during seizures in the cat. Am J Physiol 227: 1444–1451.

Hu Y, Wilson GS (1997a) A temporary local energy pool coupled to neuronal activity: fluctuations of extracellular lactate levels in rat brain monitored with rapid-response enzyme-based sensor. J Neurochem 69:1484–1490.

Hu Y, Wilson GS (1997b) Rapid changes in local extracellular rat brain glucose observed with an *in vivo* glucose sensor. J Neurochem 68:1745–1752.

Hyder F, Rothman DL, Mason GF, Rangarajan A, Behar KL, Shulman RG (1997) Oxidative glucose metabolism in rat brain during single forepaw stimulation: a spatially localized 1H[13C] nuclear magnetic resonance study. J Cereb Blood Flow Metab 17:1040–1047.

Hyder F, Patel AB, Gjedde A, Rothman DL, Behar KL, Shulman RG (2006) Neuronal-glial glucose oxidation and glutamatergic-GABAergic function. J Cereb Blood Flow Metab 26:865–877.

Hyder F, Chase JR, Behar KL, Mason GF, Siddeek M, Rothman DL, Shulman RG (1996) Increased tricarboxylic acid cycle flux in rat brain during forepaw stimulation detected with 1H[13C]NMR. Proc Natl Acad Sci USA 93:7612–7617.

Hyder F, Sanganahalli BG, Herman P, Coman D, Maandag NJ, Behar KL, Blumenfeld H, Rothman DL (2010) Neurovascular and neurometabolic couplings in dynamic calibrated fMRI: transient oxidative neuroenergetics for block-design and event-related paradigms. Front Neuroenerg 2.

Jackson VN, Halestrap AP (1996) The kinetics, substrate, and inhibitor specificity of the monocarboxylate (lactate) transporter of rat liver cells determined using the fluorescent intracellular pH indicator, 2′,7′-bis(carboxyethyl)-5(6)-carboxyfluorescein. J Biol Chem 271:861–868.

Jolivet R, Allaman I, Pellerin L, Magistretti PJ, Weber B (2010) Comment on recent modeling studies of astrocyte–neuron metabolic interactions. J Cereb Blood Flow Metab 30:1982–1986.

Kapoor R, Spence AM, Muzi M, Graham MM, Abbott GL, Krohn KA (1989) Determination of the deoxyglucose and glucose phosphorylation ratio and the lumped constant in rat brain and a transplantable rat glioma. J Neurochem 53:37–44.

Kauppinen RA, Sihra TS, Nicholls DG (1987) Aminooxyacetic acid inhibits the malate-aspartate shuttle in isolated nerve terminals and prevents the mitochondria from utilizing glycolytic substrates. Biochim Biophys Acta 930:173–178.

Kemppainen J, Aalto S, Fujimoto T, Kalliokoski KK, Langsjo J, Oikonen V, Rinne J, Nuutila P, Knuuti J (2005) High intensity exercise decreases global brain glucose uptake in humans. J Physiol 568:323–332.

Kim T, Masamoto K, Fukuda M, Vazquez A, Kim SG (2010) Frequency-dependent neural activity, CBF, and BOLD fMRI to somatosensory stimuli in isoflurane-anesthetized rats. NeuroImage 52:224–233.

King LJ, Lowry OH, Passonneau JV, Venson V (1967a) Effects of convulsants on energy reserves in the cerebral cortex. J Neurochem 14:599–611.

King LJ, Schoepfle GM, Lowry OH, Passonneau JV, Wilson S (1967b) Effects of electrical stimulation on metabolites in brain of decapitated mice. J Neurochem 14:613–618.

Koehler-Stec EM, Li K, Maher F, Vannucci SJ, Smith CB, Simpson IA (2000) Cerebral glucose utilization and glucose transporter expression: response to water deprivation and restoration. J Cereb Blood Flow Metab 20: 192–200.

Koh L, Zakharov A, Johnston M (2005) Integration of the subarachnoid space and lymphatics: is it time to embrace a new concept of cerebrospinal fluid absorption? Cerebrospinal Fluid Res 2:6.

Krebs HA (1972) The Pasteur effect and the relations between respiration and fermentation. Essays in Biochemistry 8:1–34.

Land JM, Booth RF, Berger R, Clark JB (1977) Development of mitochondrial energy metabolism in rat brain. Biochem J 164:339–348.

Langer J, Stephan J, Theis M, Rose CR (2012) Gap junctions mediate intercellular spread of sodium between hippocampal astrocytes *in situ*. Glia 60:239–252.

Lavialle M, Aumann G, Anlauf E, Prols F, Arpin M, Derouiche A (2011) Structural plasticity of perisynaptic astrocyte processes involves ezrin and metabotropic glutamate receptors. Proc Natl Acad Sci USA 108: 12915–12919.

Lear JL (1990) Glycolysis: link between PET and proton MR spectroscopic studies of the brain. Radiology 174:328–330.

Lear JL, Ackermann RF (1988) Comparison of cerebral glucose metabolic rates measured with fluorodeoxyglucose and glucose labeled in the 1, 2, 3–4, and 6 positions using double label quantitative digital autoradiography. J Cereb Blood Flow Metab 8:575–585.

Lear JL, Ackermann RF (1989) Why the deoxyglucose method has proven so useful in cerebral activation studies: the unappreciated prevalence of stimulation-induced glycolysis. J Cereb Blood Flow Metab 9:911–913.

Lebon V, Petersen KF, Cline GW, Shen J, Mason GF, Dufour S, Behar KL, Shulman GI, Rothman DL (2002) Astroglial contribution to brain energy metabolism in humans revealed by 13C nuclear magnetic resonance spectroscopy: elucidation of the dominant pathway for neurotransmitter glutamate repletion and measurement of astrocytic oxidative metabolism. J Neurosci 22:1523–1531.

Leong SF, Clark JB (1984) Regional enzyme development in rat brain. Enzymes associated with glucose utilization. Biochem J 218:131–138.

Leong SF, Lai JC, Lim L, Clark JB (1981) Energy-metabolizing enzymes in brain regions of adult and aging rats. J Neurochem 37:1548–1556.

Lin AL, Gao JH, Duong TQ, Fox PT (2010a) Functional neuroimaging: a physiological perspective. Front Neuroenerg 2:17, doi: 10.3389/fnene.2010.00017

Lin AL, Fox PT, Hardies J, Duong TQ, Gao JH (2010b) Nonlinear coupling between cerebral blood flow, oxygen consumption, and ATP production in human visual cortex. Proc Natl Acad Sci USA 107:8446–8451.

Linde R, Schmalbruch IK, Paulson OB, Madsen PL (1999) The Kety-Schmidt technique for repeated measurements of global cerebral blood flow and metabolism in the conscious rat. Acta Physiol Scand 165:395–401.

Ljunggren B, Norberg K, Siesjo BK (1974) Influence of tissue acidosis upon restitution of brain energy metabolism following total ischemia. Brain Res 77:173–186.

Lovatt D, Sonnewald U, Waagepetersen HS, Schousboe A, He W, Lin JH, Han X, Takano T, Wang S, Sim FJ, Goldman SA, Nedergaard M (2007) The transcriptome and metabolic gene signature of protoplasmic astrocytes in the adult murine cortex. J Neurosci 27:12255–12266.

Lowry OH (1975) Energy metabolism in brain and its control. In: Brain Work: The Coupling of Function, Metabolism, and Blood Flow in the Brain. Proceedings of the Alfred Benzon Symposium VIII (Ingvar DH, Lassen NA, eds), pp 48–63. Copenhagen.

Lowry OH, Passonneau JV (1964) The Relationships between substrates and enzymes of glycolysis in brain. J Biol Chem 239:31–42.

Lowry OH, Passonneau JV (1966) Kinetic evidence for multiple binding sites on phosphofructokinase. J Biol Chem 241:2268–2279.

Lowry OH, Passonneau JV, Hasselberger FX, Schulz DW (1964) Effect of ischemia on known substrates and cofactors of the glycolytic pathway in brain. J Biol Chem 239:18–30.

MacMillan V (1975) The effects of acute carbon monoxide intoxication on the cerebral energy metabolism of the rat. Can J Physiol Pharmacol 53:354–362.

Maddock RJ (2001) The lactic acid response to alkalosis in panic disorder: an integrative review. J Neuropsychiatry Clin Neurosc 13:22–34.

Madsen PL, Cruz NF, Sokoloff L, Dienel GA (1999) Cerebral oxygen/glucose ratio is low during sensory stimulation and rises above normal during recovery: excess glucose consumption during stimulation is not accounted for by lactate efflux from or accumulation in brain tissue. J Cereb Blood Flow Metab 19:393–400.

Madsen PL, Linde R, Hasselbalch SG, Paulson OB, Lassen NA (1998) Activation-induced resetting of cerebral oxygen and glucose uptake in the rat. J Cereb Blood Flow Metab 18:742–748.

Madsen PL, Hasselbalch SG, Hagemann LP, Olsen KS, Bulow J, Holm S, Wildschiodtz G, Paulson OB, Lassen NA (1995) Persistent resetting of the cerebral oxygen/glucose uptake ratio by brain activation: evidence obtained with the Kety-Schmidt technique. J Cereb Blood Flow Metab 15:485–491.

Magistretti PJ, Pellerin L, Rothman DL, Shulman RG (1999) Energy on demand. Science 283:496–497.

Mangia S, Simpson IA, Vannucci SJ, Carruthers A (2009a) The *in vivo* neuron-to-astrocyte lactate shuttle in human brain: evidence from modeling of measured lactate levels during visual stimulation. J Neurochem 109 Suppl 1:55–62.

Mangia S, Tkac I, Logothetis NK, Gruetter R, Van de Moortele PF, Ugurbil K (2007a) Dynamics of lactate concentration and blood oxygen level-dependent effect in the human visual cortex during repeated identical stimuli. J Neurosci Res 85:3340–3346.

Mangia S, Tkac I, Gruetter R, Van de Moortele PF, Maraviglia B, Ugurbil K (2007b) Sustained neuronal activation raises oxidative metabolism to a new steady-state level: evidence from 1H NMR spectroscopy in the human visual cortex. J Cereb Blood Flow Metab 27:1055–1063.

Mangia S, DiNuzzo M, Giove F, Carruthers A, Simpson IA, Vannucci SJ (2011) Response to 'comment on recent modeling studies of astrocyte–neuron metabolic interactions': much ado about nothing. J Cereb Blood Flow Metab 31:1346–1353.

Mangia S, Giove F, Tkac I, Logothetis NK, Henry PG, Olman CA, Maraviglia B, Di Salle F, Ugurbil K (2009b) Metabolic and hemodynamic events after changes in neuronal activity: current hypotheses, theoretical predictions and *in vivo* NMR experimental findings. J Cereb Blood Flow Metab 29:441–463.

Manning Fox JE, Meredith D, Halestrap AP (2000) Characterisation of human monocarboxylate transporter 4 substantiates its role in lactic acid efflux from skeletal muscle. J Physiol 529 Pt 2:285–293.

Masamoto K, Kanno I (2012) Anesthesia and the quantitative evaluation of neurovascular coupling. J Cereb Blood Flow Metab, doi:10.1038/jcbfm.2012.50

Maurer MH, Canis M, Kuschinsky W, Duelli R (2004) Correlation between local monocarboxylate transporter 1 (MCT1) and glucose transporter 1 (GLUT1) densities in the adult rat brain. Neurosci Lett 355:105–108.

McIlwain H, Bachelard HS (1969) Carbohydrate and oxidative metabolism in neural systems. In: Carbohydrate Metabolism (Florkin M, Stotz EH, eds), pp 191–218. New York, NY: Elsevier.

McIlwain H, Bachelard HS (1985) Biochemistry and the Central Nervous System, 5th Edition. New York, , NY: Churchill Livingstone

McKenna MC, Hopkins IB, Carey A (2001) Alpha-cyano-4-hydroxycinnamate decreases both glucose and lactate metabolism in neurons and astrocytes: implications for lactate as an energy substrate for neurons. J Neurosci Res 66:747–754.

McKenna MC, Waagepetersen HS, Schousboe A, Sonnewald U (2006) Neuronal and astrocytic shuttle mechanisms for cytosolic-mitochondrial transfer of reducing equivalents: current evidence and pharmacological tools. Biochem Pharmacol 71:399–407.

McKenna MC, Tildon JT, Stevenson JH, Boatright R, Huang S (1993) Regulation of energy metabolism in synaptic terminals and cultured rat brain astrocytes: differences revealed using aminooxyacetate. Dev Neurosci 15:320–329.

McKenna MC, Sonnewald U, Huang X, Stevenson J, Zielke HR (1996) Exogenous glutamate concentration regulates the metabolic fate of glutamate in astrocytes. J Neurochem 66:386–393.

McKenna MC, Dienel GA, Sonnewald U, Waagepetersen HS, Schousboe A (2012) Chapter 11–Energy Metabolism of the Brain. In: Basic Neurochemistry (Eighth Edition), pp 200–231. New York: Academic Press.

Meldrum BS, Nilsson B (1976) Cerebral blood flow and metabolic rate early and late in prolonged epileptic seizures induced in rats by bicuculline. Brain 99:523–542.

Miller AL, Hawkins RA, Veech RL (1975) Decreased rate of glucose utilization by rat brain *in vivo* after exposure to atmospheres containing high concentrations of CO2. J Neurochem 25:553–558.

Miller AL, Shamban AT, Corddry DH, Kiney CA (1982) Cerebral metabolic responses to electroconvulsive shock and their modification by hypercapnia. J Neurochem 38:916–924.

Miyaoka M, Shinohara M, Batipps M, Pettigrew KD, Kennedy CLS (1979) The relationship between the intensity of the stimulus and the metabolic response in the visual system of the rat. Acta Neurol Scand 60(Suppl 72):16–17.

Muller CP, Pum ME, Amato D, Schuttler J, Huston JP, Silva MA (2011) The *in vivo* neurochemistry of the brain during general anesthesia. J Neurochem 119:419–446.

Nakao Y, Itoh Y, Kuang TY, Cook M, Jehle J, Sokoloff L (2001) Effects of anesthesia on functional activation of cerebral blood flow and metabolism. Proc Natl Acad Sci USA 98:7593–7598.

Nedergaard M, Goldman SA (1993) Carrier-mediated transport of lactic acid in cultured neurons and astrocytes. Am J Physiol 265:R282–289.

Nehlig A (1997) Cerebral energy metabolism, glucose transport and blood flow: changes with maturation and adaptation to hypoglycaemia. Diabetes Metab 23:18–29.

Nehlig A, Pereira de Vasconcelos A (1993) Glucose and ketone body utilization by the brain of neonatal rats. Prog Neurobiol 40:163–221.

Nehlig A, de Vasconcelos AP, Boyet S (1988) Quantitative autoradiographic measurement of local cerebral glucose utilization in freely moving rats during postnatal development. J Neurosci 8:2321–2333.

Nehlig A, Wittendorp-Rechenmann E, Lam CD (2004) Selective uptake of [14C]2-deoxyglucose by neurons and astrocytes: high-resolution micro-autoradiographic imaging by cellular 14C-trajectography combined with immunohistochemistry. J Cereb Blood Flow Metab 24:1004–1014.

Nehlig A, Rudolf G, Leroy C, Rigoulot MA, Simpson IA, Vannucci SJ (2006) Pentylenetetrazol-induced status epilepticus up-regulates the expression of glucose transporter mRNAs but not proteins in the immature rat brain. Brain Res 1082:32–42.

Nelson T, Kaufman EE, Sokoloff L (1984) 2-Deoxyglucose incorporation into rat brain glycogen during measurement of local cerebral glucose utilization by the 2-deoxyglucose method. J Neurochem 43:949–956.

Nelson T, Lucignani G, Goochee J, Crane AM, Sokoloff L (1986) Invalidity of criticisms of the deoxyglucose method based on alleged glucose-6-phosphatase activity in brain. J Neurochem 46:905–919.

Newman LA, Korol DL, Gold PE (2011) Lactate produced by glycogenolysis in astrocytes regulates memory processing. PloS One 6:e28427.

Nicholls DG (2009) Spare respiratory capacity, oxidative stress and excitotoxicity. Biochem Soc Trans 37:1385–1388.

O'Neal RM, Koeppe RE (1966) Precursors *in vivo* of glutamate, aspartate and their derivatives of rat brain. J Neurochem 13:835–847.

Obel LF, Muller MS, Walls AB, Sickmann HM, Bak LK, Waagepetersen HS, Schousboe A (2012) Brain glycogen-new perspectives on its metabolic function and regulation at the subcellular level. Front Neuroenerg 4:3.

Okada Y, Lipton P (2007) Glucose, oxidative energy metabolism, and neural function in brain slices–Glycolysis plays a key role in neural activity. In: Brain Energetics. Integration of Molecular and Cellular Processes, 3 Edition (Gibson GE, Dienel GA, eds). Berlin: Springer-Verlag.

Orzi F, Lucignani G, Dow-Edwards D, Namba H, Nehlig A, Patlak CS, Pettigrew K, Schuier F, Sokoloff L (1988) Local cerebral glucose utilization in controlled graded levels of hyperglycemia in the conscious rat. J Cereb Blood Flow Metab 8:346–356.

Oz G, Tesfaye N, Kumar A, Deelchand DK, Eberly LE, Seaquist ER (2012) Brain glycogen content and metabolism in subjects with type 1 diabetes and hypoglycemia unawareness. J Cereb Blood Flow Metab 32:256–263.

Oz G, Berkich DA, Henry PG, Xu Y, LaNoue K, Hutson SM, Gruetter R (2004) Neuroglial metabolism in the awake rat brain: CO2 fixation increases with brain activity. J Neurosci 24:11273–11279.

Oz G, Kumar A, Rao JP, Kodl CT, Chow L, Eberly LE, Seaquist ER (2009) Human brain glycogen metabolism during and after hypoglycemia. Diabetes 58:1978–1985.

Oz G, Seaquist ER, Kumar A, Criego AB, Benedict LE, Rao JP, Henry PG, Van De Moortele PF, Gruetter R (2007) Human brain glycogen content and metabolism: implications on its role in brain energy metabolism. Am J Physiol. Endocrinol Metab 292:E946–951.

Pardo B, Contreras L, Serrano A, Ramos M, Kobayashi K, Iijima M, Saheki T, Satrustegui J (2006) Essential role of aralar in the transduction of small Ca2+ signals to neuronal mitochondria. J Biol Chem 281:1039–1047.

Pardo B, Rodrigues TB, Contreras L, Garzon M, Llorente-Folch I, Kobayashi K, Saheki T, Cerdan S, Satrustegui J (2011) Brain glutamine synthesis requires neuronal-born aspartate as amino donor for glial glutamate formation. J Cereb Blood Flow Metab 31:90–101.

Pardridge WM, Crane PD, Mietus LJ, Oldendorf WH (1982) Kinetics of regional blood–brain barrier transport and brain phosphorylation of glucose and 2-deoxyglucose the barbiturate-anesthetized rat. J Neurochem 38:560–568.

Patel AB, de Graaf RA, Rothman DL, Behar KL, Mason GF (2010) Evaluation of cerebral acetate transport and metabolic rates in the rat brain *in vivo* using 1H-[13C]-NMR. J Cereb Blood Flow Metab 30:1200–1213.

Paulson OB, Hasselbalch SG, Rostrup E, Knudsen GM, Pelligrino D (2010) Cerebral blood flow response to functional activation. J Cereb Blood Flow Metab 30:2–14.

Pellerin L (2005) How astrocytes feed hungry neurons. Mol Neurobiol 32: 59–72.

Pellerin L (2008) Brain energetics (thought needs food). Curr Opin Clin Nutr Metab Care 11:701–705.

Pellerin L (2010) Food for thought: the importance of glucose and other energy substrates for sustaining brain function under varying levels of activity. Diabetes Metab 36 Suppl 3:S59–63.

Pellerin L, Magistretti PJ (1994) Glutamate uptake into astrocytes stimulates aerobic glycolysis: a mechanism coupling neuronal activity to glucose utilization. Proc Natl Acad Sci USA 91:10625–10629.

Pellerin L, Magistretti PJ (2004) Neuroenergetics: calling upon astrocytes to satisfy hungry neurons. Neuroscientist 10:53–62.

Pellerin L, Magistretti PJ (2011) Sweet sixteen for ANLS. J Cereb Blood Flow Metab 32:1152–1166.

Pellerin L, Bouzier-Sore AK, Aubert A, Serres S, Merle M, Costalat R, Magistretti PJ (2007) Activity-dependent regulation of energy metabolism by astrocytes: an update. Glia 55:1251–1262.

Peng L, Swanson RA, Hertz L (2001) Effects of L-glutamate, D-aspartate, and monensin on glycolytic and oxidative glucose metabolism in mouse astrocyte cultures: further evidence that glutamate uptake is metabolically driven by oxidative metabolism. Neurochem Int 38:437–443.

Pfeuffer J, Tkac I, Gruetter R (2000) Extracellular-intracellular distribution of glucose and lactate in the rat brain assessed noninvasively by diffusion-weighted 1H nuclear magnetic resonance spectroscopy *in vivo*. J Cereb Blood Flow Metab 20:736–746.

Ponten U, Ratcheson RA, Salford LG, Siesjo BK (1973) Optimal freezing conditions for cerebral metabolites in rats. J Neurochem 21:1127–1138.

Prichard J, Rothman D, Novotny E, Petroff O, Kuwabara T, Avison M, Howseman A, Hanstock C, Shulman R (1991) Lactate rise detected by 1H NMR in human visual cortex during physiologic stimulation. Proc Natl Acad Sci USA 88:5829–5831.

Quistorff B, Secher NH, Van Lieshout JJ (2008) Lactate fuels the human brain during exercise. FASEB J 22:3443–3449.

Ramos M, del Arco A, Pardo B, Martinez-Serrano A, Martinez-Morales JR, Kobayashi K, Yasuda T, Bogonez E, Bovolenta P, Saheki T, Satrustegui J (2003) Developmental changes in the Ca^{2+}-regulated mitochondrial aspartate-glutamate carrier aralar1 in brain and prominent expression in the spinal cord. Brain Res. Dev Brain Res 143:33–46.

Reivich M, Kuhl D, Wolf A, Greenberg J, Phelps M, Ido T, Casella V, Fowler J, Hoffman E, Alavi A, Som P, Sokoloff L (1979) The [18F]fluorodeoxyglucose method for the measurement of local cerebral glucose utilization in man. Circ Res 44:127–137.

Rennels ML, Gregory TF, Blaumanis OR, Fujimoto K, Grady PA (1985) Evidence for a 'paravascular' fluid circulation in the mammalian central nervous system, provided by the rapid distribution of tracer protein throughout the brain from the subarachnoid space. Brain Res 326:47–63.

Requardt RP, Hirrlinger PG, Wilhelm F, Winkler U, Besser S, Hirrlinger J (2012) $Ca2^+$ signals of astrocytes are modulated by the NAD^+/NADH redox state. J Neurochem 120:1014–1025.

Roberts J, E.L. (2007) The support of energy metabolism in the central nervous system with substrates other than glucose. In: Brain Energetics. Integration of Molecular and Cellular Processes, 3rd Edition (Gibson GE, Dienel GA, eds), pp 137–179. Berlin: Springer-Verlag.

Roncero I, Alvarez E, Vazquez P, Blazquez E (2000) Functional glucokinase isoforms are expressed in rat brain. J Neurochem 74:1848–1857.

Rothman DL, Behar KL, Hyder F, Shulman RG (2003) *In vivo* NMR studies of the glutamate neurotransmitter flux and neuroenergetics: implications for brain function. Annu Rev Physiol 65:401–427.

Rothman DL, De Feyter HM, de Graaf RA, Mason GF, Behar KL (2011) 13C MRS studies of neuroenergetics and neurotransmitter cycling in humans. NMR Biomed 24:943–957.

Ryan AF, Woolf NK, Sharp FR (1982) Tonotopic organization in the central auditory pathway of the Mongolian gerbil: a 2-deoxyglucose study. J Comp Neurol 207:369–380.

Sakurada O, Kennedy C, Jehle J, Brown JD, Carbin GL, Sokoloff L (1978) Measurement of local cerebral blood flow with iodo [14C] antipyrine. Am J Physiol 234:H59–66.

Savaki HE, Desban M, Glowinski J, Besson MJ (1983) Local cerebral glucose consumption in the rat. II. Effects of unilateral substantia nigra stimulation in conscious and in halothane-anesthetized animals. J Comp Neurol 213:46–65.

Schaaff I, Heinisch J, Zimmermann FK (1989) Overproduction of glycolytic enzymes in yeast. Yeast 5:285–290.

Schousboe A, Bak LK, Sickmann HM, Sonnewald U, Waagepetersen HS (2007) Energy substrates to support glutamatergic and GABAergic synaptic function: role of glycogen, glucose and lactate. Neurotox Res 12:263–268.

Schuier F, Orzi F, Suda S, Lucignani G, Kennedy C, Sokoloff L (1990) Influence of plasma glucose concentration on lumped constant of the deoxyglucose method: effects of hyperglycemia in the rat. J Cereb Blood Flow Metab 10:765–773.

Schurr A, Gozal E (2011) Aerobic production and utilization of lactate satisfy increased energy demands upon neuronal activation in hippocampal slices and provide neuroprotection against oxidative stress. Front Pharmacol 2:96.

Schweigert ID, Roehrig C, da Costa F, Scheibel F, Gottfried CJ, Rotta LN, Goncalves CA, Souza DO, Perry ML (2004) High extracellular K+ levels stimulate acetate oxidation in brain slices from well and malnourished rats. Neurochem Res 29:1547–1551.

Sharp FR (1976) Relative cerebral glucose uptake of neuronal perikarya and neuropil determined with 2-deoxyglucose in resting and swimming rat. Brain Res 110:127–139.

Shen Q, Ren H, Duong TQ (2008) CBF, BOLD, CBV, and CMRO(2) fMRI signal temporal dynamics at 500-msec resolution. J Magn Reson Imaging 27:599–606.

Shestov AA, Emir UE, Kumar A, Henry PG, Seaquist ER, Oz G (2011) Simultaneous measurement of glucose transport and utilization in the human brain. Am J Physiol. Endocrinol Metab 301:E1040–1049.

Shulman RG, Rothman DL, Hyder F (1999) Stimulated changes in localized cerebral energy consumption under anesthesia. Proc Natl Acad Sci USA 96:3245–3250.

Shulman RG, Hyder F, Rothman DL (2001) Lactate efflux and the neuroenergetic basis of brain function. NMR Biomed 14:389–396.

Shulman RG, Hyder F, Rothman DL (2009) Baseline brain energy supports the state of consciousness. Proc Natl Acad Sci USA 106:11096–11101.

Siesjo BK (1978) Brain Energy Metabolism. Chichester: John Wiley & Sons.

Simard M, Arcuino G, Takano T, Liu QS, Nedergaard M (2003) Signaling at the gliovascular interface. J Neurosci 23:9254–9262.

Simpson IA, Carruthers A, Vannucci SJ (2007) Supply and demand in cerebral energy metabolism: the role of nutrient transporters. J Cereb Blood Flow Metab 27:1766–1791.

Smith D, Pernet A, Hallett WA, Bingham E, Marsden PK, Amiel SA (2003) Lactate: a preferred fuel for human brain metabolism *in vivo*. J Cereb Blood Flow Metab 23:658–664.

Snyder CD, Wilson JE (1983) Relative levels of hexokinase in isolated neuronal, astrocytic, and oligodendroglial fractions from rat brain. J Neurochem 40:1178–1181.

Sokoloff L (1986) Cerebral circulation, energy metabolism, and protein synthesis: general characteristics and principles of measurement. In: Positron Emission Tomography and Autoradiography: Principles and Applications for the Brain and Heart (Phelps M, Mazziotta J, Schelbert H, eds), pp 1–71. New York: Raven Press.

Sokoloff L, Reivich M, Kennedy C, Des Rosiers MH, Patlak CS, Pettigrew KD, Sakurada O, Shinohara M (1977) The [14C]deoxyglucose method for the measurement of local cerebral glucose utilization: theory, procedure, and normal values in the conscious and anesthetized albino rat. J Neurochem 28:897–916.

Sols A, Crane RK (1954) Substrate specificity of brain hexokinase. J Biol Chem 210:581–595.

Speizer L, Haugland R, Kutchai H (1985) Asymmetric transport of a fluorescent glucose analogue by human erythrocytes. Biochim Biophys Acta, Biomembr 815:75–84.

Sperber GO, Bill A (1985) Blood flow and glucose consumption in the optic nerve, retina and brain: effects of high intraocular pressure. Exp Eye Res 41:639–653.

Stewart MA, Passonneau JV, Lowry OH (1965) Substrate changes in peripheral nerve during ischaemia and Wallerian degeneration. J Neurochem 12:719–727.

Suh SW, Bergher JP, Anderson CM, Treadway JL, Fosgerau K, Swanson RA (2007) Astrocyte glycogen sustains neuronal activity during hypoglycemia: studies with the glycogen phosphorylase inhibitor CP-316,819 ([R-R*,S*]-5-chloro-N-[2-hydroxy-3-(methoxymethylamino)-3-oxo-1-(phenylmethyl)pro pyl]-1H-indole-2-carboxamide). J Pharmacol Exp Ther 321:45–50.

Suzuki A, Stern SA, Bozdagi O, Huntley GW, Walker RH, Magistretti PJ, Alberini CM (2011) Astrocyte-neuron lactate transport is required for long-term memory formation. Cell 144:810–823.

Swanson RA, Morton MM, Sagar SM, Sharp FR (1992) Sensory stimulation induces local cerebral glycogenolysis: demonstration by autoradiography. Neuroscience 51:451–461.

Takahashi S, Izawa Y, Suzuki N (2012) Astroglial pentose phosphate pathway rates in response to high-glucose environments. ASN NEURO, 4(2):art:e00078.doi:10.1042/AN20120002

Trivedi B, Danforth WH (1966) Effect of pH on the kinetics of frog muscle phosphofructokinase. J Biol Chem 241:4110–4112.

Tucek S, Cheng SC (1974) Provenance of the acetyl group of acetylcholine and compartmentation of acetyl-CoA and Krebs cycle intermediates in the brain *in vivo*. J Neurochem 22:893–914.

Ueki M, Linn F, Hossmann KA (1988) Functional activation of cerebral blood flow and metabolism before and after global ischemia of rat brain. J Cereb Blood Flow Metab 8:486–494.

Ueki M, Mies G, Hossmann KA (1992) Effect of alpha-chloralose, halothane, pentobarbital and nitrous oxide anesthesia on metabolic coupling in somatosensory cortex of rat. Acta Anaesthesiol Scand 36:318–322.

Uludag K, Dubowitz DJ, Yoder EJ, Restom K, Liu TT, Buxton RB (2004) Coupling of cerebral blood flow and oxygen consumption during physiological activation and deactivation measured with fMRI. NeuroImage 23:148–155.

Urbano AM, Gillham H, Groner Y, Brindle KM (2000) Effects of overexpression of the liver subunit of 6-phosphofructo-1-kinase on the metabolism of a cultured mammalian cell line. Biochem J 352 Pt 3:921–927.

Vaishnavi SN, Vlassenko AG, Rundle MM, Snyder AZ, Mintun MA, Raichle ME (2010) Regional aerobic glycolysis in the human brain. Proc Natl Acad Sci USA 107:17757–17762.

Van den Berg CJ, Bruntink R (1983) Glucose oxidation in the brain during seizures: Experiments with labeled glucose and deoxyglucose. In: Glutamine, Glutamate and GABA in the Central Nervous System (Hertz L, Kvamme E, McGeer EG, Schousboe A, eds), pp 619–624. New York, NY: Alan R Liss Inc.

van Hall G, Stromstad M, Rasmussen P, Jans O, Zaar M, Gam C, Quistorff B, Secher NH, Nielsen HB (2009) Blood lactate is an important energy source for the human brain. J Cereb Blood Flow Metab 29:1121–1129.

Vannucci SJ, Simpson IA (2003) Developmental switch in brain nutrient transporter expression in the rat. Am J Physiol. Endocrinol Metab 285:E1127–1134.

Vazquez AL, Masamoto K, Fukuda M, Kim SG (2010) Cerebral oxygen delivery and consumption during evoked neural activity. Front Neuroenerget 2:11.

Veech RL (1980) Freeze-blowing of the brain and the interpretation of the meaning of certain metabolite levels. In: Cerebral Metabolism and Neural Function (Passonneau JV, Hawkins RA, Lust WD, Welsh FA, eds), pp 34–41. Baltimore: Williams & Wilkins.

Veech RL, Hawkins RA (1974) Brain blowing: a technique for *in vivo* study of brain metabolism. In: Research Methods in Neurochemistry (Marks N, Rodnight R, eds), pp 171–185. New York: Plenum Press.

Vissing J, Andersen M, Diemer NH (1996) Exercise-induced changes in local cerebral glucose utilization in the rat. J Cereb Blood Flow Metab 16:729–736.

Volianitis S, Fabricius-Bjerre A, Overgaard A, Stromstad M, Bjarrum M, Carlson C, Petersen NT, Rasmussen P, Secher NH, Nielsen HB (2008) The cerebral metabolic ratio is not affected by oxygen availability during maximal exercise in humans. J Physiol 586:107–112.

Wang J, Li G, Wang Z, Zhang X, Yao L, Wang F, Liu S, Yin J, Ling EA, Wang L, Hao A (2012) High glucose-induced expression of inflammatory cytokines and reactive oxygen species in cultured astrocytes. Neuroscience 202:58–68.

Watanabe H, Passonneau JV (1973) Factors affecting the turnover of cerebral glycogen and limit dextrin *in vivo*. J Neurochem 20:1543–1554.

Wemmie JA (2011) Neurobiology of panic and pH chemosensation in the brain. Dialogues Clin Neurosci 13:475–483.

Wender R, Brown AM, Fern R, Swanson RA, Farrell K, Ransom BR (2000) Astrocytic glycogen influences axon function and survival during glucose deprivation in central white matter. J Neurosci 20:6804–6810.

Wilhelm F, Hirrlinger J (2012) Multifunctional roles of NAD^+ and NADH in astrocytes. Neurochem Res, doi:10.1007/s11064-012-0760-y

Wilson JE (2003) Isozymes of mammalian hexokinase: structure, subcellular localization and metabolic function. J Exp Biol 206:2049–2057.

Winkler BS, Pourcho RG, Starnes C, Slocum J, Slocum N (2003) Metabolic mapping in mammalian retina: a biochemical and 3H-2-deoxyglucose autoradiographic study. Exp Eye Res 77:327–337.

Wyss MT, Jolivet R, Buck A, Magistretti PJ, Weber B (2011) *In vivo* evidence for lactate as a neuronal energy source. J Neurosci 31:7477–7485.

Wyss MT, Weber B, Treyer V, Heer S, Pellerin L, Magistretti PJ, Buck A (2009) Stimulation-induced increases of astrocytic oxidative metabolism in rats and humans investigated with 1-11C-acetate. J Cereb Blood Flow Metab 29:44–56.

Xu S, Yang J, Li CQ, Zhu W, Shen J (2005) Metabolic alterations in focally activated primary somatosensory cortex of alpha-chloralose-anesthetized rats measured by 1H MRS at 11.7 T. NeuroImage 28:401–409.

Yang J, Shen J (2006) Increased oxygen consumption in the somatosensory cortex of alpha-chloralose anesthetized rats during forepaw stimulation determined using MRS at 11.7 Tesla. NeuroImage 32:1317–1325.

Yoshioka K, Saito M, Oh KB, Nemoto Y, Matsuoka H, Natsume M, Abe H (1996) Intracellular fate of 2-NBDG, a fluorescent probe for glucose uptake activity, in *Escherichia coli* cells. Biosci Biotechnol Biochem 60:1899–1901.

Zeller K, Rahner-Welsch S, Kuschinsky W (1997) Distribution of Glut1 glucose transporters in different brain structures compared to glucose utilization and capillary density of adult rat brains. J Cereb Blood Flow Metab 17:204–209.

Zhu XH, Zhang N, Zhang Y, Ugurbil K, Chen W (2009) New insights into central roles of cerebral oxygen metabolism in the resting and stimulus-evoked brain. J Cereb Blood Flow Metab 29:10–18.

Zielke HR, Zielke CL, Baab PJ (2007) Oxidation of (14)C-labeled compounds perfused by microdialysis in the brains of free-moving rats. J Neurosci Res 85:3145–3149.

Received 28 March 2012/8 May 2012; accepted 9 May 2012

Published as Immediate Publication 21 May 2012, doi 10.1042/AN20120021